https://doi.org/10.59761/RCR5152

Polymers based on triphenylamine: synthesis, properties, and applications

Irina A. Chuyko,[a] Pavel A. Troshin,[b,c] Sergey A. Ponomarenko,[a] Yuriy N. Luponosov[a]*

[a] *Enikolopov Institute of Synthetic Polymer Materials, Russian Academy of Sciences, 117393 Moscow, Russia*
[b] *Federal Research Center of Problems of Chemical Physics and Medicinal Chemistry, Russian Academy of Sciences, 142432 Chernogolovka, Moscow Region, Russia*
[c] *Zhengzhou Research Institute of HIT, Zhengzhou, Henan Province, 450000, China*

Triphenylamine-based conjugated polymers are a class of organic semiconductor compounds used in a variety of devices in the field of organic and hybrid optoelectronics, owing to a number of properties such as high hole mobility, efficient luminescence, high stability, and the ability to form films from solutions. The modern methods of organic and polymer synthesis make it possible to implement a variety of molecular designs for these polymers, ranging from simple conjugated macromolecules to intricate branched and cross-linked copolymers. This review analyzes the currently existing diversity of triphenylamine-based polymer structures, proposes their classification for the first time, considers the main approaches to the polymer synthesis, and, using numerous examples, demonstrates how the properties of such materials can be tuned using molecular design. Examples of application of these polymers in various modern devices are given, including perovskite solar cells, metal-ion batteries, electrochromic devices, organic light-emitting diodes, and sensors of various types.
The bibliography includes 281 references.

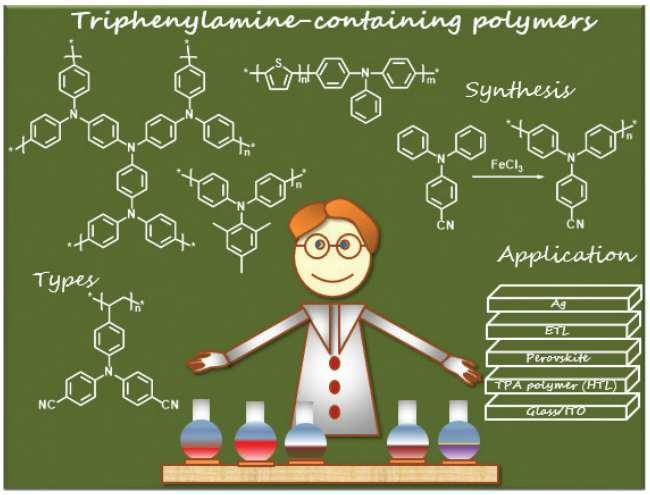

Keywords: poly(triphenylamine), TPA, donor–acceptor polymer, hole-transporting polymer, perovskite solar cell, organic light-emitting diode, sensor.

Contents

I.A.Chuyko. Junior researcher ISPM RAS. E-mail: chuyko@ispm.ru
Current research interests: organic electronics, organic synthesis, conjugated triphenylamine-based polymers, organic semiconductor materials.
P.A.Troshin. PhD, Head of Laboratory FRC PCP MC RAS.
E-mail: troshin2003@inbox.ru
Current research interests: organic electronics, organic synthesis, organic semiconductor materials.
S.A.Ponomarenko. Doctor of Chemistry, Corresponding Member of the Russian Academy of Sciences, Director at ISPM RAS.
E-mail: ponomarenko@ispm.ru
Current research interests: synthesis, research and development of organic and polymer semiconductors, luminophores, liquid crystals, self-assembling molecules and their application in various devices of organic electronics and photonics, including organic field-effect, electrochemical and light emitting transistors, solar cells, detectors and sensors based on them.
Yu.N.Luponosov. Doctor of Chemistry, Head of the Laboratory of Polymer Solar Cells ISPM RAS.
E-mail: luponosov@ispm.ru
Current research interests: development of semiconductor materials based on organic and polymeric conjugated molecules for organic and perovskite solar cells and photodetectors, organic light-emitting diodes, scintillators and various biomedical applications.

Translation: Z.P.Svitanko

Received 17 September 2024

1. Introduction

The development of organic electronics began in the 1960s when the first conducting polymer, polyacetylene, was synthesized as a dark powder.[1,2] In the 1970s, chemists succeeded in obtaining polyacetylene as a thin film. However, this conducting polymer could not be processed and was unstable in air.[3] Active research of semiconducting properties of π-conjugated polymers such as polythiophene, polypyrrole, and polyaniline started in the early 1980s.[4–6] This gave stimulus to further development of organic electronics. In 1987, an electroluminescent device was manufactured, in which organic oligomer materials were used as light-emitting elements.[7] In 1990, poly(*p*-phenylene vinylene) was synthesized and tested in a light-emitting diode, bulk heterojunction photovoltaic cell, and a solid-state laser.[8–10] This was followed by the discovery of the charge-transport properties of conjugated arylamines. They started to be used as hole-transport materials in various devices.[11,12] Polymers containing arylamine blocks were easier to process because of increased solubility and had enhanced mechanical properties.

As a rule, poly(triarylamine)s can be reversibly oxidized to form stable radical cations. Owing to this feature and to high stability in the environment, they have been actively investigated as hole-transport layers in organic and hybrid electronic devices. Conjugated polymers based on triphenylamine (TPA), particularly their simplest representative, poly(4,4′-triphenylamine) (**PTPA**), which were synthesized by Yasuhiko Ohsawa's group in 1991,[13] showed high thermal and morphological stability in combination with good hole-transport properties.[13] Further studies were directed toward the use of triphenylamine-based materials as hole-transport and electrochemically active layers in electrochromic devices[14,15] and charge-transport layers in organic light-emitting diodes (OLEDs) and organic field effect transistors (OFETs).[16–19]

Quite a few TPA-based hole-transport materials, ranging from low-molecular-weight compounds to polymers, have been studied over the past three decades.[20–24] The introduction of the propeller-shaped TPA block into molecules decreases π–π interactions and tendency for crystallization.[25,26] Materials of this type are, most often, amorphous and readily soluble and have high glass transition temperatures. An advantage of TPA-based polymers over similar low-molecular-weight compounds is that these materials are more thermally stable and have better film-forming and mechanical properties.[27–29]

Examples of simple and commercially available TPA-based polymers are poly[bis(4-phenyl)(2,4,6-trimethylphenyl)amine] (**PTAA**)[30,31] and poly(4-butylphenyldiphenylamine) (**poly-TPD**).[32,33] The **PTAA** and **poly-TPD** polymers are most commonly used as hole-transport layers in perovskite solar cells.[30,32,34–36] In the case of definite film deposition procedure and device optimization, these polymers as hole-transport materials show a relatively high hole mobility for amorphous materials equal to 4×10^{-3} cm^2 V^{-1} s^{-1} (measured by the OFET method).[30,32,37] However, their further application is restricted by the lack of possibility of fine tuning of their physicochemical properties, *e.g.*, phase transition temperature, light absorption and emission spectra, and energies of the frontier molecular orbitals, over wide ranges. Therefore, a relevant task for researchers specializing in this field is to design new molecular structures of TPA-based polymers with optimal characteristics. A possible way of molecular design and, as a consequence, tuning of polymer properties is the introduction of various electron-withdrawing groups into the monomer unit of homoconjugated polytriphenylamines[38,39] or the preparation of copolymers containing, apart from TPA, an additional electron-withdrawing aromatic group conjugated with TPA.[40]

Currently, there are a number of reviews addressing TPA-based polymers;[41–45] however, the diversity of these polymers has markedly expanded in recent years: new molecular designs, methods of synthesis, and applications appeared; this makes it difficult to navigate these issues even for specialists. Therefore, comprehensive analysis of the currently available publications in this field is required. Analysis of the data published mainly since 2010 would not only highlight the history of development of this field, but also give rise to the first classification of TPA-based polymers in terms of their chemical structure, methods of synthesis, and current applications. The present review considers TPA-based polymers of various structures ranging from simple homopolymers to cross-linked polymers, giving vivid examples illustrating both the early stage of development and the latest achievements; demonstrates ways for tuning the properties of these materials using various molecular design tools; and describes the main methods for their synthesis and the existing practical applications. Comparative analysis of the methods of synthesis of a representative series of TPA-based polymers would identify the benefits and drawbacks of each approach, while comparison of polymer properties would help to understand the key regularities in the variation of their characteristics depending on the chemical structure. The final chapter addressing the applications of the title polymers informs the reader about the modern promising areas in which these materials are used.

2. Types of triphenylamine-based polymers

Poly(triphenylamine)s are amorphous polymers possessing relatively high mobility of positive charges (holes), good thermal stability, and high glass transition temperature. They are readily soluble in various organic solvents and have good film-forming properties. The above features of poly(triphenylamine)s allow for their wide use as hole-transport layers in various optoelectronic devices.[41–45]

There are various types of triphenylamine-containing polymers. In this review, we propose a classification of these polymers, which is shown in Fig. 1. Among the polymers, it is possible to distinguish main groups, in which TPA blocks are incorporated into the backbone as repeating units: linear homopolymers[30,32,46–48] and copolymers[49–51] and polymers with a nonlinear architecture including branched[52–54] and cross-linked polymers.[55–57] Linear polymers, in which the TPA block is attached to the backbone as a side group, can be considered as a separate type.[58–60] Each type of the triphenylamine-containing polymers has advantages and disadvantages. The homopolymers are, most often, easily synthesized,[48] as their synthesis requires only one monomer, whereas the preparation of copolymers requires two or more monomers; this complicates the production of materials and increases their cost. Meanwhile, synthesis of the copolymers makes it possible to combine the properties of structurally different blocks, which significantly expands the possibilities of modification.[49] Branched TPA-based polymers, unlike the linear polymers, have a high free radical density and large surface area, which is favourable for charge transfer.[54] Most often, linear and branched polymers are readily soluble, unlike cross-linked polymers,[55] which is convenient for polymer processing and for the formation of polymer coatings and thin films from solutions. Poor solubility of cross-linked polymers can also be beneficial. For some devices, it is important that the

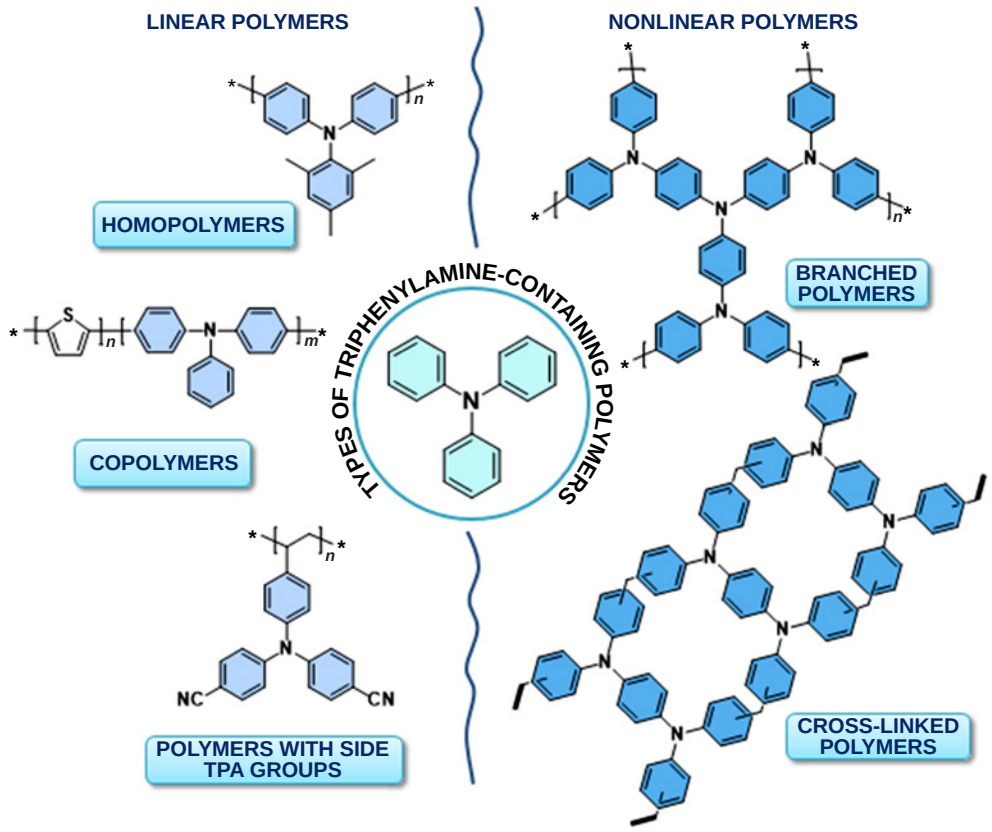

Figure 1. Classification of triphenylamine-based polymers.

functional layer deposited after the TPA-based polymer does not dissolve it during the deposition of the next layer from a solution. Films of poorly soluble cross-linked polymers can be deposited directly on the substrate of an optoelectronic device,[57] which facilitates the technique by decreasing the number of production stages. Polymers containing TPA side groups are usually prepared to improve the properties of a base polymer, for example, to increase the solubility or decrease the melting point and also to introduce one more hole-conducting moiety into the macromolecule. This Section addresses polymers of various structures: the ways of tuning the polymer properties are given and the structure–property relationships are analyzed.

2.1. Linear polymers

2.1.1. Homopolymers

The simplest representative of TPA-based homopolymers is poly(triphenylamine) PTPA[13] (structures **P1**–**P11**, **PTPA**, **PTAA**, **poly-TPD**). This polymer has no solubilizing groups in the macromolecule, which results in poor solubility and restricts the scope of its application. The solubility problem was solved by introducing various solubilizing groups into **PTPA**; *e.g.*, methyl or n-butyl groups in the most well-known and commercially available TPA-based homopolymers, **PTAA**[30,34–36] and **poly-TPD**.[32,61–64] These polymers are promising for industrial application in optoelectronic devices, owing to easy synthesis, amorphous structure, good solubility in a wide range of organic solvents, and relatively high hole mobility measured by the space charge limited current (SCLC) method ($3–4 \times 10^{-5}$ cm^2 V^{-1} s^{-1} for **PTAA** and 1×10^{-4} cm^2 V^{-1} s^{-1} for **poly-TPD**).[65,66] Over the last several years, the number of works using **PTAA** and **poly-TPD** as hole-transport layers (HTLs) has increased. However, **PTAA** and **poly-TPD** have some drawbacks related to the limited possibility of tuning the properties of materials, which are selected depending on the particular application of the polymers in specific devices. In particular, important characteristics of **PTAA** and **poly-TPD** that should be tuned are the energy levels of the highest occupied molecular orbital (HOMO) (–5.2 eV) and band gap (E_g) (~2.8 eV) and the light absorption spectra (in the 300–400 nm range).[30,32,33–36,61–64]

The properties of polymer materials based on triphenylamine can be tuned by a relatively easy, but still effective method, namely, by introducing various electron-withdrawing (EW) or electron-donating (ED) groups into the monomer unit. By introducing EW groups into the macromolecules, it is possible to vary the frontier molecular orbital levels, which determine the band gap width.[67] For semiconductors, E_g is an important value affecting the conductivity and the range of the light absorption and emission spectra.

For example, it was shown[68] that EW groups reduce the energy level of the highest occupied molecular orbital (HOMO) of the polymer and, conversely, ED groups increase this energy level. For example, the HOMO energy of the polymer containing the electron-withdrawing cyano group (**P1**) is –5.33 eV, which is lower than the HOMO energy of **PTAA** and **poly-TPD** by 0.17 eV. Conversely, the HOMO energy of polymer **P4** containing the electron-donating methoxy group increases to –4.89 eV compared to **PTAA** and **poly-TPD**.

The introduction of EW groups into the donor triphenylamine moiety can also be used to red-shift the absorption spectra of polymers. For example, as compared with **PTAA** the major absorption band of which (refers to the π–π^* transition) occurs in the range of 325–362 nm, analogous polymers **P1**, **P2**, **P3**, and **P5** show strong absorption bands corresponding to the intramolecular charge transfer in the range of 412–543 nm. In the series **PTAA** → **P1** → **P2** → **P3**, the band gap considerably

Structures P1–P11, PTPA, PTAA, poly-TPD

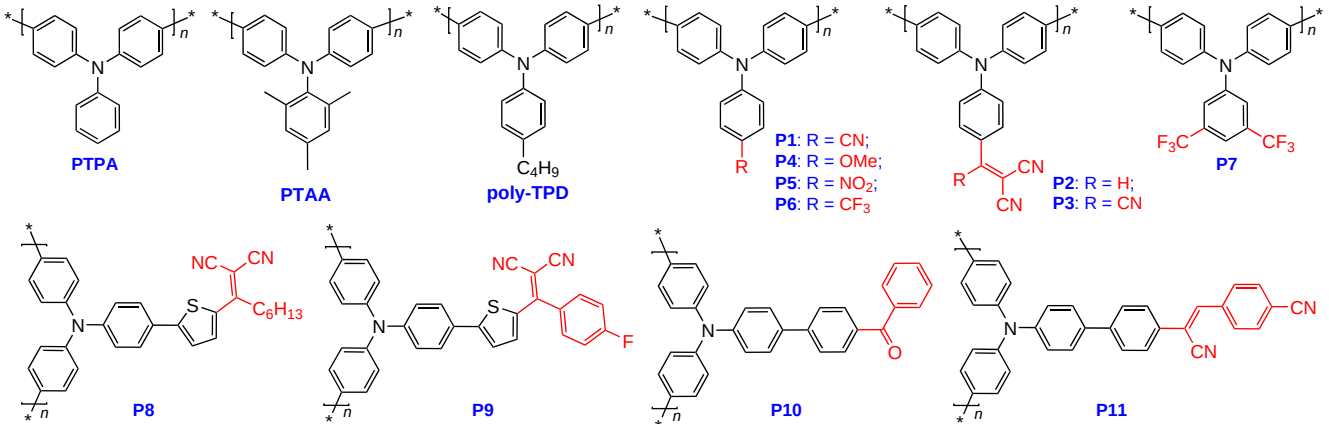

decreases from 2.98 to 1.72 eV with increasing number of cyano groups.[48]

Electron-withdrawing groups containing fluorine atoms are often used because they affect not only the HOMO energy, but also the lowest unoccupied molecular orbital (LUMO) energy,[69] and because of the steric factor, they can also shift the absorption spectrum to shorter wavelengths[70] and increase the solubility of target compounds.[71] Polymers **P6** and **P7** (Ref. 72) showed excellent solubility in DMF, chloroform, and THF, which enabled the preparation of thin films of these compounds by solution processing. They also exhibit luminescent properties and have a much higher glass transition temperature T_g (209–225°C) than **PTAA** (T_g = 73°C),[73] which can certainly expand the scope of applicability of poly(triphenylamine)s and improve the durability of devices based on them.

In order to enhance the conjugation in the molecule, ED and EW groups are linked to each other *via* a conjugated π-spacer, for example, 1,4-phenylene or 2,5-thiophene one. The introduction of a conjugated π-spacer between the ED and EW groups in the molecule leads to a decrease in the HOMO energy and the band gap width and to a red shift of the absorption bands.[74–76] For example, TPA-based homopolymers containing electron-withdrawing alkyldicyanovinyl groups connected to TPA through 2,5-thiophene π-spacers have recently been obtained. The synthesized polymers **P8** and **P9** had high thermal stability (the degradation temperature reached 558°C for **P9**), reversible electrochemical reduction, HOMO levels of –5.37 and –5.35 eV, and relatively low E_g = 2.00 and 1.93 eV, respectively; the absorption edges (λ_{edge}) reached 617 and 641 nm. For comparison, in the case of polymer **P2** containing the electron-withdrawing dicyanovinyl group directly connected to TPA, λ_{edge} = 535 nm.[48] Also, the hole mobility of **P8** and **P9** measured by the SCLC method amounted to 2.1×10^{-5} and 7.5×10^{-5} cm^2 V^{-1} s^{-1}, respectively.[27,77]

Another example of TPA-based D–A polymers containing a π-spacer between ED and EW groups was reported by Sun and Liang.[78] The polymers have a 1,4-phenylene spacer in the molecules and differ by the presence of keto (**P10**) or cyano (**P11**) electron-withdrawing group. Polymer **P10** shows two absorption peaks at 255 and 384 nm, which were assigned to π–π* transitions and intramolecular charge transfer, respectively. Both absorption bands slightly change upon variation of the solvent polarity. Polymer **P11** also exhibits two absorption bands at 329 nm and in the range from 400 to 417 nm. The latter band, unlike the bands of **P10**, is blue-shifted from 417 to 400 nm with increasing solvent polarity, which implies that **P11** has a more pronounced intramolecular charge transfer even in the ground state due to the strong electron-withdrawing properties of the CN group. Both polymers show luminescence behaviour. The photoluminescence spectra were measured in various solvents. The spectra of **P10** are red-shifted from 480 to 564 nm on going from a low-polarity solvent (toluene) to polar solvents such as acetonitrile and DMF, while a more pronounced red shift of luminescence in the 552–647 nm range is observed for **P11** upon increase in the solvent polarity. The difference between the solvatochromism observed in the photoluminescence spectra is related to the difference in the dipole moments of the macromolecules. Evidently, the dipole moment of **P11** is greater due to the presence of stronger EW substituent (cyano group) compared to that of **P10**, in which the EW properties are provided by a carbonyl group.

2.1.2. Copolymers

The addition of EW groups or conjugated π-spacers into the monomer unit is often insufficient to attain the desired characteristics of the polymers such as the optimal HOMO and LUMO levels, light absorption or emission in a particular spectral region, high decomposition and glass transition temperatures, *etc*. Therefore, researchers pay attention to another class of TPA-based macromolecules, that is, copolymers in which the chemical structure makes it possible to combine several different building blocks with diverse properties in one molecule. As an example, let us consider some recent studies dealing with the TPA-based copolymers.

For example, well-known poly(3-hexylthiophene) (P3HT), which has useful optical and electrical properties and good solubility in organic solvents, has a drawback of having poor oxidation stability at high temperatures. In order to increase the stability of P3HT, Nakashita *et al*.[49] synthesized a copolymer of 3-hexylthiophene with triphenylamine (**P12**), because poly(triphenylamine) derivatives are more stable against oxidation at high temperatures.[79,80] The loss of mass of P3HT starts at 325°C, and at a temperature of 450°C, the coke residue amounts to 40%. Copolymer **P12** demonstrates excellent thermal stability, particularly, the loss of mass by this polymer is less than 5% at 400°C in air. This result demonstrated that the presence of TPA in the polymer backbone markedly improves the thermal stability of the copolymer.

Like those of TPA-based homopolymers, the properties of the copolymers can be tuned by introducing EW groups into their macromolecules. The EW group can be represented by one of the monomers, which is most often the case. More rarely, the

Structures P12–P22

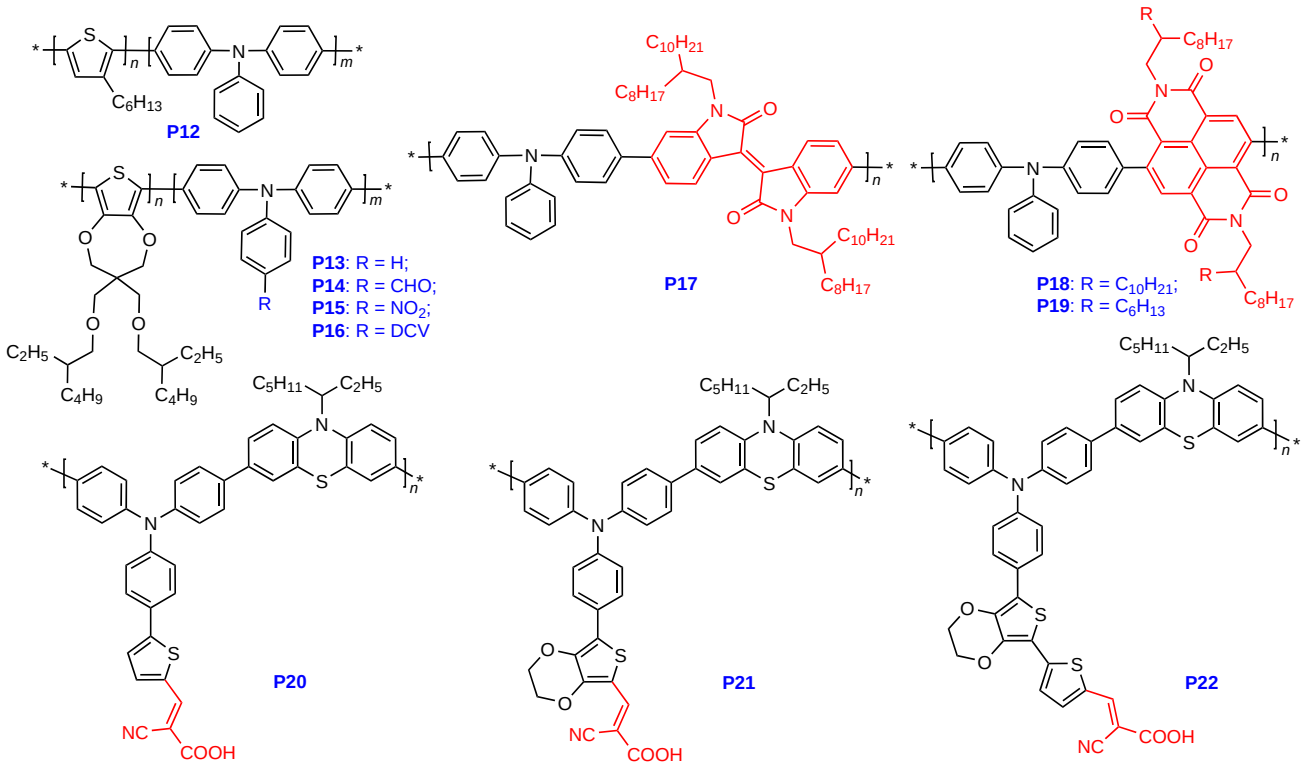

properties of these copolymers are tuned by attaching EW side groups to a TPA benzene ring. For example, Mi *et al*.[50] obtained a series of copolymers (**P13**–**P16**) based on triphenylamine and thiophene with EW groups of various strengths in the TPA *para*-position, namely, carbonyl (CHO), dicyanovinyl (DCV), and nitro (NO_2) groups. The use of EW groups in TPA resulted in a substantial decrease in the LUMO energy from –2.67 eV (**P13**) to –3.27 eV (**P16**), but barely affected the HOMO energy. This, in turn, induced a gradual decrease in E_g from 2.71 eV (**P13**) to 2.29 eV (**P16**). Owing to the long alkoxy groups at the thiophene unit, all of the polymers had good solubility in organic solvents and were able to produce thin films of acceptable quality by solution processing.

Wang *et al*.[51] prepared copolymers based on the TPA electron donor and isoindigotin (**P17**) or naphthalene diimide (**P18** and **P19**) electron acceptor. By varying the electron-withdrawing properties and planarity of the acceptor blocks *via* the replacement of isoindigotin by naphthalene diimide, the molecular orbital energies of the conjugated polymers were changed. The HOMO energies of **P17**, **P18**, and **P19** were –5.57, –5.72, and –5.65 eV, while the LUMO energies were –3.68, –3.78, and –3.81 eV, respectively. Finally, the E_g values calculated from cyclic voltammetry (CV) data were 1.89, 1.94, and 1.84 eV, respectively. The introduction of a naphthalene diimide block also induced a red shift of the absorption spectrum compared to the spectra of the other two polymers described in that study, because of more pronounced electron-withdrawing properties. In dilute solutions, **P17** exhibits two absorption peaks at 326 and 580 nm, while **P18** and **P19** show two peaks at approximately 357 and 620 nm. The variation of alkyl groups from 2-octyldodecyl to 2-hexyldecyl improved the current–voltage characteristics of organic photovoltaic devices based on these polymers, which may be attributable to differences in the thin film morphology and molecular packing influencing the charge transfer efficinecy.[81,82]

Among both homopolymers and copolymers, there are examples in which the electron-withdrawing side group is attached to TPA through a π-conjugated spacer rather than directly. For example, Wang *et al*.[83] synthesized a number of conjugated polymers **P20**, **P21**, and **P22** based on poly(triphenylamine-phenothiazine) with EW cyanoacetic side chains. In this case, phenothiazine was chosen in order to increase the conjugation in the backbone of the macromolecule. The polymers have a conjugated side chain consisting of a thiophene unit (**P20**), which alternates with either 3,4-ethylenedioxythiophene (EDOT) (**P21**) or EDOT-thiophene (**P22**) as a π-spacer. As in the previous cases, the goal of this strategy is to adjust the frontier molecular orbital energy and to broaden and red-shift the absorption spectra of the polymers. The HOMO levels of **P20**, **P21**, and **P22** derived from CV data were –5.04, –5.03, and –5.15 eV, respectively. The addition of various π-spacers between the ED and EW blocks in order to increase the conjugation in the macromolecules affected the optical properties of polymers. All polymers exhibit two sharp absorption peaks: the peak at ~350 nm is due to the π–π* transition of conjugated polymer chains and the peak at ~500 nm corresponds to the intramolecular charge transfer between the ED polymer backbone and the EW side groups. The two-band absorption is typical of compounds composed of conjugated D–A type chains. The absorption peaks of **P22** are red-shifted relative to those of **P20** or **P21**. This effect can be attributed to elongation of the π-spacer when the EDOT-thiophene unit is used rather than thiophene or EDOT alone. Meanwhile, the absorption spectrum of **P21** is virtually not red-shifted compared to that of **P20**, which is apparently due to the fact that the π-spacers in these polymers have the same length.

2.1.3. Polymers with triphenylamine side groups

One more group of triphenylamine-containing polymers include polymers with TPA side chains. The backbone of these polymers

Structures P23–P30

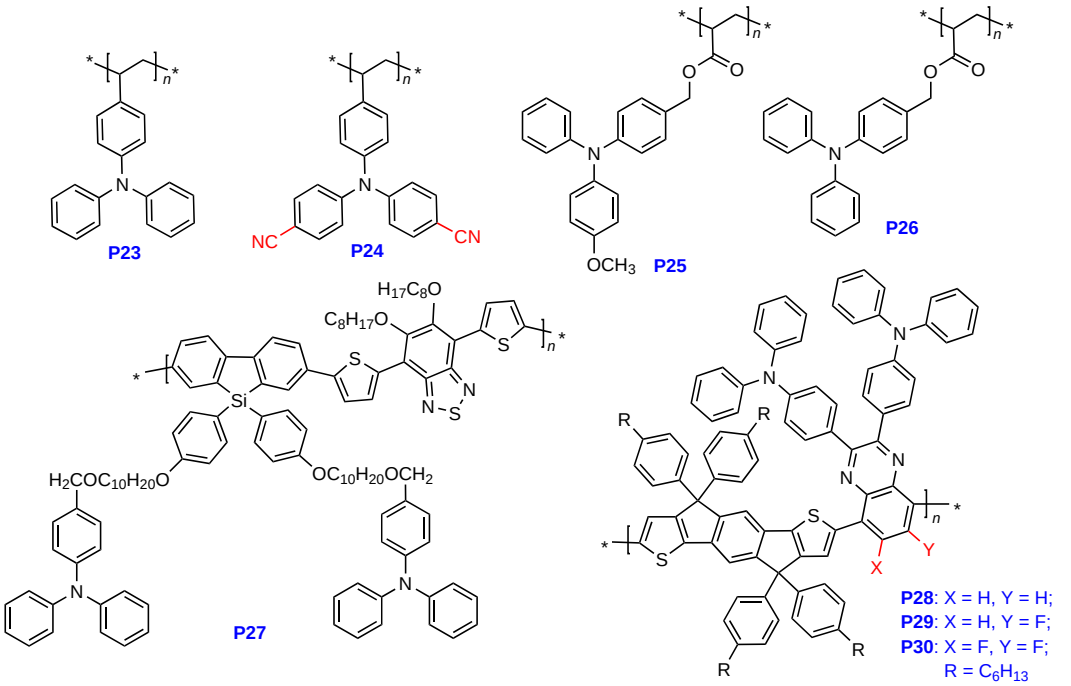

may be composed of either non-conjugated[58–60] or conjugated[84,85] units. In the former case, polymers are meant to combine the mechanical properties of known polyolefins, synthesized by radical polymerization widely used in industry, with the conducting properties of triphenylamine. In the latter case, TPA is more often introduced as an additional hole-transporting block.

A few vivid examples of polymers with TPA side chains are presented below. Fang *et al.*[58] prepared two polyolefin-based homopolymers: **P23** containing TPA groups and **P24** in which the TPA group is substituted with two EW cyano groups. Polymer **P24** has higher degradation temperature T_d (404°C) and glass transition temperature T_g (211°C) than **P23** (T_d = 387°C, T_g = 140°C) due to the presence of EW cyano groups, which enhance the intermolecular interactions. The peaks in the absorption spectra of **P23** and **P24** are located at 306 and 353 nm, while the emission peaks are at 437 and 429 nm, respectively. Both polymers exhibit luminescence, but the luminescence quantum yield in films is much higher for **P24** than for **P23**: 20.3% *vs*. 3.7%. The HOMO energy level in **P24** is –5.63 eV, which is 0.28 eV lower than that of **P23**. This HOMO energy level of **P24** promotes more efficient hole injection and improves the performance of the iridium-containing phosphorescent OLEDs investigated by Fang *et al.*[58]

Polyacrylate-based polymers with TPA side groups (**P25** and **P26**)[60] were prepared for photorefractive (PR) devices. The photoconductive TPA-containing polymers **P25** or **P26** serve as a dispersion matrix for other components and provide a charge transfer medium. The desired properties of a photoconductive polymer used in such devices include high hole mobility, high HOMO energy, and low T_g, which favours better reorientation of the chromophore in the composite. If the polymer has a high glass transition temperature, a plasticizer is added to the composite.[86] Polymers **P26** and **P25** have relatively low T_g (75 and 74°C, respectively). In this case, polyacrylate backbone was chosen exactly to reduce T_g and to obtain a low-viscosity polymer. The introduction of methoxy groups into **P25** shifts the HOMO level from –5.69 to –5.57 eV.[60]

Among the copolymers, there are also compounds in which TPA is a side group at the conjugated backbone of the macromolecule. Lian *et al.*[84] synthesized a copolymer based on 2,7-silafluorene and 5,6-bis(octyloxy)-4,7-di(thiophen-2-yl)-benzo[*c*][1,2,5]thiadiazole decorated with triphenylamine side groups (**P27**). In this design, triphenylamine groups endow the material with a lower melting temperature and higher solubility in most organic solvents. This influences the miscibility of the material in thin films with other organic semiconductors, which is important, for example, to achieve an optimal morphology in the photoactive layer of organic solar cells. In addition, in these polymers, TPA groups can form channels for efficient hole transport.

Lee *et al.*[85] reported another example of D–A conjugated polymers with TPA side groups containing different numbers of fluorine atoms: **P28**, **P29**, and **P30**. As the ED unit, the authors chose 4-hexylphenyl-substituted indacenodithiophene, because this rigid planar structure facilitates the charge transfer. The second monomer used as a basic block to form the EW unit is quinoxaline with two TPA side groups. The appearance of TPA in this copolymer induces additional charge transfer in the vertical direction towards the EW quinoxiline unit, together with the horizontal charge transfer from the ED unit of the copolymer. The hole mobility of monofluorinated **P29**, measured by the SCLC method, was 1.62×10^{-3} cm^2 V^{-1} s^{-1}, which was higher than that of **P28** (1.27×10^{-3} cm^2 V^{-1} s^{-1}) or **P30** (1.47×10^{-3} cm^2 V^{-1} s^{-1}). The mobility data proved to be comparable with those of commercial **PTAA**. The HOMO levels in fluorinated polymers **P29** and **P30** were at –5.24 and –5.30 eV, which is lower than that of non-fluorinated reference polymer **P28** (–5.20 eV).

2.2. Non-linear polymers

2.2.1. Branched polymers

The next group of TPA-based polymers are polymers consisting of branched macromolecules.[52–54,87] Branched

Structures P31–P38

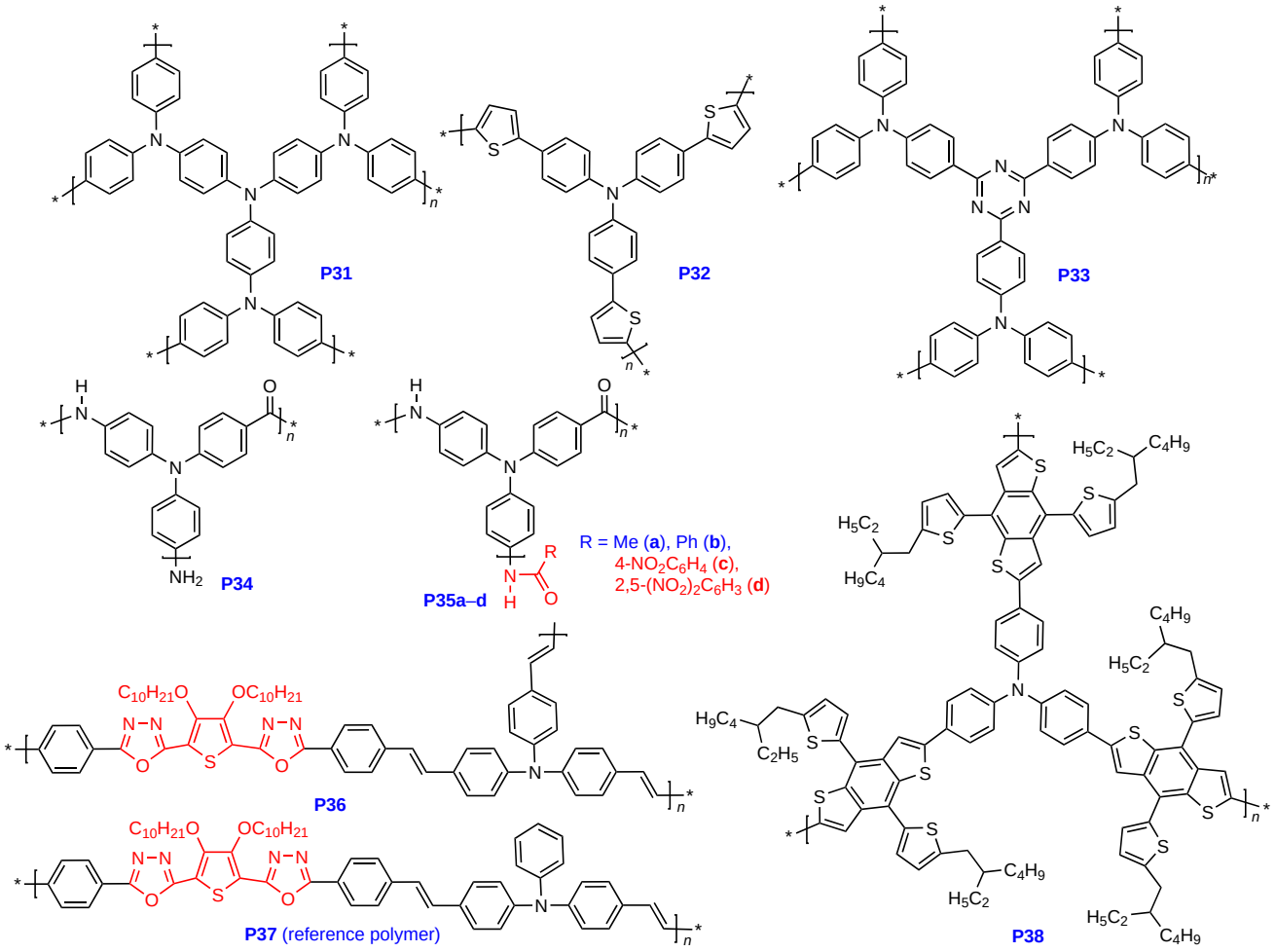

polymers have a set of interesting properties. For example, they can be used to obtain meso- or microporous materials.[54,88,89] Conjugated microporous polymers have attracted a lot of attention owing to their high specific surface area, small pore size (<2 nm), and high chemical and thermal stability in harsh environments. These polymers are often used as electrode materials for metal-ion batteries. Owing to their large specific surface area, microporous organic polymers possess enhanced electrochemical activities.

Branched polymers **P31** (Ref. 54) and **P32** (Ref. 88) have specific surface areas of 561 $m^2 g^{-1}$ and 594 $m^2 g^{-1}$, respectively, which is two orders of magnitude greater than that of linear **PTPA** (5.6 $m^2 g^{-1}$).[90,91] The branched polymer structure can provide enhanced electrolyte diffusion and may ultimately improve the performance of lithium-ion batteries, for example, increase the specific capacity, which is 143.5 mAh g^{-1} for **P31** *vs*. 109 mAh g^{-1} for linear **PTPA**.[54] The synthesized triazine-containing micro/mesoporous polymer **P33** (Ref. 89) has an even greater specific surface area (930 $m^2 g^{-1}$). As a cathode material for lithium-ion battery, compound **P33** showed a stable capacity of ~123 mAh g^{-1}.

Furthermore, some branched polymers are readily soluble in organic solvents; therefore, solution methods can be used to fabricate functional layers based on them.[92] It is known that aromatic polyamides have excellent thermal, mechanical, and chemical properties. However, the rigidity of molecules and strong hydrogen bonds result in high melting temperatures or glass transition temperatures and sparing solubility of polymers in most organic solvents. One of the methods for improving the solubility is to prepare these polymers with a branched structure and with a TPA block as the aromatic unit. For example, Wang *et al*.[93] synthesized branched polymers **P34** and **P35a–d**, readily soluble in a number of solvents such as *N*-methyl-2-pyrrolidone (NMP), dimethylacetamide (DMA), DMF, and DMSO. The branched polymers **P35a–d** are of interest due to the fact that they contain different EW and ED terminal groups that affect optical, electrochemical, and thermal properties of the materials. The photoluminescence of these branched polyamides is blue-green emission in the 430–510 nm range. Poly(triphenylamine amide) with the electron-withdrawing *p*-nitrobenzene terminal group emits at the shortest wavelength of 433 nm, while poly(triphenylamine amide) with the strong electron-donating amino terminal group (**P34**) has the longest-wavelength emission at 505 nm. The band gap width of the polymers with different terminal groups is approximately 2.93 eV irrespective of the terminal groups, since the absorption of these polymers occurs in the same spectral region, with peaks being at 354–358 nm. Meanwhile, the HOMO and LUMO energy levels do depend on the terminal groups. Polymer **P34** with ED amino groups is characterized by the highest HOMO and LUMO energies (–4.99 and –2.07 eV, respectively). Conversely, the polymer **P35c** containing the EW *p*-nitrobenzene terminal group demonstrates the lowest energies of HOMO (–5.34 eV) and LUMO (–2.42 eV). The presence of terminal groups influences the thermal properties of the polymers. Polymer **P35b** with a phenyl terminal group proved to be the most thermally stable: its

degradation temperature for a mass loss of 5% was 338°C, while that for polymer **P34** was 270°C.

Among the branched copolymers, one can also find D–A polymers, *e.g.*, branched conjugated polymer **P36**,[94] which contains TPA and 3,4-didecyloxythiophene units as electron donors and 1,3,4-oxadiazole units as electron acceptors. The introduction of the 1,3,4-oxadiazole ring into the polymer backbone enhances the polymer ability to transfer electrons. The properties of the resulting branched polymer were compared with those of analogous linear polymer **P37**. Both polymers had a good thermal stability; however, the temperature of the degradation onset proved to be higher for **P36** (375°C) than for **P37** (325°C). While comparing the optical properties, note that the absorption maximum for **P36** films (λ_{max} ~ 560 nm) is red-shifted compared to that of **P3** (λ_{max} ~ 510 nm). In addition, **P36** has a smaller band gap than **P37**. This may be due to the branched structure of **P36**, which increases the conjugation in the polymer. Polymers **P36** and **P37** also exhibit luminescent properties. The emission maximum of **P36** is red-shifted compared to that of **P37** by approximately 30 nm. The colour of the emitted light changes from yellow for **P37** to orange for **P36**. The HOMO (LUMO) energy levels estimated from CV data were –5.33 (–3.73) eV and –5.20 (–3.74) eV for **P37** and **P36**, respectively. The high HOMO levels and the low LUMO levels are caused by the alternating arrangement of the ED and EW units along the polymer chain. The E_g values amount to 1.60 (**P37**) and 1.47 (**P36**) eV. These D–A conjugated polymers containing strong ED and EW units are promising for the use in optical and photonic devices.

One more interesting example of branched polymer based on TBA and benzo[1,2-b:4,5-b′]dithiophene (BDT) is **P38**.[95] BDT has a symmetrical and planar structure, which is favourable for stronger π–π interactions and for ordered packing of molecules, thus facilitating the charge transport. This polymer has a relatively narrow band gap of 1.69 eV, with the HOMO and LUMO levels being –5.29 and –3.60 eV, respectively. The thermal stability of the polymer is relatively high (T_d = 385°C). It is worth noting that thin films of **P38** exhibit a fairly high hole mobility, which varies depending on the annealing temperature. Organic field-effect transistors with the active layer made of **P38** as an encapsulated top gate/bottom contact were fabricated to measure the hole mobility. The highest attained hole mobilities were 2.08×10^{-4} cm^2 V^{-1} s^{-1}, 1.22×10^{-3} cm^2 V^{-1} s^{-1}, 1.02×10^{-3} cm^2 V^{-1} s^{-1}, and 7.28×10^{-4} cm^2 V^{-1} s^{-1} at 0°C, 100°C, 150°C, and 200°C, respectively, which is comparable with the hole mobility of commercially available **PTAA** and **poly-TPD**.

2.2.2. Cross-linked polymers

Cross-linked polymers based on TPA are also promising materials for organic and hybrid electronics. The poor solubility or lack of solubility of cross-linked polymers in organic solvents and electrolytes allows the production of strong films resistant to dissolution. Therefore, they can be used as functional materials for the fabrication of organic and hybrid electronic devices, in which successive deposition of layers by solution-based methods is required, as the cross-linked polymer layer cannot be washed away or corroded during the deposition of a subsequent layer from a solution.

Perhaps, of most interest is the use of cross-linked TPA-based polymers as organic electrodes for metal-ion batteries because of their resistance to direct contact with the electrolyte, which improves the stability of batteries during the charge/discharge cycling. For example, films of cross-linked polymer **P39** (Ref. 55) retain the initial morphology after a few charge and discharge cycles, indicating that the cathode based on this compound is free from clear structural damages or breaks. The capacity of the battery in which **P39** is used as the cathode remains high (125 mAh g^{-1}) even after 100 cycles. Strong and solvent-resistant films of polymers **P40** (Ref. 56) and **P41** (Ref. 57) proved to be promising for the hole-transport layers of OLEDs. Polymer **P41** has a HOMO energy level of –5.30 eV, while the HOMO energy level of **P40** is –5.16 eV. The HOMO

Structures P39–P43

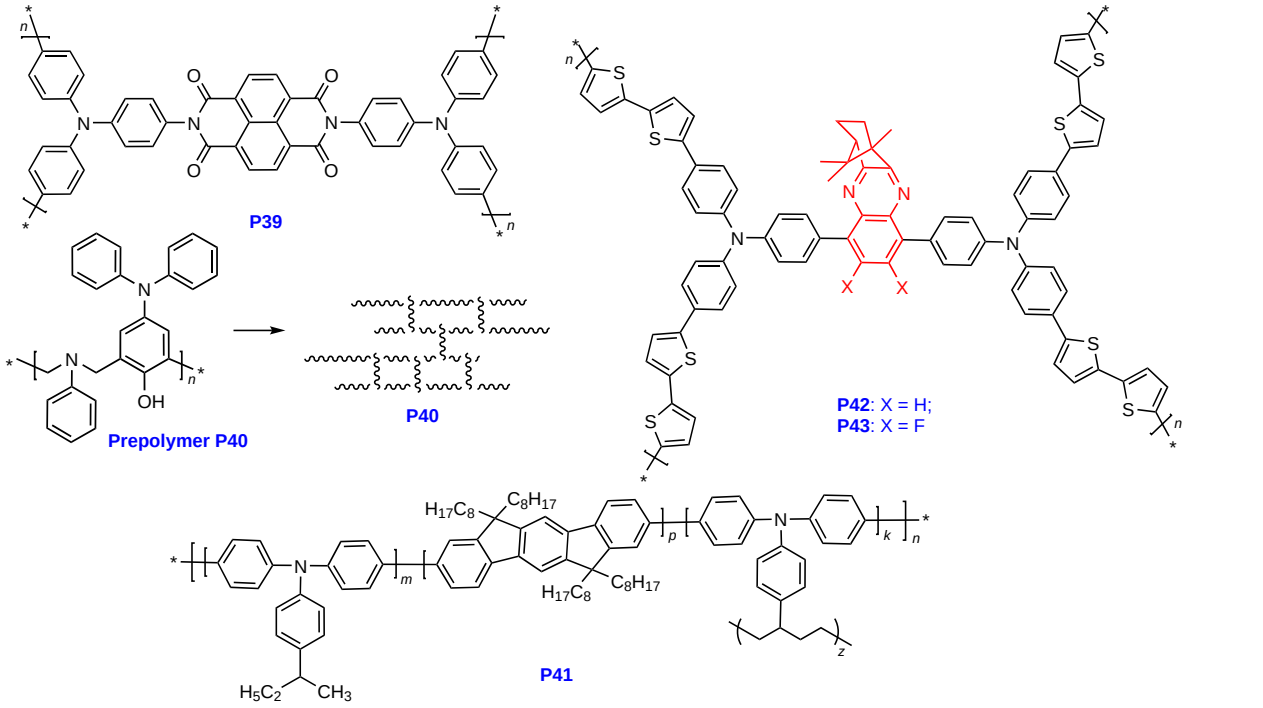

energy levels of these polymers indicate that they can perform hole injection and transport from the anode to the emission layer. The cross-linked polymer structure can enhance the charge transport properties. This fact was demonstrated in relation to polymer **P40** and its monomer (**16**) (the structure is presented in Scheme 10 in Section 3.3) used in ITO/HTL/Al devices. The current density was higher for the device using **P40** than in the case of monomer **16**, which implies higher capacity for hole injection/transport in the former case. It should be noted that the HOMO energy levels for monomer **16** and **P41** are almost identical (–5.17 and –5.16 eV, respectively). Hence, the hole injection/transport performance is largely related to the formation of the cross-linked structure.

The D–A cross-linked polymers **P42** and **P43** for electrochromic devices were obtained by electrochemical polymerization of the monomers on the ITO surface.[96] Using D–A type polymers, it is possible to attain high optical contrast and short response time in combination with the longer cycling stability and high specific capacity. Polymers **P42** and **P43** showed noticeable colour changes with a considerable optical contrast in both visible and infrared regions. The polymers exhibited electrochromic switching from light yellow to blue-grey colour with high optical contrast, fast response time, high colouration efficiency, and robust cycling stability. Both polymers provided high specific capacitance (12 mF cm^{-2} for **P42** and 9.97 mF cm^{-2} for **P43**) for a current density of 0.1 mA cm^{-2}. Efficient electrochromic energy storage devices based on these polymers have been fabricated. These devices not only powered a red LED for 25 s, but also showed obvious colour changes during the charge/discharge process.

Thus, to summarize this Section, it can be concluded that there is a wide range of triphenylamine-based polymers, each of which has certain benefits and drawbacks. Considering the target application of TPA-based polymers, researchers can select the desired structure that would be the most suitable.

3. Methods for the synthesis of triphenylamine-based polymers

The design of functional polymers based on TPA is an actively developing field of materials science. An integral part of these studies is the search for versatile and scalable methods for the synthesis of polymers, which in turn enable the design of new efficient and inexpensive functional materials for practical applications.

Usually, in the first step of the polymer synthesis, triphenylamine monomers are prepared.[97] There are various methods for the synthesis of triphenylamines. Among them, the Ullmann or Buchwald–Hartwig coupling reactions are used most frequently for this purpose.[98,99] The reactions differ in the bases, solvents, and catalysts they involve. The Ullmann amination (Goldberg reaction) is the Cu(I)-catalyzed reaction of aryl halides with amines in the presence of a base. In the Buchwald–Hartwig C–N cross-coupling, nickel or palladium complexes with suitable ligands are used as the catalysts instead of copper. Currently, TPA is a cheap and commercially available substrate. Triphenylamine derivatives (in particular, monomers) are prepared using various reactions. For example, TPA-based monomers with EW groups can be synthesized by the Knoevenagel condensation of compounds containing active methylene groups with TPA carbonyl derivatives.[48] The attachment of various π-spacers to TPA is performed, most often, *via* the Suzuki[27] or Stille[99] cross-coupling reactions; branched monomers can be obtained by the Ullmann reaction.[98,99] The synthesis of monomers is mainly a trivial reaction and is described in detail in the papers surveyed in this review; therefore, we do not consider the synthesis of monomers in detail and pass to a more detailed discussion of the polymer synthesis.

Among the wide diversity of synthetic routes to triphenylamine-based polymers (Fig. 2), two main groups of reactions can be distinguished: cross-coupling and oxidative polymerization reactions. The C–C cross-coupling reactions include Suzuki, Stille, and Yamamoto polycondensations. The Ullmann and Buchwald–Hartwig polycondensations are classified as C–N cross-coupling. There are also other methods of synthesis such as Knoevenagel polycondensation, radical polymerization, Friedel–Crafts reaction, and thermal cross-linking.

Homopolymers and copolymers are obtained, most often, by chemical oxidative polymerization or Suzuki and Stille polycondensations.[48–51] Branched polymers based on TPA can be obtained by chemical and electrochemical oxidative polymerization or by cross-coupling reactions.[54,95,100] In the case of polymers with TPA side groups, radical polymerization is used.[58–60] Conjugated polymers in which TPA is a side group are also prepared by cross-coupling methods, *e.g.*, by the Stille polycondensation.[85] The most popular method for the synthesis of cross-linked polymers is thermal cross-linking;[56,57] however, cross-linked polymers are often prepared by oxidative polymerization.[55] The methods of synthesis are considered below in more detail in relation to the above TPA-based polymers.

3.1. Coupling reactions

A method for the synthesis of TPA-based polymers is based on coupling reactions (see Fig. 2), which include C–C cross-coupling reactions such as Stille,[50,85] Suzuki,[51,101] and Yamamoto[46,102] cross-coupling and Ullmann arylation[101,103] and the Buchwald–Hartwig C–N cross-coupling.[104–106]

An important and obvious requirement for the polymer synthesis by cross-coupling reactions is the presence of two or more bifunctional compounds, except for the Yamamoto reaction, which requires only one type of bifunctional compound. When monomers with more than two functional groups are used, cross-coupling can give branched or cross-linked polymers.

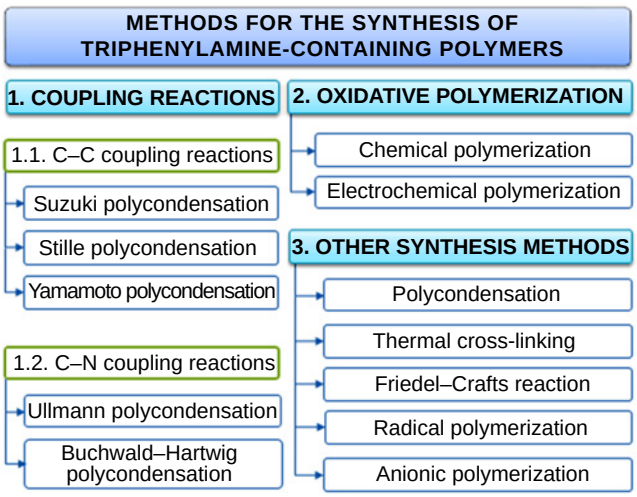

Figure 2. Synthetic routes to TPA-based polymers.

Scheme 1

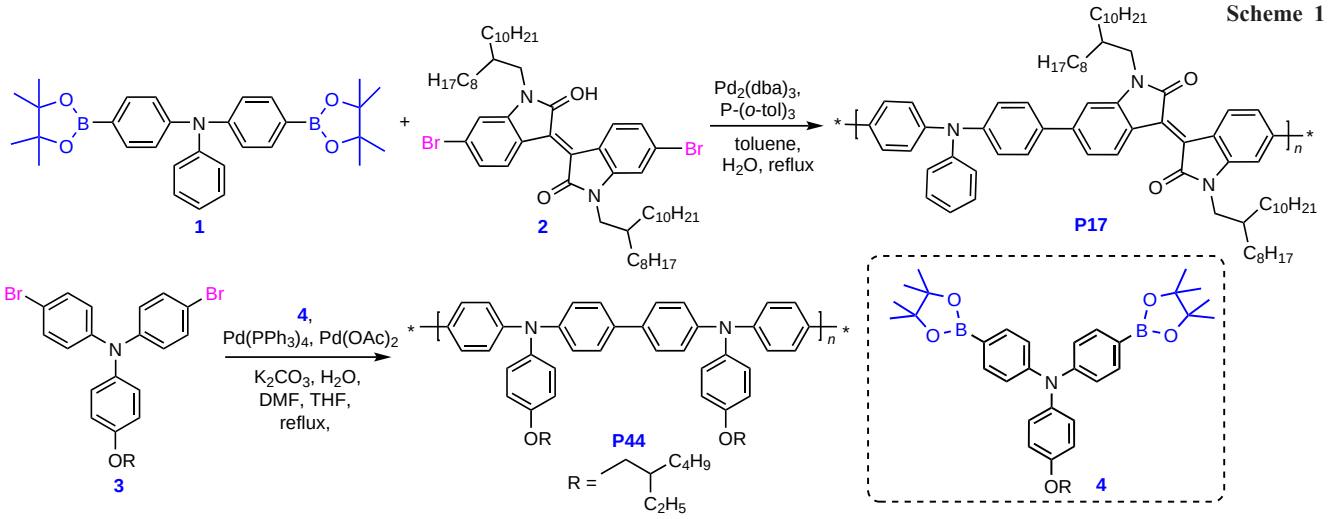

The Suzuki cross-coupling is a highly important reaction for the formation of C–C bonds, which is used to obtain π-conjugated polymers. The C–C bond formation by the Suzuki reaction has a number of benefits such as high yields of products under relatively mild reaction conditions, good reproducibility, high stereo- and regioselectivity, and the use of readily available reactants.[107] One monomer in this reaction is usually an organohalogen compound, while the other one is an organoboron compound. Organoboron compounds are markedly less toxic than organotin derivatives used in the similar Stille cross-coupling reactions. Furthermore, they have high thermal and chemical stability and are relatively inert to moisture and oxygen. These advantages make Suzuki cross-coupling one of the most potent tools for the synthesis of conjugated polymers.[31,107–111]

Section 2 of the review considers some polymers obtained by the Suzuki polycondensation, for example, series of polymers **P17**–**P19** (Ref. 51) or **P20**–**P22**.[83] Scheme 1 depicts the synthesis of TPA-based copolymers by this method. The copolymerization involved two monomers, one of which is TPA organoboron derivative (**1**) and the other is brominated isoindigotin (**2**). The reaction was carried out in the presence of *tris*(dibenzylideneacetone)dipalladium(0) $Pd_2(dba)_3$ and *tris*(*o*-tolyl)phosphine P(*o*-tol)$_3$ in toluene and water. The polymer was purified in a Soxhlet extractor and isolated in 66% yield. The number-average molecular weight (M_n) was 36.2 kDa and the polydispersity index ($Đ_M$) was 3.2.[51]

In the case of synthesis of TPA-based homopolymers, only TPA-based monomers (**3**, **4**) are used, but they differ in the type of functional groups. For example, homopolymer **P44** was synthesized in THF in the presence of aqueous K_2CO_3 solution as a base and DMF using palladium catalysts, *tetrakis*-(triphenylphosphine)palladium $Pd(PPh_3)_4$ and palladium(II) acetate $Pd(OAc)_2$ (see Scheme 1).[112] After purification, the product yield was 66% [M_n = 10.3 kDa, weight-average molecular weight (M_w) is 15.8 kDa].

The catalytic system and the solvent are important factors for the Suzuki polycondensation. They have a pronounced effect on the cross-coupling product yield and molecular-weight characteristics. The polycondensation of triphenylamine derivatives described in the literature is performed, most often, with catalytic systems such as $Pd(OAc)_2/PPh_3$ and $Pd_2(dba)_3$/P(*o*-tol)$_3$.[109] The standard solvents for Suzuki polycondensation are toluene, THF, or 1,2,4-trichlorobenzene, but the choice of solvent is usually dictated by the solubility of the reactants and products.

An alternative to the Suzuki reaction is the Stille cross-coupling. In the previous Sections, we described polymers obtained by this method, namely, copolymers **P13**–**P16** (Ref. 50) and polymers with TPA side groups **P28**–**P30**.[85] Branched polymers, for example **P38**, can also be prepared in this way.[95] An example of Stille polycondensation is shown in Scheme 2. The reaction was carried out between *tris*(4-bromophenyl)amine (**5**) and *bis*(trimethyltin)-4,8-*bis*[5-(2-ethylhexyl)thiophen-2-yl]benzo[1,2-b;4,5-b']dithiophene (**6**) in the presence of $Pd(PPh_3)_4$ in a mixture of dry DMF and dry toluene (the product yield was 76%; M_n = 11.8 kDa, M_w = 22.7 kDa).

In the Stille reaction, an organotin compound reacts with an organohalogen compound in the presence of a palladium catalyst to give a new C–C bond. Organotin compounds are more stable than organoboron compounds. This advantage makes it possible to prepare polymers with higher molecular weights and narrower molecular weight distributions. One more advantage of the Stille polycondensation is the absence of bases, which could affect the reactivity and stability of the monomers sensitive to an alkaline medium.[113,114]

A significant problem faced by the Stille polycondensation is the toxicity of tin-containing monomers. Improper handling and disposal of these compounds can cause environmental pollution and be harmful to human health. In addition, it is difficult to completely remove the remaining tin-containing impurities from the final products and chemical ware.[115] One more problem, which is, by the way, also inherent in the Suzuki polycondensation, is the presence of phosphine ligands in the catalytic system. They are sensitive to air and water, expensive, and toxic, although still less toxic than organotin compounds.[114,116]

An important issue concerns the stoichiometry of the Stille and Suzuki cross-coupling reactions. To achieve high molecular weights, a precise stoichiometric balance between the monomers is needed. This requires monomers with a high degree of purity, which necessitates additional purification. Furthermore, under cross-coupling conditions, some monomers may be involved in the side homocoupling reactions, which may give rise to defects in the main chain of conjugation, thus affecting the properties of the resulting polymers. An additional difficulty is to purify the product from the palladium catalyst, because the remainder of the catalyst is known to affect the electronic properties of the

Scheme 2

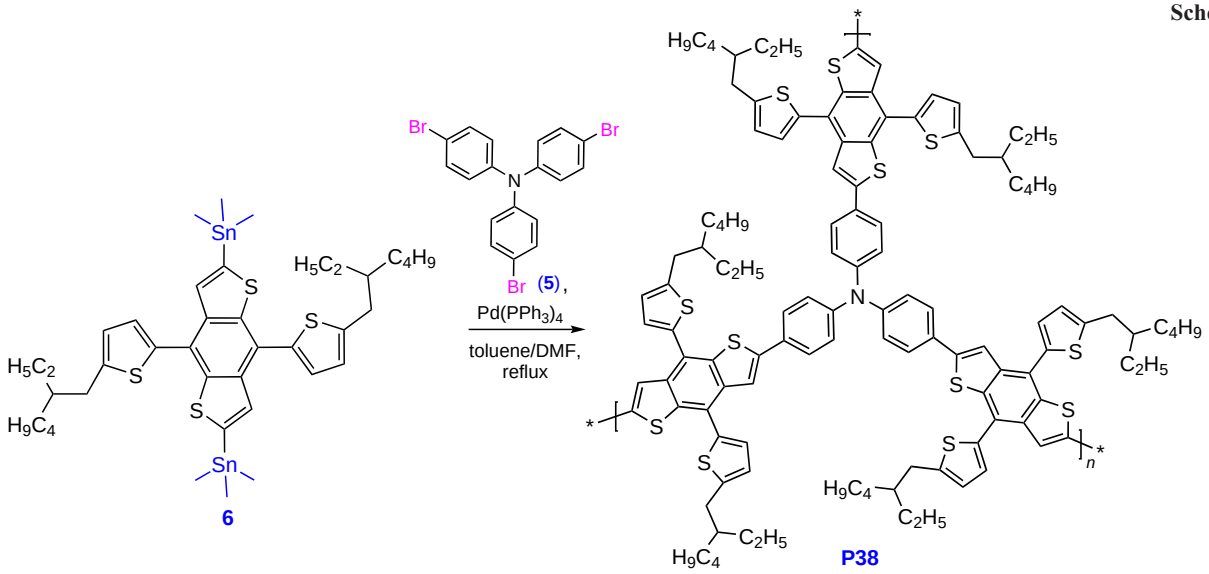

final product. It is noteworthy that both the Suzuki and Stille polycondensations require removing of the terminal functional groups that influence the properties and stability of the target polymers. This is usually achieved by blocking the terminal groups with a monofunctional halogen-, tin-, or boron-containing compound such as *p*-bromobenzene and phenylboronic acid.[114–116]

Using different catalytic complexes, it is possible to vary the molecular weight of polymers. For example, it was shown that the palladium catalyst $Pd(PPh_3)_4$ often used in the Stille polycondensation is susceptible to oxidation, resulting in the formation of Ph_3PO, which inhibits the polycondensation reaction. In one study, this catalyst was replaced by more stable dichlorobis(tri-*o*-tolylphosphine)palladium(II) $PdCl_2[P(o\text{-}Tol)_3]_2$, which promoted the formation of high-molecular-weight (M_w = 48.4 kDa, M_n = 47.3 kDa) polymers based on TPA containing 1,2,3-benzotriazole and thiophene moieties.[113] In some cases, the length of polymer chains is controlled by varying the duration of synthesis. For example, carrying out the Stille polycondensation for 4, 24, and 48 h was accompanied by increasing M_n. This gave poly(triphenylamine-2,2′-bithiophene) polymers with cyanoacrylic acid moieties as acceptors with M_n of 1.7, 2.9, and 3.5 kDa, respectively.[117]

One more way to produce conjugated polymers is the Yamamoto polycondensation.[46,102,118,119] As mentioned above, the advantage of this reaction is that only one type of monomer, a bifunctional halogen-containing monomer, is needed for the Yamamoto cross-coupling, unlike the Stille or Suzuki polycondensations, which additionally require the presence of monomers with tin- or boron-based functional groups. However, in this method, it is very important to maintain the stoichiometry of compounds incorporated in the cross-coupling catalytic complex.

The Yamamoto reaction is usually catalyzed by nickel complexes. A popular catalytic system is a solution of *bis*(1,5-cyclooctadiene) nickel(0) $Ni(COD)_2$, 1,5-cyclooctadiene (COD), and 2,2′-bipyridine (BPY) in THF.[46,102] *Bis*(1,5-cyclooctadiene) nickel(0) and BPY are used in a slight excess with respect to 1,5-cyclooctadiene.[118] Alternatively, a catalytic system consisting of $NiCl_2$, BPY, and zinc dust can be used. In this case, the nickel complex with BPY is formed *in situ*.[119] In some cases, DMF is employed as a solvent. Zinc dust, which serves as a reducing agent, should be taken in a large excess. In some cases, apart from these components, triphenylphosphine is added and DMA serves as the solvent.[120]

An example of preparation of triphenylamine-based polymers by the Yamamoto polycondensation is shown in Scheme 3. Polymers **P45a**–**c** were obtained by adding the monomers in THF to a solution of the catalyst consisting of $Ni(COD)_2$, COD, and BPY in dry THF.[102]

Scheme 3

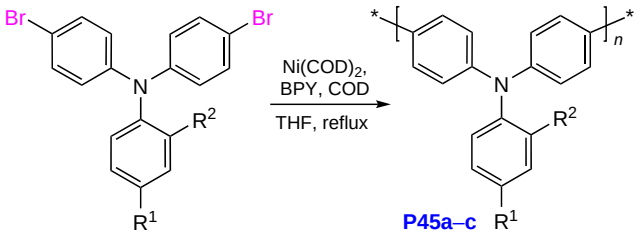

P45a: R^1 = CH_3, R^2 = CH_3; 51% yield, M_w = 17.6 kDa, 1.94 $Đ_M$;
P45b: R^1 = F, R^2 = CH_3; 52% yield, M_w = 25.0 kDa, 1.90 $Đ_M$;
P45c: R^1 = F, R^2 = F; 53% yield, M_w = 27.9 kDa, 2.00 $Đ_M$

An alternative method for the synthesis of polymers by the C–C cross-coupling is *N*-arylation, *e.g.*, the Ullmann (Goldberg reaction)[103] or Buchwald–Hartwig amination.[104–106] These reactions are also classified as C–N cross-coupling.

The Ullmann reaction is used more rarely to obtain triphenylamine polymers than the Suzuki or Stille polycondensations. The classical copper-catalyzed Ullmann reaction between a secondary diamine and a diiodide[121] at high temperatures of about 200°C is unsuitable for the preparation of some polymers, since in this case, numerous side reactions take place to give insoluble oligomeric products. An example of Ullmann synthesis of TPA-based polymers[103] is shown in Scheme 4. Three TPA-based polymers were synthesized from stoichiometric amounts of *N*,*N*′-diphenylbenzidine (**7**) and the corresponding bis(iodophenoxy)alkanes **8a**–**c** in the presence of copper metal and K_2CO_3 and 18-crown-6 in dry *o*-dichlorobenzene (*o*-DHB). After purification, poly[*bis*(triphenylamine) ethers] **P46a**–**c** were isolated in more than 80% yields (M_n varied from 8 to 15 kDa, M_w was from 50 to 60 kDa.

One more synthetic approach to TPA-based polymers is the Buchwald–Hartwig C–N cross-coupling.[104–106] Typical components of these reactions include palladium catalysts,

Scheme 4

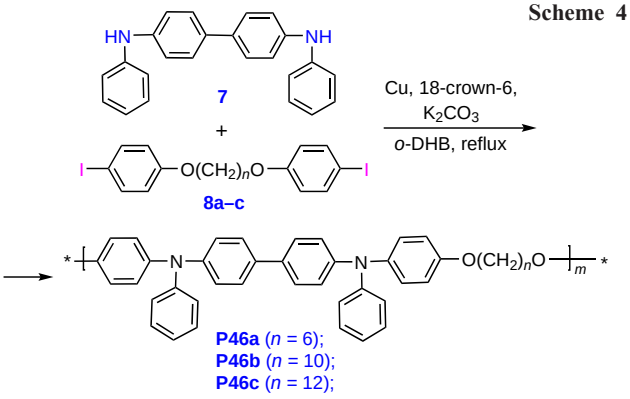

$Pd(dba)_2$ or $Pd(OAc)_2$, phosphine ligands such as dicyclohexyl[2′,4′,6′-*tris*(propan-2-yl)[1,1′-biphenyl]-2-yl]-phosphane (XPhos) or *tris*(*tert*-butyl)phosphine PBu^t_3, and sodium *tert*-butoxide $NaOBu^t$; most often, toluene is used as the solvent. Polymer **P47** was synthesized in this way from *tris*(4-bromophenyl)amine **10** and 2,6-diaminoanthra-9,10-quinone **11** in 75% yield (Scheme 5).[106] No data on the polymer MW are given, probably, due to the poor solubility of the cross-linked polymer.

3.2. Oxidative polymerization reactions

Oxidative polymerization is another method to prepare conducting polymers based on arylamines. The oxidative polymerization of arylamines can be induced by various oxidants such as $S_2O_8^{2-}$, $Cr_2O_7^{2-}$, ClO_3^-, VO_3^-, MnO_4^-, IO_4^-, H_2O_2, Ce^{4+}, Fe^{3+}, Cu^{2+}, Ag^+, or hydrogen tetrachloroaurate(III) $H[AuCl_4]$.[122] A commonly used oxidant is iron(III) chloride (Refs 27, 33, 48, 49, 54, 55, 88, 89, 123–128). It is applicable to the synthesis of TPA-based polymers of all classes described in the review: homopolymers,[27,33,48,123–125,129] copolymers,[49,126,127] branched polymers containing triphenylamine units,[54,88,89,128] and even cross-linked polymers.[55] The simplicity of synthesis and the use of available $FeCl_3$ oxidant make this method least costly,[33] unlike the cross-coupling reactions, which require expensive palladium catalysts,[31] or the same oxidative polymerization, but using the complex CuCl(OH)TMEDA oxidant.[130]

The procedure of oxidative polymerization has a significant effect on the polymer yield, molecular weight, and the amount of soluble fraction. A number of publications[123–125] describe the synthesis of TPA-based polymers (Scheme 6) containing various alkyl substituents (**P48a–c**) or the electron-donating methoxy group (**P48d**) using chloroform as the solvent. It was noticed that when the catalyst is added in the beginning of the reaction, a heterogeneous system is produced, resulting in the formation of an oligomeric product. The formation of a high-molecular-weight product requires fractional supply of the catalyst at 1-hour intervals during the reaction.[109–111] The additional feeding of iron(III) chloride to the reaction mixture may also be attributed to the fact that the catalyst is partly soluble in chloroform, while formation of the polymer requires a heterogeneous system. Moreover, hydrochloric acid released upon the polymerization reacts with $FeCl_3$ to give iron(III) complexes and thus decreases the content of the active oxidant in the system.[131]

Scheme 6

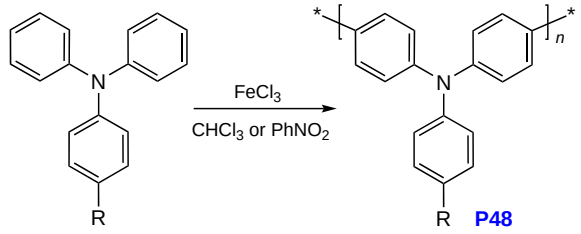

P48: R = CH_3 (**a**), Bu^t (**b**), Bu^n (**c**), OCH_3 (**d**), CN (**e**), NO_2 (**f**)

Takahashi *et al.*[123] demonstrated that the product yield and molecular weight are influenced by the $FeCl_3$/monomer molar ratio. It was found that at a low ratio equal to 2 : 1, no high-molecular-weight product is formed. When the ratio is too high (5 : 1), a large amount of gel fraction is produced; this implies cross-linking of macromolecules or attainment of too high molecular weight. As a result, the amount of insoluble fraction of the polymer increases under these conditions and the resulting polymer cannot be investigated or used in practice. According to this study, the optimal $FeCl_3$ to monomer ratio was 4 : 1.[123]

Study of the effect of temperature and reaction time on the polymer molecular weight[123] demonstrated that low temperature (30 to 40°C) does not provide high MW of the polymer even when the reaction time is long. Meanwhile, at 60°C, high molecular weight and high yield (>96%) of the soluble polymer were attained in 4 h, while longer reaction times at this temperature led to gelation of up to ~96% and low molecular weight.

One more, less common, solvent used in the oxidative polymerization is nitrobenzene.[27,125] It was used, for example, to prepare triphenylamine polymers (**P48e–f**) containing an electron-donating methoxy group and electron-withdrawing cyano and nitro groups (see Scheme 6). In this case, the reaction was carried out for 18–24 h at room temperature, with the polymer MW being controlled by introducing electron-withdrawing groups. The EW groups effectively increase the rate of oxidative coupling, as they increase the oxidation potentials and decrease the electrochemical stability of molecules. Thus, conjugated polymers with cyano

Scheme 5

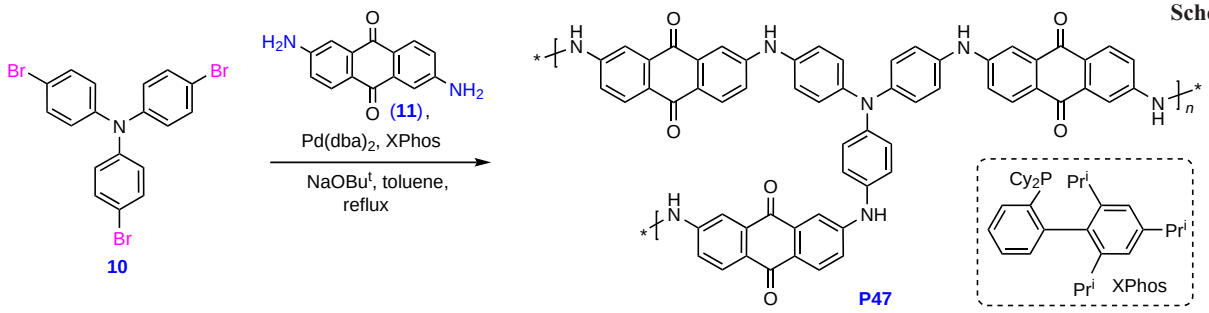

(M_w = 26.2 kDa, M_n = 14.4 kDa) and nitro groups (M_w = 1260 kDa, M_n = 365 kDa) have markedly higher molecular weights that the polymer with a methoxy group (M_w = 3.3 kDa, M_n = 1.9 kDa).[125]

The oxidative polymerization can be induced not only by chemical reagents (oxidants),[122,132] but also by electrochemical methods (electrochemical polymerization).[100,133–136] The electrochemical polymerization is often used for simultaneous polymer synthesis and fabrication of films on the electrode surface. The electrochemical polymerization technique allows the polymer to form a layer with high adhesion on the electrode surface. Electropolymerization considerably decreases the time of experiment and usually can solve the solubility problem arising when the traditional solution-based methods are used to fabricate the polymer films. The production of polymers by electrochemical polymerization can also be regarded as a green method, because the monomer oxidation is controlled by the voltage and current and does not require the use of a solvent or catalyst and their subsequent disposal.[137] This method is often employed to obtain triphenylamine-based branched polymers,[100,134,138] cross-linked polymers,[139–141] and, in some cases, linear homopolymers[142,143] from the corresponding monomers. For example, in the synthesis of polymer **P49** (Scheme 7), the electropolymerization was carried out on ITO-coated glass plates using a 1 mM solution of monomer **12** in a toluene–acetonitrile mixture (4 : 1 v/v) containing 0.1 M tetrabutylammonium hexafluorophosphate ($NBu^n_4PF_6$). The polymer layer on the electrode surface was formed *via* 30 successive oxidation–reduction cycles in the potential range from 0 to 1.7 V. Polymers **P50** and **P51** were prepared in the same way[143] (see Scheme 7).

A drawback of this method is the fact that upon electrochemical synthesis, various structural defects may appear in the conjugated polymer and doping counter-ions may remain in the product, which markedly deteriorates the properties of the resulting materials.[144–146]

Scheme 7

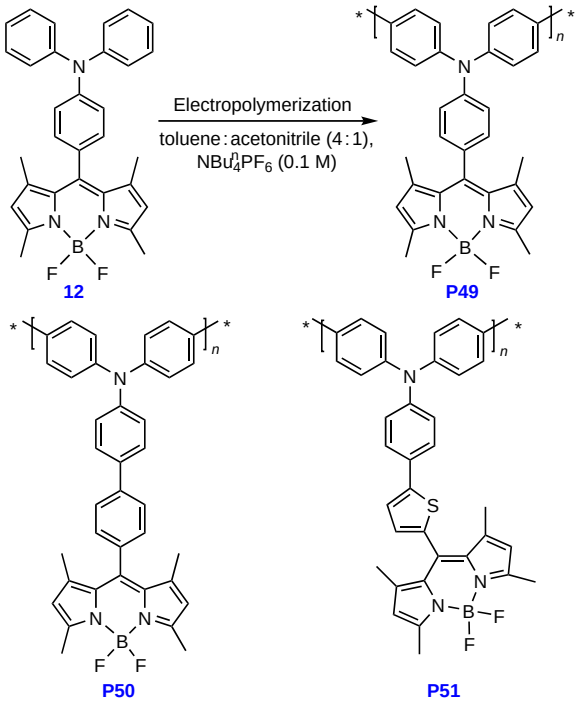

3.3. Miscellaneous methods for the preparation of triphenylamine-based polymers

Apart from cross-coupling and oxidative polymerization, there are also other methods for the preparation of triphenylamine-containing polymers. One such method is conventional polycondensation. At least from the environmental standpoint, the preparation of conjugated polymers by conventional polycondensation has advantages over the methods of synthesis described above. For example, the Knoevenagel condensation is sometimes used, in which an aldehyde group reacts with an activated methylene group in the presence of a base.[147,148] The methylene group is often activated using the EW cyano group.[149] The Knoevenagel polycondensation has a high potential for the synthesis of conjugated polymers for several reasons. First, the reaction does not involve organometallic reagents and, hence, the formation of toxic organic by-products is ruled out. The only by-product is water. Second, the Knoevenagel polycondensation does not require expensive catalysts based on noble metals or phosphorus-containing ligands; therefore, the total cost of the synthesis is lower. Third, the base used as a catalyst for the Knoevenagel polycondensation can be easily removed after the reaction and the catalyst impurity in the copolymer can be avoided.[147,150] The bases commonly used in the Knoevenagel polycondensation include tetra-n-butyammonium hydroxide (Bu^n_4NOH) or piperidine, while THF, ethanol, *tert*-butyl alcohol, and xylene are used as solvents.

This reaction also has drawbacks including the appearance of structural defects, which, in turn, deteriorates the optical properties of the obtained compounds[148] and the difficulty of achieving high molecular weight of the polymers due to the steric factor and the difficulty of precise control of the molar ratio between the two monomers.[151] Examples of the Knoevenagel polycondensation used to prepare TPA-based polymers[151] are presented in Scheme 8. Polymers **P52**–**P54** were obtained by the condensation of 4,4′-[(4-butylphenyl) imido]dibenzaldehyde **14** with *para*-, *meta*-, or *ortho*-phenylenediacetonitrile **13** in THF in the presence of $^nBu_4NOH$. The decrease in MW of polymers along the above series of isomers is mainly caused by steric hindrances.

Among the ways to produce TPA-based polymers, mention should be made of the formation of polyimides and polyamides.[93,152–154] For example, polycondensation reactions to produce TPA-containing polyamides involve aromatic dianhydrides and TPA derivatives containing amino groups in the molecules. Polymer **P55** was obtained in this way (Scheme 9). The polycondensation was conducted for piomellitic acid dianhydride (PMDA) and *N*,*N*-bis(4-aminophenyl)-

Scheme 8

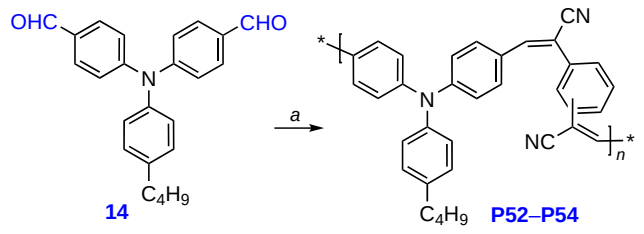

(*a*) NCH_2C–⟨⟩–CH_2CN (**13**: *p*-/*m*-/*o*-), Bu^n_4NOH, THF;
P52: *p*- (65% yield, M_n = 11.5 kDa, M_w = 31 kDa);
P53: *m*- (61% yield, M_n = 6.2 kDa, M_w = 14 kDa);
P54: *o*- (57% yield, M_n = 2 kDa, M_w = 3 kDa)

Scheme 9

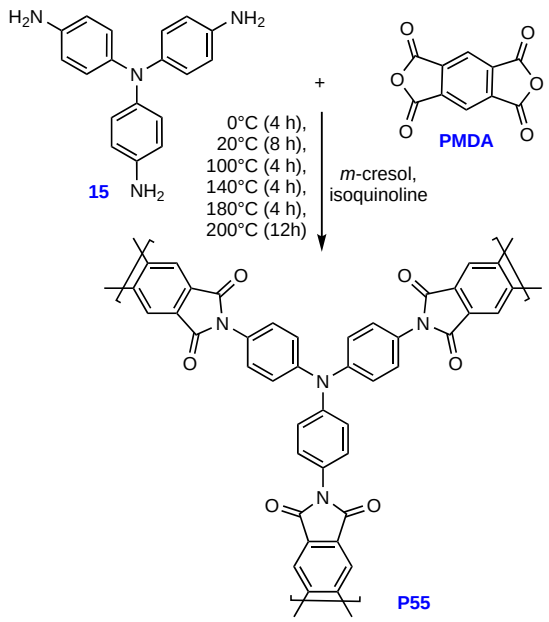

benzene-1,4-diamine (**15**) in *m*-cresol in the presence of isoquinoline as the catalyst. After purification, the target polymer was obtained in 64% yield.[153]

Cross-linked polymers are prepared by thermal cross-linking.[141,155] This approach was used, for example, to obtain polymers **P40** and **P41** (Scheme 10) described in Section 2.2.2.[56,57] This process gives strong films that are resistant to solvents. Polymer **P40** results from benzoxazine ring opening in monomer **16** on heating at 220°C for 30 min (see Scheme 10).[56] The thermal cross-linking is performed directly on the substrate of the device being manufactured; in this particular case, this was a glass substrate for OLED with the ITO/**P40**/NPB/Alq_3/LiF/Al structure,[†]

Scheme 10

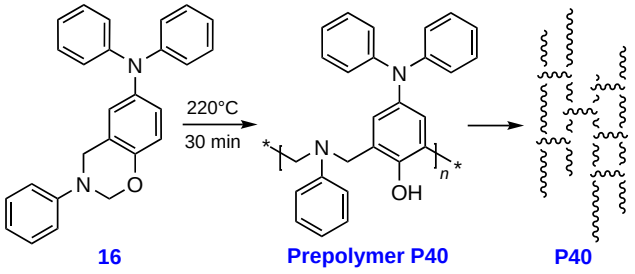

Polymer **P41** was synthesized by the Suzuki polycondensation, and the cross-linked polymer was formed after spin casting of copolymer films from a solution in chlorobenzene and subsequent thermal annealing of the film at 150°C for 24 min (Scheme 11).[57]

The thermal cross-linking can also be accomplished by treatment of monomers that have styrene terminal groups in the molecules. For example, two TPA-based derivatives **17** and **18** or two tetraphenylethylene-based derivatives **19** and **20** functionalized with terminal styrene groups were subjected to

Scheme 11

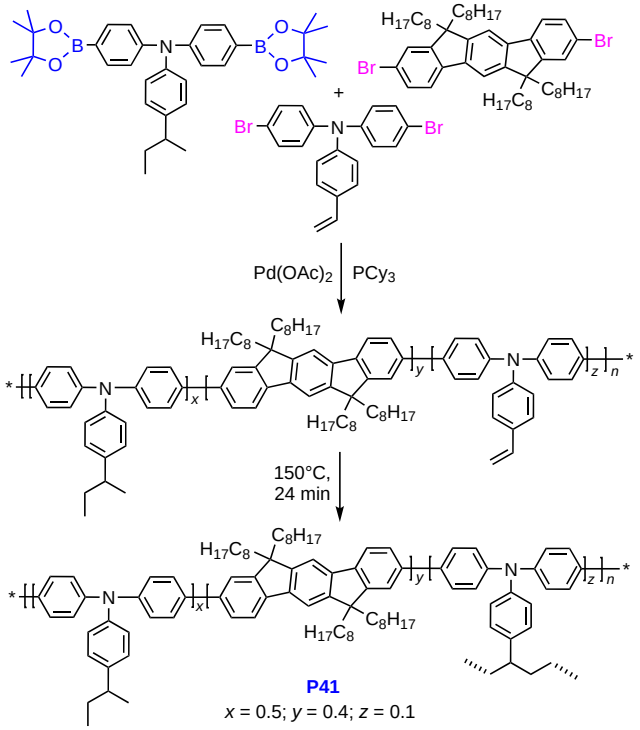

heat treatment to give cross-linked polymers **P56** and **P57** (Scheme 12).[156]

One more approach to the synthesis of TPA-based polymers is the Friedel–Crafts acylation. This gave microporous cross-linked polymers **P58**–**P60** (Scheme 13).[157] The polymers were prepared by the reaction of *N*,*N*,*N*′,*N*′-tetraphenylbenzene-1,4-diamine with cyanuric chloride, 1,4-dimethoxybenzene, and dimethoxymethane, respectively. Anhydrous $FeCl_3$ or $AlCl_3$ was used as the catalyst. The authors note that the structures of **P59** and **P60** can be more complex than those depicted in the Scheme because of the possible homocoupling and cross-linking reactions.

Considering polymers with TPA side chains such as **P23** and **P24** (Scheme 14), these polymers are mainly obtained by radical polymerization,[58–60] in this particular case, using benzoyl peroxide (BPO) as the initiator in the presence of 2,2,6,6-tetramethylpiperidin-1-oxyl (TEMPO).[58]

The molecular weight of these polymers can be controlled if living anionic polymerization is used instead of the radical polymerization (Scheme 15, polymer **P61**). In this case, *sec*-butyllithium or potassium naphthalenide is used to initiate polymerization in THF at –30 or –78°C. This procedure gives polymers with low $Đ_M \leqslant 1.12$.[158,159]

As can be seen, numerous methods are used for the synthesis of triphenylamine-based polymers. There are versatile methods that are suitable for the preparation of both homopolymers and copolymers and also branched and cross-linked polymers. These methods include Suzuki and Stille polycondensations and the oxidative polymerization. There are methods that make it possible to obtain the polymer directly on the substrate of a future device, which is especially relevant to the synthesis of branched and cross-linked polymers. In the former case, electrochemical polymerization is used, while in the latter case, thermal cross-linking is utilized. When choosing the method for the preparation of polymers, researchers usually proceed from the desired structure and also pay attention to the ease of synthesis,

[†] NPB is *N*,*N*′-di(1-naphthyl)-*N*,*N*′-diphenyl-(1,1′-biphenyl)-4,4′-diamine (hole-transport layer), Alq_3 is aluminium tris(8-hydroxyquinoline) (emitting layer and electron-transport layer) in which **P40** acted as the hole-injecting and hole-transport layer.

Scheme 12

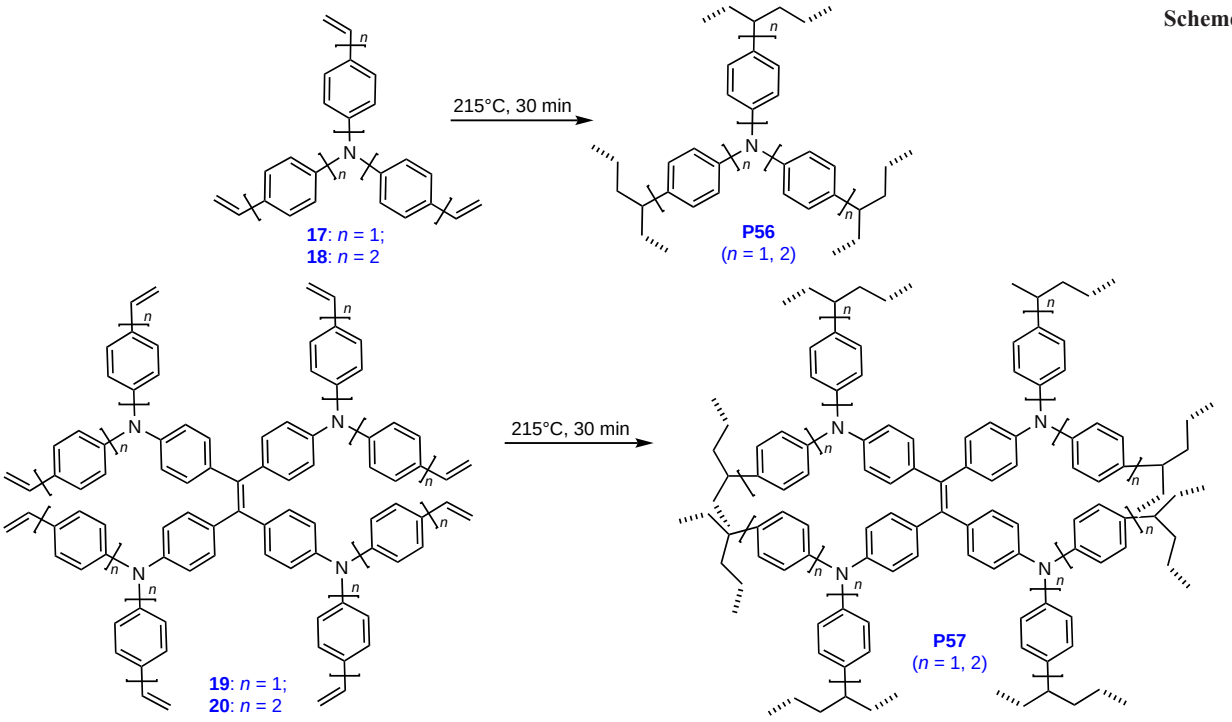

Scheme 13

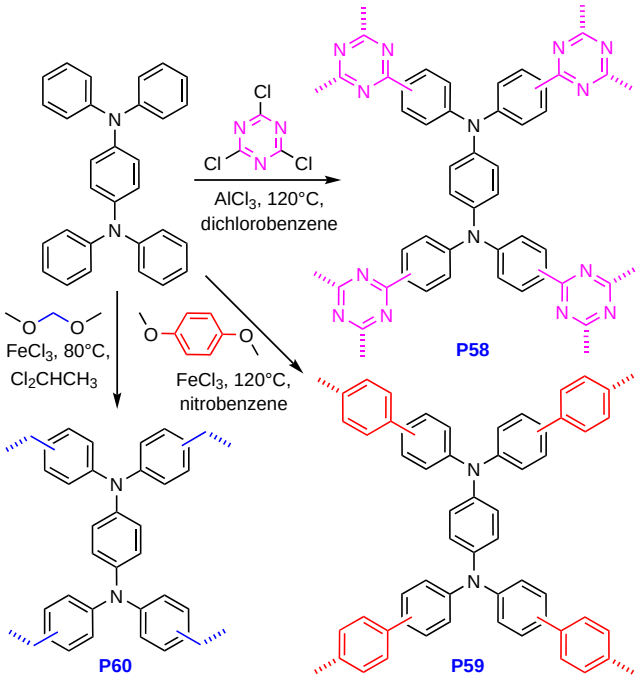

Scheme 14

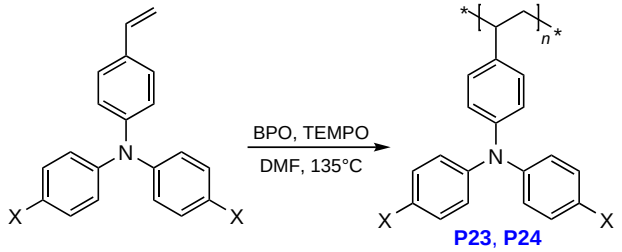

P23: X = H, M_n = 10200, $Đ_M$ = 1.27;
P24: X = CN, M_n = 23400, $Đ_M$ = 1.24

Scheme 15

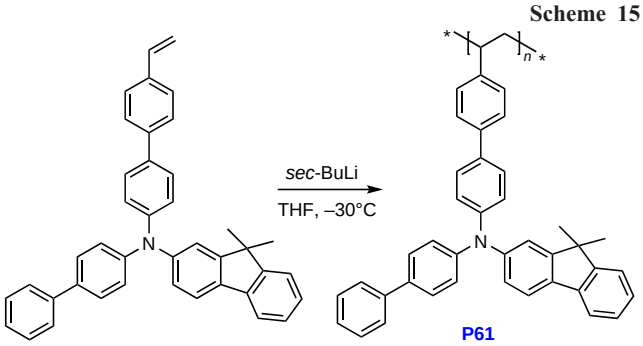

availability and toxicity of reagents, reproducibility, and the ease of purification of the products. The oxidative polymerization in the presence of $FeCl_3$ is perhaps the most versatile and accessible method for the synthesis of triphenylamine-based polymers.

4. Applications of triphenylamine-based polymers

The electron-donating properties of TPA derivatives, which are attributable to the presence of nitrogen lone pairs of electrons, make it possible to use the materials based on these compounds as hole-transport layers (HTLs).[160–163] It is known that HTLs play a crucial role in achieving high performance and long service life of various optoelectronic devices.[164] Owing to the simple synthesis and easy modification of TPA derivatives and the possibility of fine tuning of various characteristics of materials based on them,[165–167] they can be used as HTLs in perovskite solar cells (PSC), electrochromic devices, and OLEDs. The electron-rich nature of triphenylamine also enables the use of this material as an organic cathode for metal-ion batteries, *i.e.*, for electrochemical energy storage and for the design of high-performance memory devices.[168,169]

4.1. Perovskite solar cells

In recent decades, the attention of researchers has been drawn to the methods for efficient conversion of solar energy that could replace traditional fossil fuels.[170–173] Perovskite solar cells are photoelectric systems that certainly mark the most significant breakthrough in photoelectric technologies since the 1970s.[174] A typical cell structure of a perovskite solar battery is shown in Fig. 3. A basic perovskite solar cell consists of a film of perovskite material sandwiched between two electrodes.[165,175] However, additional layers are used to improve the stability and efficiency of these devices. In recent years, the attention of researchers has been focused on the search for appropriate hole-transport materials, which not only provide the transport of positive charges from the perovskite layer to the anode, but also prevent direct contact between the perovskite and the metallic electrode, thus minimizing charge recombination and preventing degradation processes at the metal–perovskite interface.[176] Hole-transport materials (HTMs) should meet certain criteria. They should be thermally and photochemically stable, and their HOMO energy level should be slightly higher than that of the active layer to provide for efficient hole transport. For example, top of the valence band of perovskite materials such as $MAPbI_3$ and $(FAPbI_3)_{0.85}(MAPbBr_3)_{0.15}$[‡] are –5.40 and –5.65 eV, respectively, whereas HOMO energy levels for poly(triphenylamine)s, which are often used as hole-transport layers in combination with perovskites, range from –5.50 eV to –5.10 eV. Hole-transport materials should possess a reasonable hole mobility for effective charge transfer to the electrode. Most often, the hole mobility varies from 10^{-3} to 10^{-5} $cm^2\ V^{-1}\ s^{-1}$. A good solubility of the polymer is also desirable to ensure good film-forming properties; furthermore, if the polymer layer is deposited over the perovskite layer, the solubility in orthogonal (usually non-polar) solvents is important. In order to avoid phase transitions during the device operation, polymers must have high T_g (>100°C).[177] In this Section, we consider relevant examples of such HTLs and analyze how the structure of polymers affects their performance as HTLs and output parameters of perovskite solar cells.

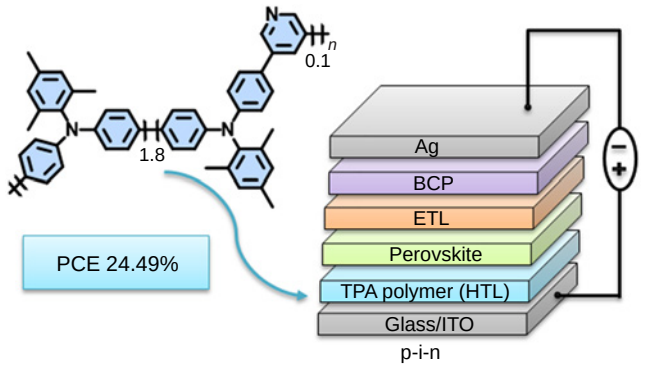

Figure 3. Structure of a perovskite solar cell. Designations: ITO is indium tin oxide (anode), HTL is the hole-transport layer, ETL is the electron-transport layer, BCP (bathocuproine or 2,9-dimethyl-4,7-diphenyl-1,10-phenanthroline) is the hole-blocking layer, Ag is the silver cathode, PCE is power conversion efficiency.

[‡] The perovskite has a structure ABX_3, where A is a monovalent cation [caesium, methylammonium (MA^+), or formamidinium (FA^+)], B is the divalent metal cation (Pb^{2+}), and X is halogen (Cl^-, I^-, or Br^-)

TPA-based polymers are promising hole-transport materials for perovskite solar cells.[31,33,73,109,178,179] Power conversion efficiency of PSCs using commercially available **PTAA** as HTL is as high as 23.8%,[30] which makes them comparable with traditional silicon-based solar cells. However, to attain high PCE for these **PTAA**-based PSCs, additional components are required to enhance the charge transfer efficiency. Traditionally, lithium *bis*(trifluoromethanesulfonyl)imide (LiTFSI) and 4-*tert*-butylpyridine (*t*-BPy) are used as dopants for this purpose; they increase the hole conductivity of **PTAA** and decrease the HOMO level down to the top of the valence band of perovskites (–5.4 to –5.9 eV).[180–182] However, the introduction of LiTFSI deteriorates the stability of devices and decreases the adhesion of **PTAA** to the substrate.[180,181,183] 4-*tert*-Butylpyridine has a low boiling point (196°C); therefore, it is volatile and unstable at elevated temperatures during the manufacture and long operation.[184] Also, *t*-BPy is corrosive: it reacts with PbI_2, and this causes chemical decomposition of the perovskite film.[185] Therefore, researchers look for new structures of triphenylamine hole-transport materials that would have high efficiency in perovskite solar cells without any dopants.[186]

A lot of efforts have been made to develop new polymer HTMs, but most PSCs based on undoped triphenylamine polymers showed PCE around 12–18%,[187–190] in some cases, PCE was 20%,[33,191–193] and only in few studies, PCE of more than 20% were attained.[194–197] The enhancement of performance of the device by an optimal combination of molecular orbital energy levels, hole mobility, layer morphology, and stability of the triphenylamine polymer is still a challenging and relevant task. A potent strategy for the design of highly efficient polymeric semiconductors is the use of conjugated D–A polymers.[198–201]

Table 1. HOMO and LUMO energy levels, hole mobilities of TPA polymers and PCE for PSCs with HTLs based on TPA polymers.

Polymer	HOMO, eV	LUMO, eV	μ, $cm^2 \cdot V^{-1} \cdot s^{-1}$	PCE (%)	Ref.
PTAA	–5.20	–1.80	4.00×10^{-3}	18.10 (23.80)	30, 45, 210, 211
Poly-TPD	–5.40	–2.40	1.00×10^{-4}	19.24 (22.10)	62, 65, 212
P62	–5.44	–2.45	2.00×10^{-3}	14.40	201
P63	–5.52	–2.49	3.00×10^{-4}	11.10	201
P64	–5.26	–2.35	9.07×10^{-5}	18.54	194
P65	–5.28	–2.42	3.51×10^{-4}	21.00	194
P66	–5.49	–2.41	3.89×10^{-4}	17.60	203
P67	–5.50	–2.46	6.66×10^{-4}	19.23	203
P68	–5.53	–2.54	9.44×10^{-4}	22.30	195
P69	–5.22	–2.25	1.95×10^{-4}	24.49	196
P70	–5.24	–2.29	1.54×10^{-4}	23.17	196
P71	–5.10	–3.20	5.06×10^{-2}	19.33	208
P72	–5.26	–2.43	н.д.	20.86	204
P73	–5.30	–2.22	4.27×10^{-5}	18.66	197
P74	–5.30	–2.24	2.42×10^{-4}	20.02	197
P75	–5.21	–2.08	8.05×10^{-5}	18.72	197
P76	–5.33	–2.31	6.25×10^{-5}	20.25	209
P77	–5.32	–2.27	4.47×10^{-5}	20.09	209

Note. The values in parentheses are PCEs for devices manufactured using dopants in HTLs μ is the hole mobility.

Structures P62–P77

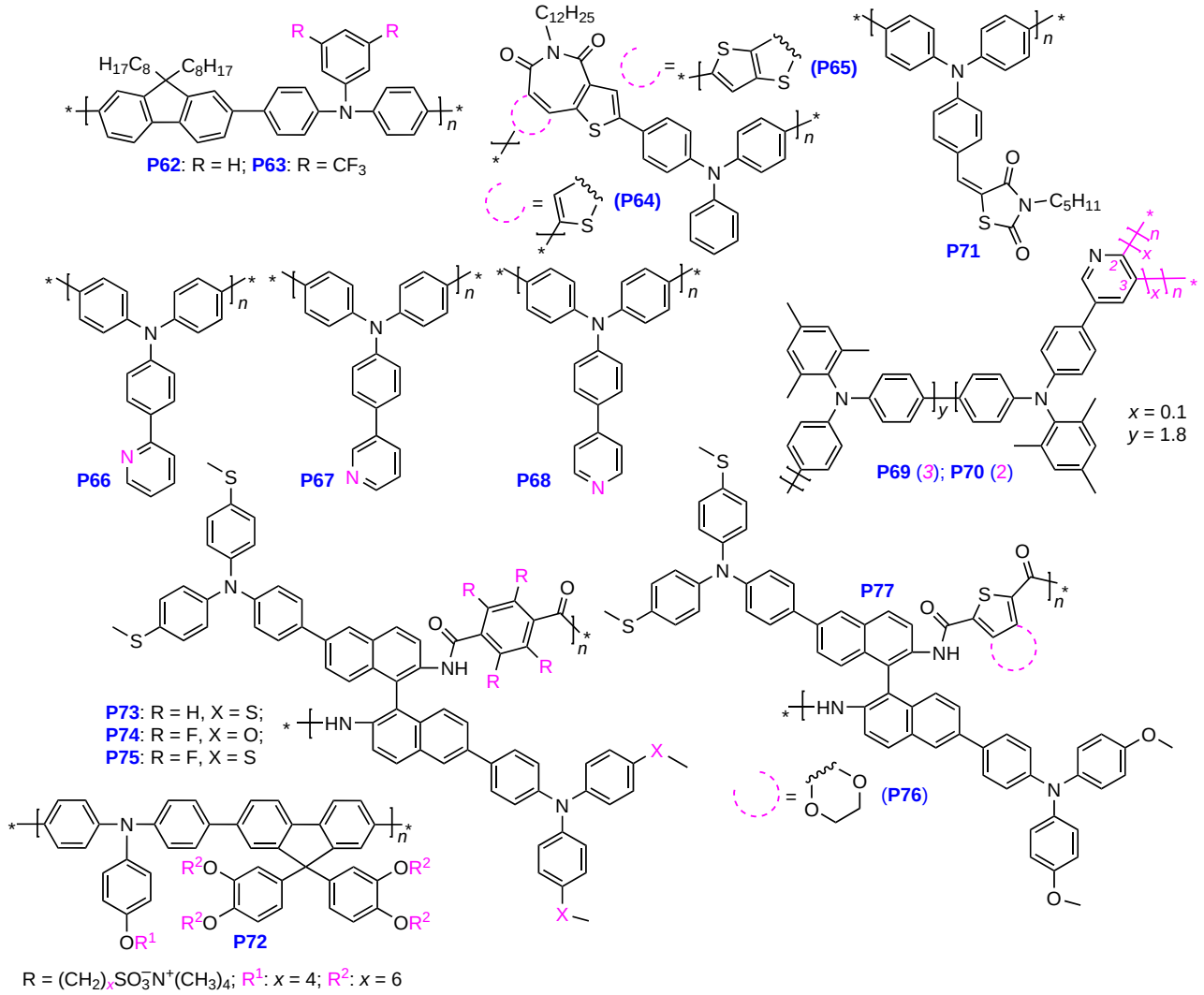

We will consider the most vivid examples of studies using undoped HTLs based on TPA polymers (structures **P62**–**P77**, Table 1). Zhang *et al.*[201] obtained donor-acceptor copolymers **P62** and **P63**. After the introduction of one or two electronegative trifluoromethyl groups into the TPA unit, the HOMO levels of **P62** and **P63** were reduced to –5.44 and –5.52 eV, respectively. This increased the open-circuit voltage (V_{oc}) to 1.28 and 1.30 V, respectively (as compared to the model copolymer without fluoromethyl groups, which had V_{oc} = 1.23 V in PSC), while the energy loss decreased from 0.69 eV for the copolymer without a fluoromethyl group to 0.64 and 0.62 eV for **P62** and **P63**, respectively. The power conversion efficiency of PSC based on polymer **P61** reached 14.4%, whereas the device based on **P62** showed PCE of only 11.1%, which is apparently related to the decrease in the hole mobility of the polymer caused by introduction of a larger number of trifluoromethyl groups. The hole mobility of copolymer **P63** (3×10^{-4} cm^2 V^{-1} s^{-1}) proved to be an order of magnitude lower than that for **P62** (2×10^{-3} cm^2 V^{-1} s^{-1}).

Recently, D–A copolymers based on TPA were synthesized; they showed the highest PCE value among PSCs based on undoped HTLs: approximately 18% for **P64** and 21% for **P65** (see Table 1).[194] Both copolymers contain thiophene-imide derivatives as electron-withdrawing units. Owing to the EW character and planar and rigid structure of these units, both polymers demonstrate well-matched HOMO (–5.26 and –5.28 eV, respectively) and LUMO (–2.35 and –2.42 eV, respectively) energy levels and an acceptable hole mobility (9.07×10^{-5} and 3.51×10^{-4} cm^2 V^{-1} s^{-1}, respectively), which makes them promising as undoped HTLs in PSCs.

Recently, researchers have paid attention to the applicability of TPA-based polymers with so-called anchor groups for p-i-n type perovskite solar cells.[195–197,202–204] The anchor groups are able to form chemical bonds with contacting materials (in this case, perovskite, metallic electrode, or metal oxide charge transport layer) and to passivate surface defects. As anchor groups, fragments of acids or bases, in particular carboxylic or organophosphorus acids, or various amines can be used.[205,206] The introduction of anchor groups also results in the fact that, unlike **PTAA** or **poly-TPD**, which have high hydrophobicity, polymers containing anchor groups are hydrophilic, which facilitates the perovskite crystallization on HTLs. Crystallization of perovskite films on the surface of commonly used hydrophobic **PTAA** or **poly-TPD** with alkyl substituents is a fairly complicated task. The successful formation of perovskite usually requires the use of additional hydrophilic interfacial layers, for example, poly[9,9-bis(3′-(*N*,*N*-dimethyl)-*N*-ethylammonium-propyl-2,7-fluorene]-*alt*-2,7-(9,9-dioctylfluorene) dibromide (PFN-Br).[207]

The introduction into the polymer of anchor groups capable of non-covalent interactions with perovskite makes it possible to deposit the photoactive layer on top of HTL without the use of additional interfacial layers. For example, a series of polymers (structures **P62**–**P77**, Table 1) in which an anchor pyridine group was attached to TPA in the *ortho*- (**P65**), *meta*- (**P66**), or *para*-position (**P68**), have recently been obtained.[195,203] This not only decreased the HOMO energies, but also increased the film wettability and endowed HTM with the ability to passivate defects. It was shown that the hydrophilicity and passivation efficiency gradually increase from **P66** to **P67** and to **P68** because of increasing effect of the lone electron pair of the nitrogen atom of the pyridine group, which enhances the interfacial contact and interaction with the perovskite. As the result, the interlayer non-radiative recombination is suppressed, which results in increasing open-circuit voltage and PCE for p-i-n type devices. The highest PCE of more than 22% was attained for a device with HTL based on **P68**.

High PCE values were attained for PSCs in which copolymers **P69** and **P70**,[196] containing pyridine moieties in the backbone, were used as HTLs (see Table 1). It was found that bonds between the pyridine units and Pb^{2+} ions in the perovskite material affect simultaneously the molecular conformation of HTM and the crystallinity of the resulting perovskite film. It was found that **P68** has a more ordered molecular regularity than **P70**. Perovskite films formed on the surface of **P69** exhibit higher crystallinity and lower density of defects than perovskites deposited on **P70** or **PTAA**. Perovskite solar cells with p-i-n architecture based on undoped **P69** showed an impressively high PCE of 24.89%. Moreover, devices based on **P69** have long durability, and the unencapsulated device retains more than 93% of the original efficiency after 800 h of operation.

Quite recently, Wang *et al*.[208] synthesized a TPA polymer **P71**, modified with a rhodanine group (see Table 1), which proved to be moderately hydrophobic. The water contact angle of a **P71** film is 46.23°, while that of the perovskite/ITO layer is 57.5°. Meanwhile the contact angle between **P71** and perovskite/ITO is 7.44°. Moreover, the **P71** contact angle on ITO is only 7.24°C, indicating good wettability, which is related to the formation of weak non-covalent bonds between nitrogen and sulfur atoms with the lone pair on rhodanine and In_2O_3 SnO_2 (ITO). In addition, the authors noted that **P71** improves the crystallinity of perovskites and passivates defects in the perovskite film to a certain extent. The device based on **P71** had PCE of 19.33%.

Another type of anchor group was applied in the synthesis of polymer **P72** (Table 1), which has SO_3^- and $N(CH_3)_4^+$ terminal ionic groups.[204] The enhanced wettability (or compatibility) of perovskite deposited on **P72** expands the possibility of scalable manufacture of large-area devices. Polymer **P72** showed not only good hole extraction from the perovskite due to good relationship between the HOMO level of the polymer (–5.26 eV) and the perovskite valence band (–5.36 eV), but also effective passivation of interfacial defects due to the presence of side-chain ionic groups; this increases the crystallinity of perovskite material and reduces the number of surface defects and/or traps. A 1 cm^2 module fabricated using **P72** as HTL had PCE of 20.86%.

The use of HTMs with a defect passivation function is an efficient method for suppressing the non-radiative recombination in PSCs caused by the defects in the perovskite structure. As can be seen from the above examples, most of these materials are meant for passivation of coordinatively unsaturated Pb^{2+} ions on the perovskite layer. The migration processes of MA^+, FA^+, or halides also cause a number of adverse effects, which sharply decrease the efficiency and stability of devices.

Recently, Luo *et al*.[197] presented polymers **P73**–**P75** (see Table 1), which are able to simultaneously passivate both the MA^+/Pb^{2+} cations and the I^- anionic defects in perovskite. The carbonyl group in **P75** is favourable for the passivation of low-coordinate Pb^{2+} and defects related to halide ions. Simultaneously, F atoms interact with MA^+ in perovskite *via* the formation of the NH···F hydrogen bonds. Also, polymer **P74** was found to contain the O=CNH···F intermolecular hydrogen bonds, which may be favourable for the existence of a more planar conformation; this made it possible to attain a relatively high hole mobility (2.42×10^{-4} cm^2 V^{-1} s^{-1}). The devices with **P75**-based HTLs demonstrated PCE of more than 20.5% and long durability and, hence, they surpass devices based on **P73** (PCE = 19.03%) or **P74** (PCE = 19.07%).

Zhao *et al*.[209] synthesized two polymers **P76** and **P77** structurally similar to **P73**–**P75** described above (see Table 1). The authors demonstrated how the problem related to the use of toxic solvents during the manufacture of PSCs can be efficiently solved, because an important condition for commercialization of these compounds is to develop environmentally benign production processes. It is known that the introduction of large conjugated units into the polymer chain with the goal to provide high hole mobility inevitably deteriorates HTM solubility in green solvents. In polymers **P76** and **P77**, the amide group is a flexible polymer base, while the 3,4-ethylenedioxythiophene and thiophene units serve as π-spacers. The results demonstrate that the combination of amide bonds and thiophene units increases the solubility of HTM in green 2-methylanisole (the solubility of both polymers in this solvent is greater than 10 g L^{-1}). It was also noticed that the polymers effectively passivate defects on the surface of polycrystalline perovskite due to the anchor carbonyl groups. In addition, the electron-withdrawing properties of carbonyl groups enhance the intermolecular hydrogen bond initiated by amide bonds and thus provide high hole mobility (see Table 1). Owing to the excellent hole mobility and passivation effect, high efficiency of perovskite solar cells was achieved: PCE was 20.25% for **P76** and 20.09% for **P77**, respectively. In addition, the devices had good durability compared to the reference **PTAA**.

While considering polymers as HTLs, it is important to note the influence of molecular weight on the properties of materials and output characteristics of the devices. For example, it was found that **PTAA** with high MW has a better mechanical resistance to damage.[213] As regards the efficiency of the device, it was found that PCE tends to increase with increasing MW. Ko *et al*.[181] investigated the effect of **PTAA** molecular weight in the range from 10 to 50 kDa.[181] The highest PCE (~17%) was attained when MW was 40 kDa. Another research group[214] investigated a wider range of MW from 10 to 115 kDa. They were able to attain a higher PCE (~18%) for a device based on **PTAA** with the highest MW (115 kDa). The authors found that the polymer with higher MW formed a more homogeneous film. It is of interest that systems based on high-molecular-weight **PTAA** exhibit a lower charge mobility than undoped systems based on low-molecular-weight **PTAA**, but, conversely, a higher charge mobility than the systems based on low-molecular-weight **PTAA** when doped.[213] The molecular-weight distribution (MWD) is also important. The more narrow MWDs provide the better output characteristics of the devices.[31]

Thus, study of TPA-based polymers as HTLs in PSCs is an actively developing field. The use of various methods of molecular design allows the synthesis of polymers with optimal

properties compared to those of well-known commercially available analogues such as **PTAA** and **poly-TPD**, thus providing high output characteristics of PSCs without the use of dopants in HTLs. Of special note are D–A polymers and compounds containing anchor groups in the molecules. The efficiency of the best devices based on undoped TPA polymers exceeds today 24%.

4.2. Metal-ion batteries

The modern society is characterized by rapidly increasing demand for the use of electrical devices such as electrical cars, laptop computers, and cell phones, which necessitates the manufacture of new rechargeable batteries with improved performance. The cathode materials for lithium-ion batteries are traditionally manufactured using lithium compounds (*e.g.*, $LiCoO_2$, $LiMn_2O_4$, $LiFePO_4$), but rapid progress of electrical devices is restricted by a number of problems such as toxicity, moderate capacity, limited natural resources of lithium, and difficulty of recycling and disposal of battery components.[215–217] The switching from inorganic to organic electrode materials may increase the specific characteristics of batteries and charging rate, and, what is most important, enable their manufacture from renewable non-toxic resources.[52–54,89,218]

High redox stability, ease of synthesis, and good hole-transport properties make TPA-based polymers quite promising organic cathode materials not only for lithium-ion batteries but also for sodium- and potassium-based batteries.[219–225] A few interesting examples of the application of TPA polymers in this field are considered below.

The capacities of lithium-ion batteries based on classical linear TPA polymers are moderate. For example, the battery using **P48a** (see Scheme 6) has a capacity of approximately 100 mA h g^{-1}, with the capacity of 90 mA h g^{-1} being retained after 1000 cycles.[226,227] This value is lower than that of the commonly used $LiCoO_2$ (approximately 140 mA h g^{-1}), which thus hinders further studies of polymers of this type as cathodes for high-energy batteries. Compound **P78** (Ref. 228) is structurally similar to **P48a**, but has a higher density of free radicals than **PTPA**, due to the higher proportion of tertiary nitrogen atoms per repeating unit; this provides a higher capacity for this compound, which reaches 130 mA h g^{-1}. However, even this type of polymers still suffers from certain drawbacks, such as poor long-term cyclability. The discharge capacity of **P79** drops from 130 to 110.6 mA h g^{-1} as soon as after 50 cycles.[228]

In order to increase the capacity characteristics, additional groups with theoretically high specific capacity are introduced into the molecules of TPA-based polymers. For example, Huang *et al.*[229] introduced anthraquinone units into the side chain and thus obtained polymer **P79** with a high theoretical specific capacity of 214 mA h g^{-1}, which is approximately two times as high as that of **PTPA**. It is noteworthy that comparison of the performances of **P79** and the starting monomer, carried out by the authors, showed that the battery capacity can be influenced by the solubility of the cathode material, usually dialkyl or alkylene carbonate, in the electrolyte. A lower solubility of the material in the electrolyte results in increased stability and capacity performance of the device. Both the monomer and polymer **P79** had a high starting specific capacity of approximately 129 and 159 mA h g^{-1}, respectively; however, the cycling stability and rate performance were better for polymer **P79** than for the monomer. The rate performance of the monomer and polymer **P79** were estimated by charging and discharging the cells with the monomer and the polymer as electrode material at current densities from 0.1C to 2C and then back to 0.1C. In the range from 0.1C to 2C, the discharge capacity of the monomer decreases from 129 to 38 mA h g^{-1}, while when the current density returns to 0.1C, the capacity can recover up to 71 mA h g^{-1}. In the case of polymer **P79**, the capacity decreases from 151 to 50 mA h g^{-1}, while the repeated discharge to 0.1C may result in the capacity recovery up to 106 mA h g^{-1}. It was also emphasized that the polymer degradation was much slower due to the lower solubility of the polymer in the electrolyte.

Copolymer **P80** has an initial specific capacity of 1221.8 mA h g^{-1}, which decreases to 854.9 mA h g^{-1} after 50 charge cycles up to 2.5 V. Subsequently, the capacity slowly decreases, being at a 772.4 mA h g^{-1} level after 500 cycles. As

Structures P78–P84

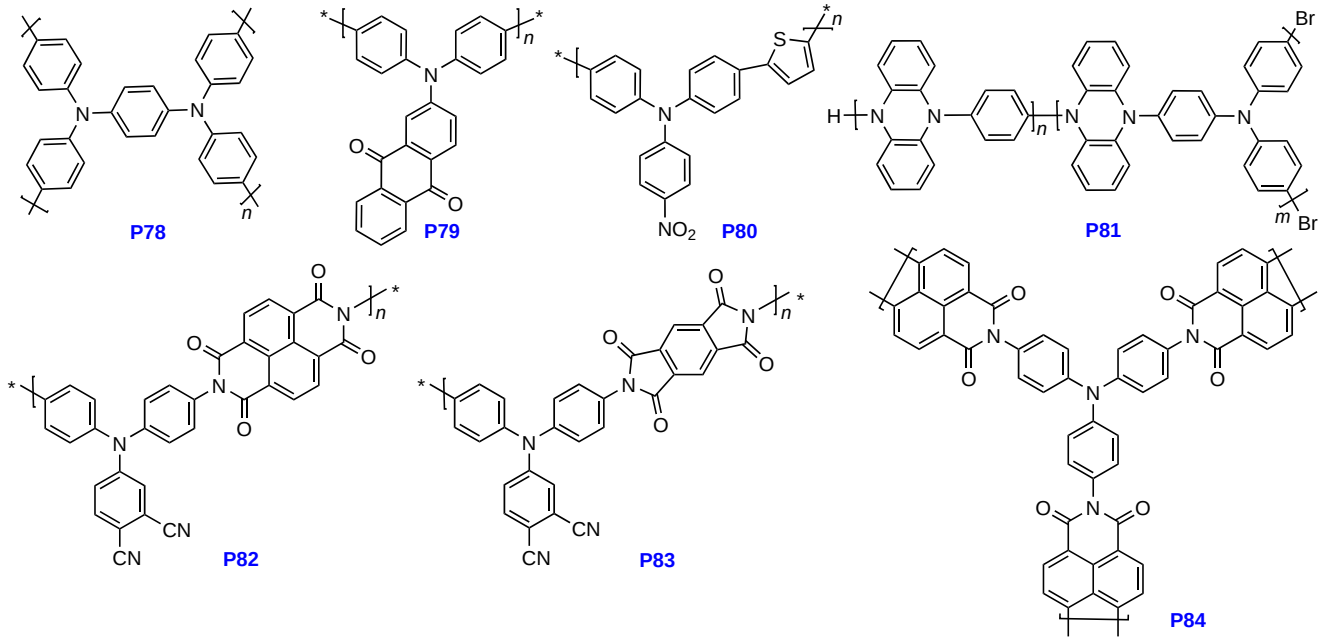

the charge increases up to 4 V, the capacity decreases to 210 mA h g^{-1}. This pronounced decrease in the capacity is due to the damage of the electrode material structure related to the dissolution in the electrolyte.[218]

Of most interest for the application in lithium-ion batteries are branched[52–54] and cross-linked polymers.[230–232] Since polymers of this type have low solubility and a large surface area providing enhanced diffusion of the electrolyte, this can finally improve the performance of lithium-ion batteries compared to those using linear polymers. For example, branched polymer **P31** obtained by Kang *et al*.,[52] which had a mesoporous structure with a surface area of 560.58 m^2 g^{-1}, showed a capacity of 133.1 mA h g^{-1}, equal to 92.8% of the theoretical capacity (143.5 mA h g^{-1}). Furthermore, the problem of decreasing capacity of the batteries caused by the partial solubility of the cathode material in the electrolyte is absent in the case of cross-linked polymers, because they are completely insoluble. For example, cross-linked polymer **P81** (Ref. 230) used as the material can provide a reversible capacity of up to 220 mA h g^{-1} with a minor degradation after 1000 cycles.

Copolymers based on TPA derivatives and imides are promising as electrode materials for lithium-ion batteries due to known properties of polyimides such as high thermal and thermooxidative stability, solvent resistance, good mechanical properties, and high chemical stability. Recently, Labasan *et al*.[152] reported the synthesis of compounds **P82** and **P83** by polycondensation of 4,4′-diamino-3″,4″-dicyanotriphenylamine (DiCN-TPA) with pyromellitic dianhydride and 1,4,5,8-naphthalenetetracarboxylic dianhydride, respectively.[152] The incorporation of DiCN-TPA into the polymer molecule resulted in a disordered arrangement of chains, which was reflected as high glass transition temperatures of 205°C and 480°C for **P83** and **P82**, respectively. The electrochemical testing of these polymers as cathode materials showed that **P82** provides a reversible specific capacity of 150 mA h g^{-1} at 0.1 A g^{-1} and stability for up to 1000 cycles, which is presumably related to the polymer structure and greater π-conjugation. Compound **P83** used as an anode provides a high specific capacity of up to 1600 mA h g^{-1} at 0.1 A g^{-1} after 100 cycles. Good cyclability and excellent battery performance indicate that **P82** and **P83** are promising organic materials for next-generation lithium-ion batteries.

Among branched TPA-based copolymers, interesting examples are porous three-dimensional polymers **P55** (see Scheme 9) and **P84**, which were prepared by introducing a binding TPA unit into polyimides based on pyromellitic acid (**P85**) and naphthalene-1,4,5,8-tetracarboxylic acid (**P86**).[153] These polymers were studied as anodes for lithium-ion batteries, they both had a large surface area (738 m^2 g^{-1} for **P85** and 456 m^2 g^{-1} for **P86**) and a well-formed porosity. The porous structure with a large surface area provides a better diffusion of Li^+. The polymers had a high reversible capacity and good rate performance. It is of interest that the capacity of porous polymer **P55** gradually increased from 385 to 420.3 mA h g^{-1} after 100 cycles. Polymer **P84** demonstrated a reasonable stability during cycling, but the capacity decreased by 4.65% after 100 cycles (from 312 to 297.5 mA h g^{-1}).

Thus, the application of TPA-based polymers as cathode materials for metal-ion batteries has been widely developed in recent years and has already achieved some success. In relation to the polymer materials discussed in this Section, it can be noticed that branched and cross-linked polymers and often polyimides are materials of choice. The devices based on these polymers show high capacity and cycling stability compared to the devices based on linear TPA homopolymers.

4.3. Electrochromic devices

Compounds that possess electrochromism, that is, reversibly change their light absorption spectra as a result of redox reactions induced by application of an external potential, are of interest for the possible use in smart windows, displays, electron skin, and self-dimming mirrors for cars.[233–235] Triphenylamine and its derivatives are propeller-shaped molecules in which the central nitrogen atom is an electrically active site and is linked to three aromatic rings. This nitrogen atom is easily oxidized to give a coloured radical cation, which is highly stable. The polymers in which arylamine moieties contain two or more non-equivalent nitrogen atoms undergo the corresponding number (two or more) of colour change processes. In addition, the electrochemical properties of TPA vary upon the introduction of ED and EW groups into the benzene rings, which allows fine tuning of electrochromic properties as well. This largely accounts for the fact that TPA-based conjugated polymers have been actively investigated for many years as electrochromic materials and are distinguished among other classes by their high electrochemical stability, bright colour over a broad range, high optical contrast, and short response time.[29,135,236–239]

The polymers meant for the electrochromic devices are usually formed as uniform thin films on a substrate coated with a semitransparent ITO electrode. The quality of the film affects the electrochromic properties of the devices. A smooth and uniform film surface may increase the contact area with the electrodes and facilitate the ion diffusion. As a rule, the films are obtained by electrochemical polymerization[100,136,240,241] or by solution-based methods, *e.g*., spin coating.[50,135,242]

In order to obtain high-quality films by spin coating, polymers must have good solubility. For example, Ma *et al*.[239] prepared six electrochromic polymers containing triphenylamine and benzothiadiazole units: **P85a**–**d**, **P86**, and **P87**.[239] All polymers were readily soluble in polar aprotic solvents such as nmP, DMA, and DMF. The films of these polymers exhibited reversible electrochromic colour change, high optical transparency, and good colouration efficiency. The colour of the **P87**-based film changed from reddish-brown (neutral form) to blue (oxidized state). The **P85a**–**d** and **P86** films demonstrated a colour change from yellow (neutral form) to green (oxidized state) upon the application of the external potential. The highest colouration efficiency (270 cm^2 C^{-1}) was found for polymer **P85b**. The best colouration time (3.8 s) and bleaching time (3.6 s) was found for polymer **P85c**.

The polymers **P10** and **P11** obtained by oxidative polymerization also proved to be readily soluble in common organic solvents.[78] The films were spin-coated on glass substrates from solutions of the polymers in chloroform (20 g L^{-1}). The D–A structure of these polymers provides for intramolecular charge transfer, which affects both the electrochemical redox process and the ion insertion/extraction processes, thus determining the oxidation/reduction rates of films based on these materials. Polymer **P10** containing the EW carbonyl group has a markedly higher ion diffusion coefficient than **P11**, which results in an almost four times shorter response time (0.19 s). It was found that this fast response is determined by the ion diffusion coefficient related to the character of intramolecular charge transfer. This difference is probably attributable to various interactions between electrolyte ions and

Structures P85–P87

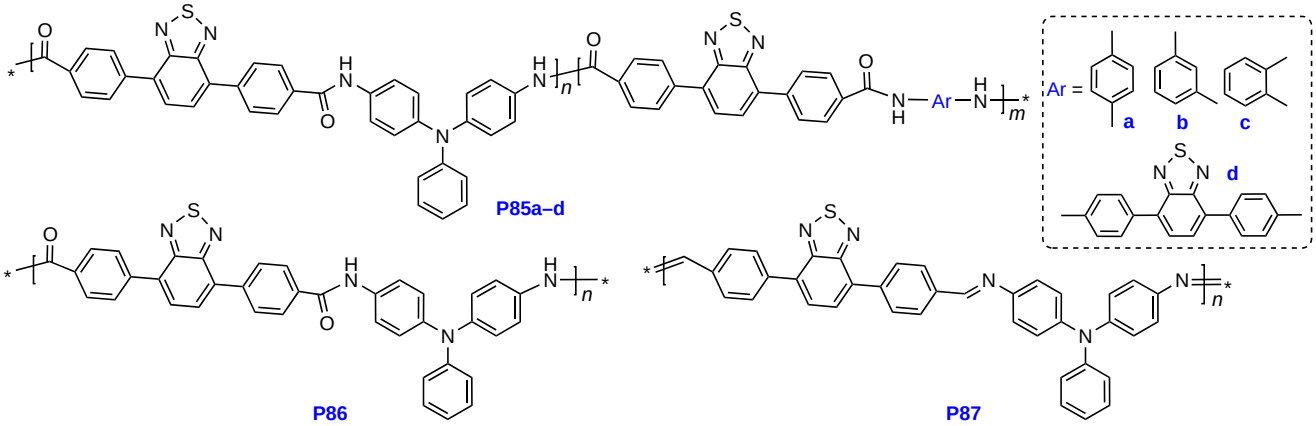

polar polymer molecules with different intramolecular charge transfer characteristics.

Recently, Chern *et al.*[154] obtained polyamides **P88**–**P90**, the backbone of which includes TPA blocks. Polymer **P88** contains *ortho*- and *para*-methoxy groups and three electroactive nitrogen sites in four benzene rings; **P89** has *para*-methyl groups and three electroactive nitrogen sites; and **P90** has two electroactive nitrogen sites and methoxy-substituents in the *para*-position. The solubility of the polymers was tested in various solvents. In this series, polymer **P88** showed a good solubility in NMP, DMA, *o*-chlorophenol, *m*-cresol, and cyclohexanone. Polymer **P90** proved to be soluble in NMP, DMA, DMF, DMSO, and *m*-cresol.[243] Polymer **P89** was soluble only in NMP and *o*-chlorophenol; this can be attributed to the presence of methoxyphenyl side groups preventing an ordered packing of the molecules in the two first-mentioned polymers. Polymer **P88** exhibited pronounced electrochromic behaviour, including multiple colour changes (from colourless to grass green, green, and blue), fast response, high contrast of the change in the optical transmittance, and stability. The introduction of electron-donating methoxy substituents in the *ortho*- and *para*-positions of the TPA benzene rings and three electroactive nitrogen sites increases the stability of the electrochromic behaviour of **P88** compared to **P89**, which has a weaker ED substituent (methyl).

Structures P88–P94

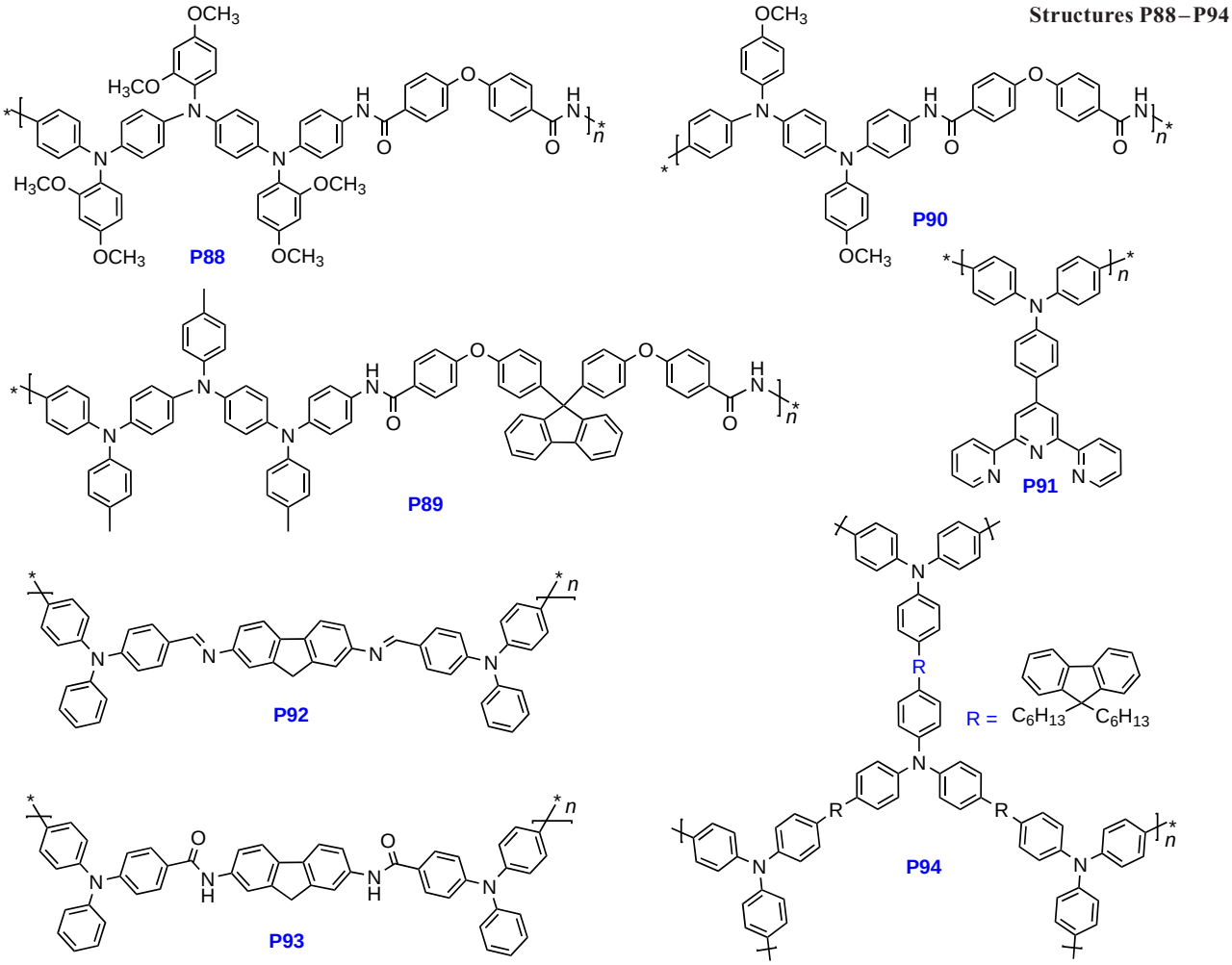

The decrease in the colouration efficiency was only 4.1 and 2.5% at 422 and 1252 nm, respectively, after 15 000 switching cycles. The colour changes of **P88** and **P89** during the electrochemical oxidation differ, which indicates that introduction of substituents with different ED strengths into the benzene ring can be used for fine tuning of the colour. In the first oxidation step, polymer **P88**, containing larger number of electroactive nitrogen sites than **P90**, absorbs light at longer wavelength in the near IR range because of the transfer of electrons from the neutral to radical-cation centre of TPA, resulting in enhanced electrochemical stability. Remarkably, the stability of each radical-cation centre of TPA-based polymers depends on both the electron-donating ability of substituents and the resonance delocalization of electrons over the electroactive nitrogen sites.

To obtain mechanically stable solvent-resistant films, methods in which the film is formed during the polymer synthesis are chosen.[236,244] The electrochemical polymerization has a number of advantages for polymer synthesis such as high rate and the fact that the film is formed directly on the electrode surface. This feature not only expands the range of polymers candidates, but also eliminates the film casting procedure. Films obtained by electropolymerization have good adhesion and electrical contact to the electrode surface. The materials exhibit fast response time, high optical contrast, good electrochromic efficiency, and robust stability.[245,246] This method, for example, was used to obtain films of polymer **P91**, which can reversibly change colour between orange (neutral state) and blue (oxidized state), with the high colouration efficiency (229 $cm^2\ C^{-1}$ at 750 nm) being retained in the electrolyte solution.[142] Guven *et al.*[135] used electrochemical polymerization to obtain polymer **P92** and **P93** films, which showed colour change from yellow to dark blue (**P93**) and from pale yellow to pale blue (**P92**). These films have the record-fast switching time: 1.61 s at 362 nm (**P93**) and 0.69 s at 390 nm (**P92**) and high colouration efficiency: 114 $cm^2\ C^{-1}$ (**P93**) and 192 $cm^2\ C^{-1}$ (**P92**).

The D–A homopolymers **P49**–**P51** considered above (see Scheme 7) were synthesized for the use in electrochromic devices.[143] They demonstrated fast and reversible eletrochromic colour switching. The colour of polymers both in the neutral and oxidized states was controlled by varying the π-spacer between TPA and the EW group. Neutral **P49** film (0 V) is orange-coloured, and a new peak in the light absorption spectrum appears at 720 nm at a potential above 0.8 V, with the peak intensity gradually increasing upon increase in the applied voltage (Fig. 4). When a voltage of 1.2 V is applied, the colour becomes dark green. When there is additional π-spacer between TPA and the EW group, the absorption spectra of polymers **P50** and **P51** are red-shifted compared to that of their analogue **P49**. Polymer **P50** shows a light pink colour, and **P51** proved to be light brown. As the applied voltage increases, a new absorption band appears at approximately 810 nm, and the band intensity gradually increases. As a result, both polymers **P50** and **P51** are grey at applied voltages of 1.1 and 1.2 V, respectively.

Electrochromic supercapacitors with polymers **P49**–**P51** became the subject of research owing to their ability to combine electrochromic behaviour and energy storage process, and the energy storage state of the supercapacitor can be monitored *via* colour changes during charge/discharge cycles.[247,248] Supercapacitors based on these polymers exhibited reversible colour change during charge/discharge processes (Fig. 5), which makes them promising materials for smart windows.

One more way to obtain polymer films directly on the substrate surface is the interfacial Suzuki polycondensation.[110] The triphenylamine-containing film of **P94** obtained by this method showed a high optical contrast (72.8%), good electrochromic efficiency (138.26 $cm^2\ C^{-1}$), and robust stability. The **P94** film was transparent and yellow in the neutral state, orange-red in the intermediate state, and blue-green in the oxidized state.

Thus, electrochromic materials based on TPA polymers have fast response time, high contrast, and colour diversity and can be effectively used in a broad range of electrochemical devices. These materials are sensitive to external stimuli and are applicable for smart windows, displays, *etc*. Although considerable advances have already been made along this

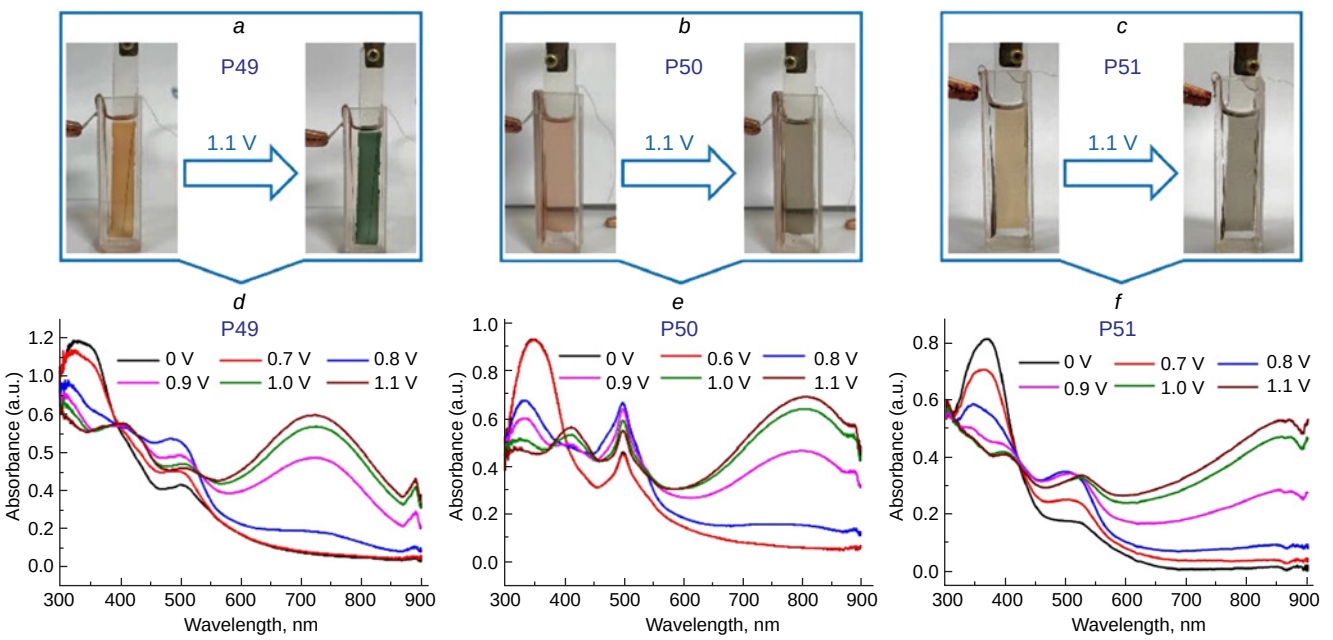

Figure 4. Colour change (*a*–*c*) and light absorption spectra (*d*–*f*) of thin films of **P49**, **P50**, and **P51**, respectively, on the glass/ITO surface in 0.1 M $Pr^i_4NPF_6$/toluene and acetonitrile (4 : 1 v/v) at various applied voltages.[143] Published with permission from Elsevier.

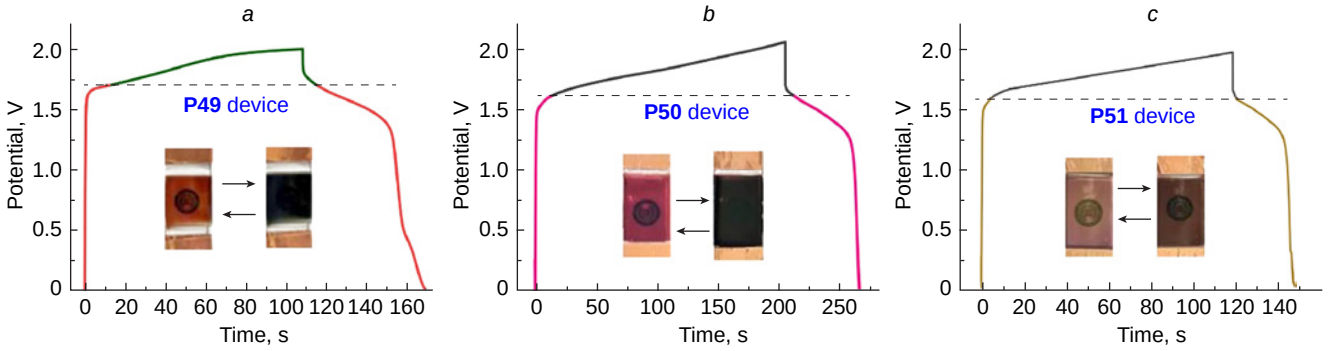

Figure 5. Charge/discharge curves and corresponding colour change of electrochromic supercapacitors based on **P49** (*a*), **P50** (*b*), and **P51** (*c*) at a current density of 0.06 mA cm^{-2}.[143] Published with permission from Elsevier.

line, much remains to be done to bring a variety of electrochromic devices into everyday use. For example, challenges related to the scalability and durability of devices have to be resolved.

4.4. Miscellaneous applications

Organic light-emitting diodes attract a lot of attention due to their application in TV and phone displays and light sources.[249–251] Currently, considerable progress has been achieved in this area, including the development of structurally diverse conjugated polymers that perform various functions in OLED devices.[252] The performance of these devices is largely determined by the efficiency of charge carrier injection and transport. The high LUMO (≈–2.30 eV) and HOMO (≈–5.00 eV) levels and high hole mobilities in the vertical direction make TPA-based polymers promising materials for hole transport and blocking the electrons. In combination with the fact that TPA-based hole-conducting polymers have high chemical and thermal stability, amorphous nature, good film-forming properties, and solubility in organic solvents, they are being actively investigated for the development of high-performance organic and perovskite light-emitting devices.[57,63,111,253–257]

For example, cross-linked polymer **P95** was synthesized for the use as HTL in OLEDs and perovskite light-emitting diodes (PeLEDs).[258] The use of cross-linked polymers in these devices gives rise to HTLs resistant to the action of solvents, which is important for implementing solution-based methods of manufacture of multilayer devices. In this case, it becomes possible to deposit subsequent layers on top of HTLs from organic solvents without partial dissolution of the underlying film or component mixing. Moreover, a denser and more uniform cross-linked film implies an optimal morphology, which improves the charge transport, decreases the number of defects, and enhances the performance of the device. The HOMO energy level for cross-linked polymer **P95** was –5.25 eV, which is between the PEDOT:PSS level (–5.00 eV) and the emitting layer (in this case, $CsPbBr_2$) (–6.20 eV); this results in better hole injection compared to that for light-emitting diodes without **P95**. The LUMO energy level of **P95** is also suitable for suppressing the back electron transfer from the emitting layer to the anode. The polymer has a relatively high hole mobility of 1.22×10^{-4} cm^2 V^{-1} s^{-1}. The films of **P95**, unlike that of non-cross-linked **P96**, were highly stable to solvents and provided a better external quantum efficiency of light-emitting diodes and operational stability. Both PeLED and OLED fabricated using cross-linked **P95** had the maximum

Structures P95–P97, PODPF

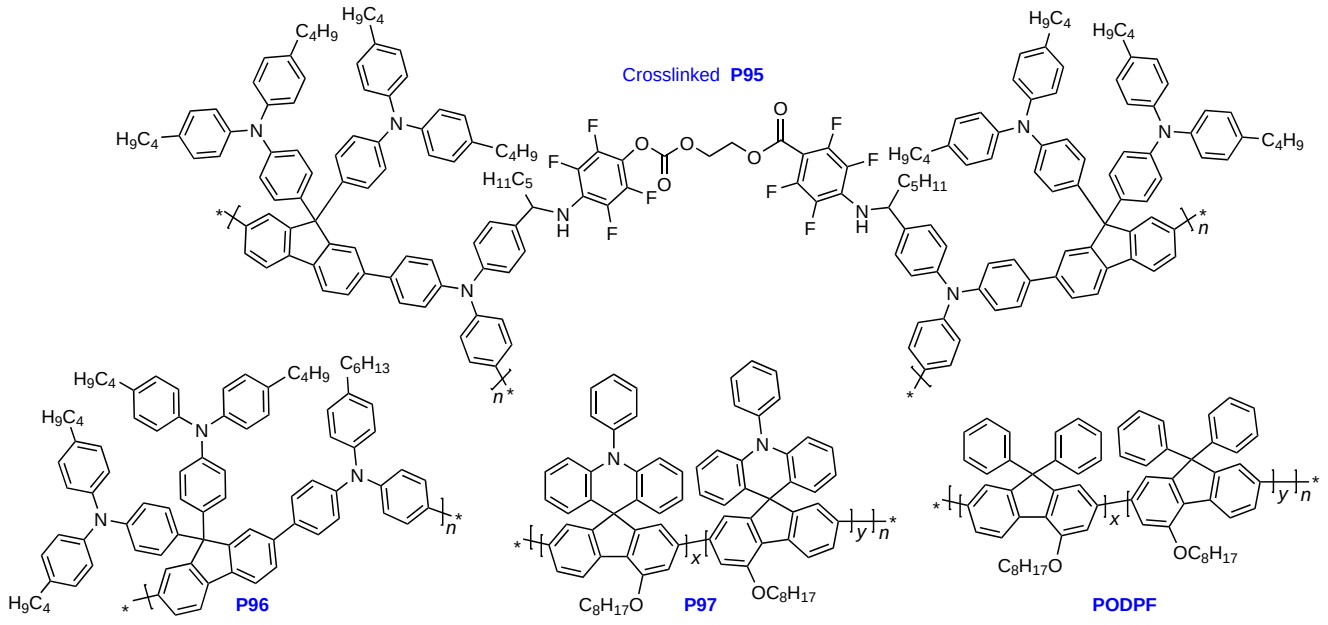

luminance of 175 and 4260 cd m^{-2} and the highest external quantum efficiency of 4.16 and 10.86%, respectively. These data indicate that TPA polymers are promising materials for HTLs of efficient polymer light-emitting devices.

The use of TPA-based polymers in OLEDs is not limited to only the fabrication of HTLs. There are quite a few examples in which these polymers act as emission materials with different emission colours and high quantum efficiency.[259–261] The problem of fabrication of efficient and stable large-area blue OLEDs is well known. A recent study reports the synthesis of originally designed polymer **P97**.[261] In essence, this polymer is a polyfluorene with spiro-coupled TPA units to improve the hole injection from electrodes and hole transport. The **P97** films provide a better transport than the model polyfluorene without TPA (**PODPF**). The good solubility of **P97** made it possible to fabricate large-area OLEDs (9 cm^2) by the blade coating method, which implies uniform deposition of a solution of the material on the substrate using a moving blade;[262] the OLEDs showed ultradeep-blue stable emission with a very narrow electroluminescence band (only 36 nm width at half height). The external quantum efficiency of the best **P97**-based devices was 1.54%, which is markedly higher than that of the model polyfluorene **PODPF** (1.17%). Moreover, passive matrix displays of 20×20 pixels were manufactured by 3D printing, which confirmed the efficiency of spiro-functionalization in optoelectronics.

One more emerging application of hole-conducting TPA polymers is their use in photorefractive (PR) composites for holographic purposes: displays and memory devices.[263–268] Characteristics of PR polymers such as high photoelectric sensitivity, two-beam coupling gain, modulation of the refractive index, diffraction efficiency, and short (millisecond range) hologram recording times, as well as the possibility of multiple real-time recording and erasing of holograms make these materials promising for photonic applications.[269] As a rule, typical photorefractive composites include photoconductive polymers, non-linear optical chromophores, plasticizers, and sensitizers. The photoconductive polymer performs the key function providing the medium for charge transfer. For example, Giang *et al*.[265] used the following system: poly((4-diphenylamino)benzyl acrylate) (**P26**) as a photoconductive TPA polymer; (4-(azapan-1-yl)-benzylidene)malononitrile (7DCST) as a chromophore; (4-(diphenylamino)phenyl)-methanol (TPAOH) or 2,4,6-trimethyl-*N*,*N*-diphenylaniline (TAA) as a plasticizer; and methyl [6,6]-phenyl-C_{61}-butyrate (PCBM) as a sensitizer (Fig. 6).[265] The characteristics of the PR composite based on **P26** photoconductive polymer were found to be improved by the addition of the TPAOH triphenylamine plasticizer. The plasticizer increases the free volume of the polymer and increases the orientational mobility of the chromophore.[270] For example, the response time decreases with increasing concentration of TPAOH because of increasing softness of the composite material and increasing orientation mobility of the chromophore. The addition of the plasticizer also induces the highly efficient charge transfer in the photoconductive matrix. The replacement of TPAOH by TAA decreases the photocurrent (by a factor of up to 100) and impairs the response time of the diffraction light beam due to the low scattering effect.

The photoconductive polymer with a higher HOMO level, *i.e*., the more easily ionizing polymer, is preferable for attaining the desirable photoconductivity. In addition, the use of high-HOMO polymer for PR composites helps to avoid the accumulation of traps, which deteriorate the performance of PR devices. The photorefractive characteristics of the composites were compared using two types of photoconductive polymers– **P26** and its full analogue **P25**, but containing an ED methoxy group in the *p*-position of the benzene ring (see Fig. 6). The methoxy group in **P25** not only elevates the HOMO level of the polymer, but also increases the chromophore orientation, thus improving the performance of devices.

Apart from the above applications, TPA-based polymers are widely used in a variety of sensors: humidity sensors[271] (*e.g*. for agriculture), sensors for acid vapour detection,[272] chemosensors for selective detection of metal ions[273] needed at industrial plants, sensors for detection of nitroaromatic explosives,[274,275] and biosensors for medicine.[276,277]

For example, Dong *et al*.[274] fabricated sensors based on poly(triphenylamine) derivatives **P98** and **P99** (Fig. 7) to detect 2,4,6-trinitrotoluene (TNT). The incorporation of tetraphenylethylene units into the backbone and side chain endows polymers with the so-called aggregation-induced emission enhancement (AIE) effect and high fluorescence quantum yields in the solid state. The electron-donating TPA blocks are incorporated into polymer backbone to enhance binding of the polymer to an analyte with potent EW groups. For TNT detection, disperse nanoaggregates of the polymers were prepared in a water/THF mixture. It was found that the fluorescence intensity of **P98** and **P99** gradually decreases with increasing TNT concentration, indicating a sensitive reaction between the polymer and the analyte. When the TNT concentration was 93 mM, the fluorescence of both polymers was quenched by more than 85%. The limit of detection was 0.8 and 0.5 mM for **P99** and **P98**, respectively. It is noteworthy that no considerable spectral changes take place during fluorescence quenching, which means that no new emitting molecular centres are formed. The mechanism of photoluminescence quenching of the polymers under the action of TNT includes an electron transfer between the excited states of **P98**/**P99** and TNT, since there is no overlap between the absorption spectra of the polymer

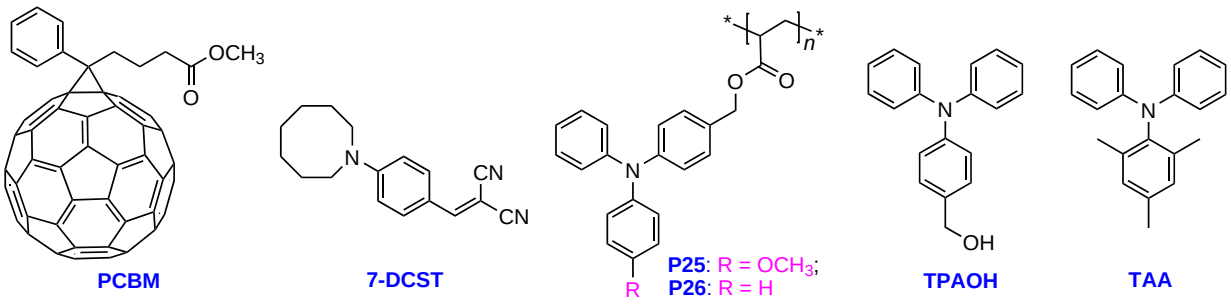

Figure 6. Structures of components of the PR composite.

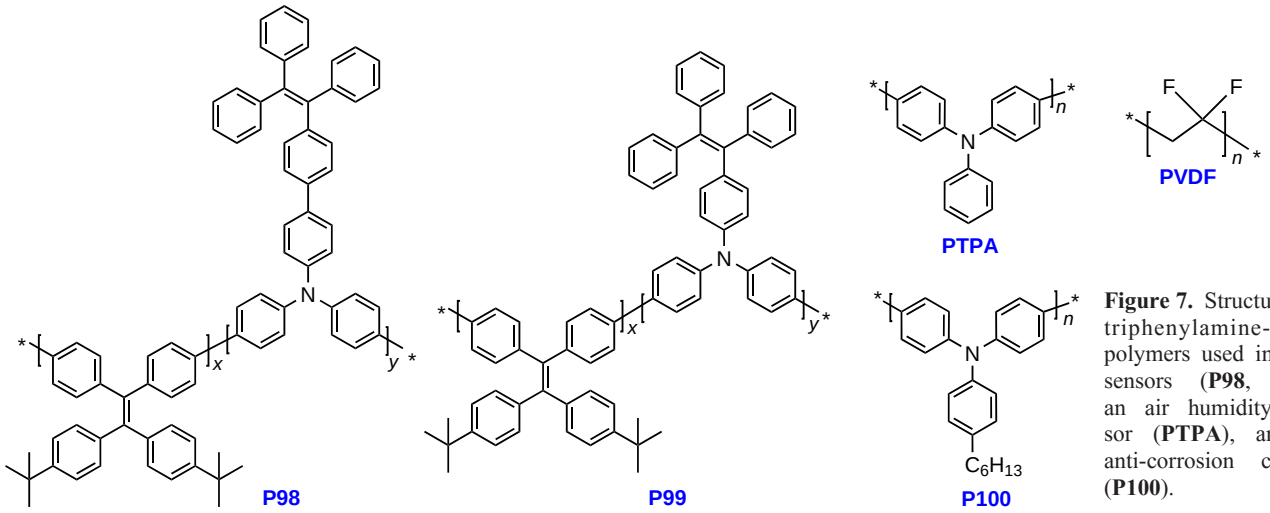

Figure 7. Structures of triphenylamine-based polymers used in TNT sensors (**P98**, **P99**), an air humidity sensor (**PTPA**), and as anti-corrosion coating (**P100**).

and the analyte, which is a necessary condition for the Förster type energy transfer. The tests using paper strips impregnated with solutions of polymers showed good prospects for their practical use as solid-state sensors to detect nitroaromatic explosives. The original emission of the paper strips was bright green; however, on contact with both dilute TNT solutions of various concentrations and TNT vapour, fluorescence of **P98** and **P99** was gradually quenched (Fig. 8).

Cheng *et al.*[271] described a flexible air humidity sensor characterized by high sensitivity and robustness, which was fabricated by electrospinning of the **PTPA**-containing polyvinylidene fluoride (PVDF) nanowires (see Fig. 7). The experiments showed that the addition of conductive **PTPA** increases the dielectric constant and water adsorption due to the extensive PVDF surface and the reaction of **PTPA** with water. The PVDF/**PTPA** film has a broad range of sensitivity (20–90%), short response/reduction time (33/28 s), and long-term stability (more than 100 cycles), being superior to most of known polymer-based humidity sensors. This publication opens a new way for the design of sensitive, flexible, and robust humidity sensors.

Other interesting applications of triphenylamine polymers include the development of a photocatalytic system for efficient carbon dioxide conversion and hydrogen generation,[278] UV-sensitive organic memory phototransistors,[279] and highly efficient hydrophobic coatings.[280,281] For example, polymer **P100** is deposited on the iron surface as a corrosion-protective layer.[281] First, **P100** was spin-coated on a pretreated iron plate, and then the plate was heat-treated at various temperatures (up to 80°C) in order to study the effect of heat treatment of **P100** on the corrosion behaviour of iron. According to the results, the contact angle of the **P100** film increased from 81.6° at room temperature to 100° after heat treatment at 80°C. In addition, it was found that the heat treatment improves the **P100** adhesion to the iron plate and gives rise to a thin passivating iron oxide film. The efficiency of corrosion protection increases from 90% for pure **P100** to 99.9% for **P100** pretreated at 80°C.

The brief insight into the applications demonstrates that TPA polymers are versatile compounds that can be used not only as hole-transport materials, but also as emitting layers in OLEDs, photorefractive materials in holographic devices, active components in various sensors, and even as anti-corrosive coatings. There is every reason to believe that these research areas would develop and expand in the future.

5. Conclusion

The chemistry, physical chemistry, and physics of triphenylamine-based polymers have been actively investigated in recent years. The variability of modern methods of synthesis and molecular design techniques, together with the relatively simple and diversified chemistry of triphenylamines, makes it possible to obtain a variety of unique structures of these compounds. In this review, the first classification of TPA polymers and methods for their synthesis were proposed.

A molecular design area actively developed in recent years is related to D–A polymers. The use of electron-withdrawing and electron-donating groups of various nature provides the possibility of fine tuning of HOMO and LUMO energies, the ranges of absorption and emission spectra, and the hole mobility of these polymers.

While considering various approaches to the synthesis of TPA-based polymers, one can distinguish the most popular methods such as Suzuki and Stille polycondensations and oxidative polymerization. The latter is perhaps the most facile and simultaneously the most versatile method, because it is suitable for the synthesis of homopolymers, copolymers, branched and cross-linked polymers. However, despite the

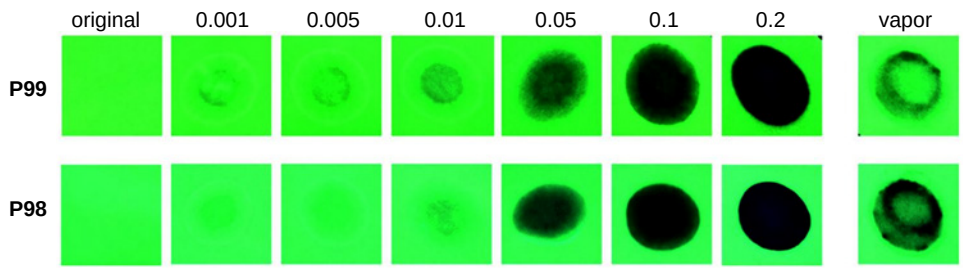

Figure 8. Paper test strips impregnated with **P98** or **P99** before and after application of TNT solutions in THF on the strips (0.001, 0.005, 0.01, 0.05, 0.1, and 0.2 mg mL^{-1} concentration, respectively) and after the strips were kept over TNT vapour for 5 min.[274] Published with permission from the Royal Society of Chemistry.

variety of methods for the polymer synthesis, the real scaling-up of processes remains a challenge, as the synthesis of monomers is very labour-intensive for most of the promising materials. Nevertheless, poly(triphenylamine)s still comply with the criteria of industrial applicability more than other classes of conjugated polymers.

Polymers of this type are widely used in the fields of organic and hybrid electronics and photonics. In numerous studies, these polymers are tested as HTLs in perovskite solar cells. Currently, there is a broad range of TPA-based polymers, which are successfully used as HTLs in perovskite solar cells, and the resulting devices have PCEs of up to 24.49%, which is comparable with traditional silicon-based solar cells. It is noteworthy that, unlike commercially known **PTAA** and **poly-TPD** homopolymers, structurally similar D–A polymers, including those with anchor groups, can be successfully used as undoped HTLs in perovskite solar cells owing to their higher hole mobility, which markedly increases the durability of these devices.

Triphenylamine-based polymers, especially branched and cross-linked ones, are also of interest as electrode materials for lithium-ion batteries, because they can replace traditional cathode materials based on inorganic transition metal oxides and solve the problems of toxicity of inorganic materials, moderate capacity, difficulty of processing and disposal of battery components. Due to the high density of redox-active centres and high specific surface area favourable for electrolyte diffusion, the devices using TPA-based polymers are characterized by high performance, high capacity, and stability during charge/discharge processes over a large number of cycles.

The ability to change colour allows the use of TPA-based polymers in electrochromic devices. Polymers exhibit a broad scale of colours, fast response time, redox stability, and high coloration efficiency. These properties of the polymers make them promising for the application in displays, sensors, and smart windows. In addition, these polymers find their applications as hole-transport and light-emitting layers in OLEDs, in sensors and transducers, and in photorefractive devices, which attests to the importance of further studies of TPA-based polymers and their good prospects in the future.

From the chemistry standpoint, further research into TPA polymers should be aimed at the synthesis of polymers and monomers by less expensive and environmentally benign methods that can be scaled-up for industrial production. As regards devices, optimization of particular characteristics and switching from laboratory prototypes to industrial products are important areas for further investigations. The issues concerning the stability and durability also remain open for some directions. It can be expected that active studies of these materials in the coming years would be concerned with biotechnology and medicine.

The study was supported by the Ministry of Science and Higher Education of the Russian Federation (grant No. 075-15-2024-532).

6. The list of abbreviations and symbols

The following abbreviations and symbols are used in the review:

$Đ_M$ — polydispersity index,
E_g — band gap,
M_n — number-average molecular weight,
M_w — weight-average molecular weight,
T_d — degradation temperature,
T_g — glass transition temperature,
μ — hole mobility,
λ_{edge} — absorption edge,
λ_{max} — absorption maximum.
CV — cyclic voltammetry,
D–A — donor–acceptor,
DMA — dimethylacetamide,
ED — electron-donating,
EW — electron-withdrawing,
HOMO — the highest occupied molecular orbital,
HTM — hole-transport material,
HTL — hole-transport layer,
ITO — indium tin oxide,
LUMO — the lowest unoccupied molecuar orbital,
MW — molecular weight,
NMP — *N*-methyl-2-pyrrolidone,
OLED — organic light-emitting diode,
PEDOT:PSS — poly(3,4-ethylenedioxythiophene) polystyene sulfonate complex,
PR — photorefractive,
PSC — perovskite solar cell,
PTAA — poly[bis(4-phenyl)(2,4,6-trimethylphenyl)amine],
PTPA — poly(4,4′-triphenylamine),
poly-TPD — poly(4-butylphenyldiphenylamine),
SCLC — space charge limited current,
TNT — 2,4,6-triniitrotoluene,
TPA — triphenylamine.

7. References

1. A.Moliton, R.C.Hiorns. *Polym. Int*., **61**, 337 (2012); https://doi.org/10.1002/pi.4173
2. D.J.Berets, D.S.Trans. *Faraday Soc*., **64**, 823 (1968); https://doi.org/10.1039/TF9686400823
3. T.Ito, H.Shirakawa, S.Ikeda. *J. Polym. Sci.: Polym. Chem. Ed*., **12**, 11 (1974); https://doi.org/10.1002/pol.1974.170120102
4. G.Tourillon, F.Garnier. *J. Electroanal. Chem. Interf. Electrochem*., **135**, 173 (1982); https://doi.org/10.1016/0022-0728(82)90015-8
5. A.F.Diaz, K.K.Kanazawa, G.P.Gardini. *J. Chem. Soc., Chem. Commun*., 635 (1979); https://doi.org/10.1039/C39790000635
6. A.F.Diaz, J.A.Logan. *J. Electroanal. Chem. Interf. Electrochem*., **111**, 111 (1980); https://doi.org/10.1016/S0022-0728(80)80081-7
7. C.W.Tang, S.A.VanSlyke. *Appl. Phys. Lett*., **51**, 913 (1987); https://doi.org/10.1063/1.98799
8. J.H.Burroughes, D.D.C.Bradley, A.R.Brown, R.N.Marks, K.Mackay, R.H.Friend, P.L.Burns, A.B.Holmes. *Nature*, **347**, 539 (1990); https://doi.org/10.1038/347539a0
9. G.Yu, J.Gao, J.C.Hummelen, F.Wudl, A.J.Heeger. *Science*, **270**, 1789 (1995); https://doi.org/10.1126/science.270.5243.1789
10. F.Hide, M.A.Díaz-García, B.J.Schwartz, M.R.Andersson, Q.Pei, A.J.Heeger. *Science*, **273**, 1833 (1996); https://doi.org/10.1126/science.273.5283.1833
11. A.V.Vannikov, A.D.Grishina, S.V.Novikov. *Russ. Chem. Rev*., **63**, 103 (1994); https://doi.org/10.1070/rc1994v063n02abeh000074
12. H.Kuhn. In *Intrinsically Conducting Polymers: an Emerging Technology*. (Ed. M.Aldissi). *NATO ASI Series E.* (Kluwer Academic Publishers, 1993). P. 25
13. M.Ishikawa, M.Kawai, Y.Ohsawa. *Synth. Met*., **40**, 231 (1991); https://doi.org/10.1016/0379-6779(91)91778-9
14. C.-H.Yang, F.-J.Liu, L.-R.Huang, T.-L.Wang, W.-C.Lin, M.Sato, C.-H.Chen, C.-C.Chang. *J. Electroanal. Chem.*, **617**, 101 (2008); https://doi.org/10.1016/j.jelechem.2008.01.015

15. S.Beaupre, J.Dumas, M.Leclerc. *Chem. Mater*., **18**, 4011 (2006); https://doi.org/10.1021/cm060407o
16. H.Choi, H.M.Ko, J.Ko. *Dyes Pigm*., **126**, 179 (2016); https://doi.org/10.1016/j.dyepig.2015.11.025
17. Y.Tao, Q.Wang, C.Yang, C.Zhong, J.Qin, D.Ma. *Adv. Funct. Mater*., **20**, 2923 (2010); https://doi.org/10.1002/adfm.201000669
18. A.Cravino, S.Roquet, O.Alévêque, P.Leriche, P.Frère, J.Roncali. *Chem. Mater*., **18**, 2584 (2006); https://doi.org/10.1021/cm060257h
19. I.K.Yakushchenko, M.G.Kaplunov, O.N.Efimov, M.Yu. Belov, S.N.Shamaev. *Phys. Chem. Chem. Phys*., **1**, 1783 (1999); https://doi.org/10.1039/A808613C
20. Yu.N.Luponosov, A.N.Solodukhin, S.A.Ponomarenko. *Polym. Sci., Ser. C*, **56**, 105 (2014); https://doi.org/10.1134/S181123821401007X
21. Y.N.Luponosov, J.Min, A.N.Solodukhin, O.V.Kozlov, M.A.Obrezkova, S.M.Peregudova, T.Ameri, S.N.Chvalun, M.S.Pshenichnikov, C.J.Brabec, S.A.Ponomarenko. *Org. Electron*., **32**, 157 (2016), https://doi.org/ 10.1016/j.orgel.2016.02.027
22. A.Farokhi, H.Shahroosvand, G.D.Monache, M.Pilkington, M.K.Nazeeruddin. *Chem. Soc. Rev*., **51**, 5974 (2022); https://doi.org/10.1039/D1CS01157J
23. C.H.Teh, R.Daik, E.L.Lim, C.C.Yap, M.A.Ibrahim, N.A.Ludin, K.Sopian, M.A.Mat Teridi. *J. Mater. Chem. A*, **4**, 15788 (2016); https://doi.org/10.1039/C6TA06987H
24. F.Peng, J.Xu, Y.Zhang, R.He, W.Yang, Y.Cao. *Polym. Chem*., **10**, 1367 (2019); https://doi.org/10.1039/C8PY01677A
25. D.O.Balakirev, Yu.N.Luponosov, A.L.Mannanov, P.S.Savchenko, Yu.Minenkov, D.Yu.Paraschuk, S.A.Ponomarenko. *Dyes Pigm*., **181**, 108523 (2020); https://doi.org/10.1016/j.dyepig.2020.108523
26. Yu.N.Luponosov, A.N.Solodukhin, A.L.Mannanov, P.S.Savchenko, Y.Minenkov, D.Yu.Paraschuk, S.A.Ponomarenko. *Dyes Pigm.*, **177**, 108260 (2020); https://doi.org/10.1016/j.dyepig.2020.108260
27. Yu.N.Luponosov, A.N.Solodukhin, I.A.Chuyko, S.M.Peregudova, S.A.Ponomarenko. *New J. Chem*., **46**, 12311 (2022); https://doi.org/10.1039/D2NJ01758J
28. G.-S.Liou, S.-H.Hsiao. *J. Polym. Sci. Part A: Polym. Chem*., **41**, 94 (2003); https://doi.org/10.1002/pola.10552
29. J.Jeong, R.S.Kumar, M.Naveen, Y.A.Son. *RSC Adv*., **6**, 78984 (2016); https://doi.org/10.1039/C6RA12112H
30. Y.Wang, L.Duan, M.Zhang, Z.Hameiri, X.Liu, Y.Bai, X.Hao. *Sol. RRL*, **6**, 2200234 (2022); https://doi.org/10.1002/solr.202200234
31. M.M.Tepliakova, A.V.Akkuratov, S.A.Tsarev, P.A.Troshin. *Tetrahedron Lett.*, **61**, 152317 (2020); https://doi.org/10.1016/j.tetlet.2020.152317
32. A.Alexander, A.B.Pillai, V.K.Pulikodan, A.Joseph, M.Raees, M.A.G.Namboothiry. *J. Appl. Phys*., **134**, 085002 (2023); https://doi.org/10.1063/5.0164413
33. O.A.Kraevaya, A.F.Latypova, A.A.Sokolova, A.A.Seleznyova, N.A.Emelianov, N.A.Slesarenko, V.Yu.Markov, L.A.Frolova, P.A.Troshin. *Sustain. Energy Fuels*, **6**, 3485 (2022); https://doi.org/10.1039/D2SE00492E
34. Q.Zhao, R.Wu, Z.Zhang, J.Xiong, Z.He, B.Fan, Z.Dai, B.Yang, X.Xue, P.Cai, S.Zhan, X.Zhang, J.Zhang. *Org. Electron.*, **71**, 106 (2019); https://doi.org/10.1016/j.orgel.2019.05.019
35. C.-H.Kuan, G.-S.Luo, S.Narra, S.Maity, H.Hiramatsu, Y.-W.Tsai, J.-M.Lin, C.-H.Hou, J.-J.Shyue, E.W.-G.Diau. *Chem. Eng. J*., **450**, 138037 (2022); https://doi.org/10.1016/j.cej.2022.138037
36. L.Hu, L.Zhang, W.Ren, C.Zhang, Y.Wu, Y.Liu, Q.Sun, Z.Dai, Y.Cui, L.Cai, F.Zhu, Y.Hao. *J. Mater. Chem. C*, **10**, 9714 (2022); https://doi.org/10.1039/D2TC01494G
37. W.Zhang, J.Smith, R.Hamilton, M.Heeney, J.Kirkpatrick, K.Song, S.E.Watkins, T.Anthopoulos, I.McCulloch. *J. Am. Chem. Soc*., **131**, 10814 (2009); https://doi.org/10.1021/ja9034818
38. K.Mahesh, S.Karpagam, K.Pandian. *Top. Curr. Chem*., **377**, 12 (2019); https://doi.org/10.1007/s41061-019-0237-4
39. D.O.Balakirev, A.N.Solodukhin, S.M.Peregudova, E.A.Svidchenko, N.M.Surin, Yu.V.Fedorov, S.A.Ponomarenko, Yu. N.Luponosov. *Dyes Pigm*., **208**, 110777 (2023); https://doi.org/10.1016/j.dyepig.2022.110777
40. W.Zhang, J.Smith, R.Hamilton, M.Heeney, J.Kirkpatrick, K.Song, S.E.Watkins, T.Anthopoulos, I.McCulloch. *J. Am. Chem. Soc*., **131**, 10814 (2009); https://doi.org/10.1021/ja9034818
41. A.Iwan, D.Sek. *Prog. Polym. Sci*., **36**, 1277 (2011); https://doi.org/10.1016/j.progpolymsci.2011.05.001
42. H.-J.Yen, G.-S.Liou. *Polym. Chem*., **9**, 3001 (2018); https://doi.org/10.1039/C8PY00367J
43. H.-J.Yen, G.-S.Liou. *Prog. Polym. Sci*., **89**, 250 (2019); https://doi.org/10.1016/j.progpolymsci.2018.12.001
44. P.Agarwala, D.Kabra. *J. Mater. Chem. A*, **5**, 1348 (2017); https://doi.org/10.1039/C6TA08449D
45. C.Kim, D.H.Lee, S.Kim, J.Kim, T.Park, J.B.Arockiam, J.Lim. *Sol. RRL*, **8**, 2400048 (2024); https://doi.org/10.1002/solr.202400048
46. K.Neumann, M.Thelakkat. *RSC Adv*., **4**, 43550 (2014); https://doi.org/10.1039/C4RA05564
47. M.W.Thesen, B.Höfer, M.Debeaux, S.Janietz, A.Wedel, A.Köhler, H.-H.Johannes, Hartmut Krueger. *J. Polym. Sci. Part A: Polym. Chem*., **48**, 3217 (2010); https://doi.org/10.1002/pola.24127
48. J.-H.Wu, G.-S.Liou. *ACS Appl. Mater. Interfaces*, **7**, 15988 (2015); https://doi.org/10.1021/acsami.5b04123
49. T.Nakashita, R.Sugimoto, T.A.P.Hai. *Bull. Chem. Soc. Jpn*., **89**, 1328 (2016); https://doi.org/10.1246/bcsj.20160248
50. S.Mi, J.Wu, J.Liu, J.Zheng, C.Xu. *Org. Electron*., **23**, 116 (2015); https://doi.org/10.1016/j.orgel.2015.04.014
51. X.Wang, L.Lv, W.Gu, X.Wang, T.Dong, Z.Yang, H.Cao, H.Huang. *Dyes Pigm*., **140**, 141 (2017); https://doi.org/10.1016/j.dyepig.2017.01.041
52. I.Kang, T.Lee, Y.R.Yoon, J.W.Kim, B.-K.Kim, J.Lee, J.H.Lee, S.Y.Kim. *Materials*, **14**, 7885 (2021); https://doi.org/10.3390/ma14247885
53. K.Yamamoto, D.Suemas, K.Masuda, K.Aita, T.Endo. *ACS Appl. Mater. Interface*, **10**, 6346 (2018); https://doi.org/10.1021/acsami.7b17943
54. C.Su, H.He, L.Xu, K.Zhao, C.Zhengc, C.Zhang. *J. Mater. Chem. A*, **5**, 2701 (2017); https://doi.org/10.1039/C6TA10127E
55. S.Chen, T.Jia, G.Zhou, C.Zhang, Q.Hou, Y.Wang, S.Luo, G.Shi, Y.Zeng. *J. Electrochem. Soc*., **166**, A2543 (2019); https://doi.org/10.1149/2.0941912jes
56. H.-K.Shih, Y.-L.Chu, F.-C.Chang, C.-Y.Zhu, S.-W.Kuo. *Polym. Chem*., **6**, 6227 (2015); https://doi.org/10.1039/C5PY00882D
57. Z.Zhong, X.Wang, T.Guo, J.Cui, L.Ying, J.Peng, Y.Cao. *Org. Electron*., **53**, 35 (2018); https://doi.org/10.1016/j.orgel.2017.10.038
58. Y.-K.Fang, W.-Y.Lee, C.-S.Tuan, L.-H.Lu, W.-J.Teng, W.-C.Chen. *Polym. J*., **42**, 327 (2010); https://doi.org/10.1038/pj.2010.1
59. K.-M.Yeh, C.-C.Lee, Y.Chen. *Synth. Met*., **158**, 565 (2008); https://doi.org/10.1016/j.synthmet.2008.04.001
60. H.N.Giang, K.Kinashi, W.Sakai, N.Tsutsumi. *J. Photochem. Photobiol. A: Chem*., **291**, 26 (2014); https://doi.org/10.1016/j.jphotochem.2014.06.008
61. W.Xu, T.Du, M.Sachs, T.J.Macdonald, G.Min, L.Mohan, K.Stewart, C.-T.Lin, J.Wu, R.Pacalaj, S.A.Haque, M.A.McLachlan, J.R.Durrant. *Cell Rep. Phys. Sci*., **3**, 100890 (2022); https://doi.org/10.1016/j.xcrp.2022.100890
62. X.Hu, C.Tao, J.Liang, C.Chen, X.Zheng, J.Li, J.Li, Y.Liu, G.Fang. *Sol. Energy*, **218**, 368 (2021); https://doi.org/10.1016/j.solener.2021.02.064
63. H.Zhang, W.Hui, Z.Wang, M.Li, H.Xi, Y.Zheng, X.Liu. *Mater. Today Energy*, **30**, 101159 (2022); https://doi.org/10.1016/j.mtener.2022.101159

64. Z.Safari, M.B.Zarandi, A.Giuri, F.Bisconti, S.Carallo, A.Listorti, C.E.Corcione, M.R.Nateghi, A.Rizzo, S.Colella. *Nanomaterials*, **9**, 1627 (2019); https://doi.org/10.3390/nano9111627
65. Y.Yao, C.Cheng, C.Zhang, H.Hu, K.Wang, S.De Wolf. *Adv. Mater*., **34**, 2203794 (2022); https://doi.org/10.1002/adma.202203794
66. F.M.Rombach, S.A.Haque, T.J.Macdonald. *Energy Environ. Sci*., **14**, 5161 (2021); https://doi.org/10.1039/D1EE02095A
67. M.C.Scharber, N.S.Sariciftci. *Adv. Mater. Technol*., **6**, 2000857 (2021); https://doi.org/10.1002/admt.202000857
68. C.Su, X.Zhu, L.Xu, N.Zhou, H.He, C.Zhang. *Electrochim. Acta*, **196**, 440 (2016); https://doi.org/10.1016/j.electacta.2016.02.169
69. F.Babudri, G.M.Farinola, F.Naso, R.Ragni. *Chem. Commun*., 1003 (2007); https://doi.org/10.1039/B611336B
70. J.C.Chen, C.J.Chiang, Y.C.Liu. *Synth. Met*., **160**, 1953 (2010); https://doi.org/10.1016/j.synthmet.2010.07.015
71. B.Y.Myung, J.J.Kim, T.H.Yoon. *J. Polym. Sci. Part A: Polym. Chem*., **40**, 4217 (2002); https://doi.org/10.1002/pola.10512
72. G.Kim, F.Basarir, T.-H.Yoon. *Synth. Met*., **161**, 2092 (2011); https://doi.org/10.1016/j.synthmet.2011.07.026
73. R.Hashimoto, M.A.Truong, A.Gopal, A.I.Rafieh, T.Nakamura, R.Murdey, A.Wakamiya. *J. Photopolym. Sci. Technol*., **33**, 505 (2020); https://doi.org/10.2494/photopolymer.33.505
74. Y.N.Luponosov, A.N.Solodukhin, A.L.Mannanov, P.S.Savchenko, B.A.-L.Raul, S.M.Peregudova, N.M.Surin, A.V.Bakirov, M.A.Shcherbina, S.N.Chvalun, M.S.Pshenichnikov, D.Y.Paraschuk, S.A.Ponomarenko. *Mater. Today Energy*, **22**, 100863 (2021); https://doi.org/10.1016/j.mtener.2021.100863
75. E.D.Papkovskaya, D.O.Balakirev, J.Min, Yu.N.Luponosov. *Mater. Today Energy*, **43**, 101591 (2024); https://doi.org/10.1016/j.mtener.2024.101591
76. G.R.Kumar, S.K.Sarkar, P.Thilagar, *Chem. – Eur. J*., **22**, 17215 (2016); https://doi.org/10.1002/chem.201603349
77. T.S.Le, I.A.Chuyko, L.O.Luchnikov, K.A.Ilicheva, P.O.Sukhorukova, D.O.Balakirev, N.S.Saratovsky, A.O.Alekseev, S.S.Kozlov, D.S.Muratov, V.V.Voronov, P.A.Gostishchev, D.A.Kiselev, T.S.Ilina, A.A.Vasilev, A.Y.Polyakov, E.A.Svidchenko, O.A.Maloshitskaya, Yu.N.Luponosov, D.S.Saranin. *Sol. RRL,* **8**, 2400437 (2024); https://doi.org/10.1002/solr.202400437
78. J.Sun, Z.Liang. *ACS Appl. Mater. Interface*., **8** (28),18301 (2016); https://doi.org/10.1021/acsami.6b05661
79. W.Zhang, C.Wang G.Liu, X.Zhu, X.Chen, L.Pan, H.Tan, W.Xue, Z.Ji, J.Wang, Y.Chen, R.-W.Li. *Chem. Commun*., **50**, 11856 (2014); https://doi.org/10.1039/C4CC04696J
80. K.Ogino, A.Kanegae, R.Yamaguchi, H.Sato, J.Kurjata. *Macromol. Rapid Commun*., **20**, 103 (1999); https://doi.org/10.1002/(SICI)1521-3927(19990301)20:3<103::AID-MARC103>3.0.CO;2-Q
81. F.Huiting, M.Dong, M.Xiangyi, S.Xiaobo, H.Lijun, F.Yuzun, L.Yan, M.Wei, S.Yanming, W.Zhaohui. *J. Mater. Chem. A*, **5**, 3475 (2017); https://doi.org/10.1039/C6TA09049D
82. D.F.Nugraha, Y.Yu, J.W.Yoon, H.Ahn, J.A.Prayogo, D.R.Whang, J.Lee, H.Choi, D.W.Chang. *J. Mater. Chem. C*, **11**, 14009 (2023); https://doi.org/10.1039/D3TC02514D
83. G.Wang, Y.Wu, W.Ding, G.Yu, Z.Hu, H.Wang, S.Liu, Y.Zoua, C.Pan. *J. Mater. Chem. A*, **3**, 14217 (2015); https://doi.org/10.1039/C5TA03425F
84. S.Lian, W.Zheng, G.Jin, B.Xiao, Z.Liu, X.Li, Y.Pan, J.Huang, L.Hou, Y.Mo, H.Wu. *Dyes Pigm*., **149**, 133 (2018); https://doi.org/10.1016/j.dyepig.2017.07.011
85. S.W.Lee, M.Jeong, D.R.Whang, J.H.Kim, D.W.Chang. *Macromol. Res*., **28**, 1297 (2020); https://doi.org/10.1007/s13233-020-8167-0
86. H.N.Giang, K Kinashi, W.Sakai, N.Tsutsumi. *Polym. J*., **46**, 59 (2014); https://doi.org/10.1038/pj.2013.68
87. R.-C.Lina, S.-W.Kuo. *RSC Adv*., **8**, 13592 (2018); https://doi.org/10.1039/C8RA00506K
88. T.Geng, Z.Zhu, X.Wang, H.Xia, Y.Wang, D.Li. *Sens. Actuators B: Chem*., **244**, 334 (2017); https://doi.org/10.1016/j.snb.2017.01.005
89. Z.Chen, C.Su, X.Zhu, R.Xu, L.Xu, C.Zhang. *J. Polym. Sci. Part A: Polym. Chem*., **56**, 2574 (2018); https://doi.org/10.1002/pola.29239
90. J.K.Feng, Y.L.Cao, X.P.Ai, H.X.Yang. *J. Power Sources*., **177**, 199 (2008); https://doi.org/10.1016/j.jpowsour.2007.10.086
91. U.S.Schubert, A.Winter, G.R.Newkome. *An Introduction to Redox Polymers for Energy-Storage Applications*. (1st Edn). (Wiley-VCH, 2023). 544 p.; https://doi.org/10.1002/9783527843466
92. S.I.Bhat, Y.Ahmadi , S.Ahmad. *Ind. Eng. Chem. Res*., **57**, 10754 (2018); https://doi.org/10.1021/acs.iecr.8b01969
93. K.-L.Wang, S.-T.Huang, L.-G.Hsieh, G.-S.Huang. *Polymer*, **49**, 4087 (2008); https://doi.org/10.1016/j.polymer.2008.07.053
94. K.R.P.Kumar, M.G.Murali, D.Udayakumar. *Des. Monomers Polym*., **17**, 7 (2013); https://doi.org/10.1080/15685551.2013.771313
95. C.Bathula, A.B.Appiagyei, H.Yadav, A.Kumar K., S.Ramesh, N.K.Shrestha,S.Shinde, H.-S.Kim, H.S.Kim, L.V.Reddy, A.Mohammed. *Nanomaterials*, **9**, 1787 (2019); https://doi.org/10.3390/nano9121787
96. J.Tao, H.Chen, Y.Han, X.-P.Zhang, S.Peng, Z.Wu, H.Liu, J.Liu. *Eur. Polym. J*., 215, 113229 (2024); https://doi.org/10.1016/j.eurpolymj.2024.113229
97. T.Manifar, S.Rohani. *Canad. J. Chem. Engin.*, **82**, 323 (2008); https://doi.org/10.1002/cjce.5450820213
98. R.Rybakiewicz, M.Zagorska, A.Pron. *Chem. Pap*., **71**, 243 (2017); https://doi.org/10.1007/s11696-016-0097-0
99. V.N.Charushin, E.V.Verbitskiy, O.N.Chupakhin, D.V.Vorobyeva, P.S.Gribanov, S.N.Osipov, A.V.Ivanov, S.V.Martynovskaya, E.F.Sagitova, V.D.Dyachenko, I.V.Dyachenko, S.G.Krivokolysko, V.V.Dotsenko, A.V.Aksenov, D.A.Aksenov, N.A.Aksenov, A.A.Larini, L.L.Fershtat, V.M.Muzalevskiy, V.G.Nenajdenko, A.V.Gulevskaya, A.F.Pozharskii, E.A.Filatova, K.V.Belyaeva, B.A.Trofimov, I.A.Balova, N.A.Danilkina, A.I.Govdi, A.S.Tikhomirov, A.E.Shchekotikhin, M.S.Novikov, N.V.Rostovskii, A.F.Khlebnikov, Yu.N.Klimochkin, M.V.Leonova, I.M.Tkachenko, V.A.O.Mamedov, V.L.Mamedova, N.A.Zhukova, V.E.Semenov, O.G.Sinyashin, O.V.Borshchev, Yu.N.Luponosov, S.A.Ponomarenko, A.S.Fisyuk, A.S.Kostyuchenko, V.G.Ilkin, T.V.Beryozkina, V.A.Bakulev, A.S.Gazizov, A.A.Zagidullin, A.A.Karasik, M.E.Kukushkin, E.K.Beloglazkina, N.E.Golantsov, A.A.Festa, L.G.Voskresensky, V.S.Moshkin, E.M.Buev, V.Ya.Sosnovskikh, I.A.Mironova, P.S.Postnikovt, V.V.Zhdankin, M.S.O.Yusubov, I.A.Yaremenko, V.A.Vil, I.B.Krylov, A.O.Terent'ev, Yu.G.Gorbunova, A.G.Martynov, A.Yu.Tsivadze, P.A.Stuzhin, S.S.Ivanova, O.I.Koifman, O.N.Burov, M.E.Kletskii, S.V.Kurbatov, O.I.Yarovaya, K.P.Volcho, N.F.Salakhutdinov, M.A.Panova, Ya.V.Burgart, V.I.Saloutin, A.R.Sitdikova, E.S.Shchegravina, A.Yu.Fedorov. *Russ. Chem. Rev*., **93** (7), RCR5125 (2024); https://doi.org/10.59761/RCR5125
100. D.C.Santra, S.Nad, S.Malik. *J. Electroanal. Chem*., **823**, 203 (2018); https://doi.org/10.1016/j.jelechem.2018.06.015
101. L.Maa, H.Ma. *RSC Adv*., **9**, 18098 (2019); https://doi.org/10.1039/C9RA02469G
102. Y.Kim, E.H.Jung, G.Kim, D.Kim, B.J.Kim, J.Seo. *Adv. Energy Mater*., **8**, 1801668 (2018); https://doi.org/10.1002/aenm.201801668
103. J.Ostrauskaite, H.R.Karickal, A.Leopold, D.Haarerb, M.Thelakkat. *J. Mater. Chem.*, **12**, 58 (2002); https://doi.org/10.1039/B105930K
104. N.Li, Y.Wang, Z.Li. *Chin. J. Org. Chem*., **44**, 1 (2024); https://doi.org/10.6023/cjoc202404016
105. M.M.H.Desoky, F.Cruciani, P.Quagliotto, G.Viscardi. *J. Mol. Struct*., **1304**, 137635 (2024); https://doi.org/10.1016/j.molstruc.2024.137635

106. Y.Liao, H.Wang, M.Zhu, A.Thomas. *Adv. Mater*., **30**, 1705710 (2018); https://doi.org/10.1002/adma.201705710
107. A.Krishna , A.V.Lunchev, A.C.Grimsdale. In *Synthetic Methods for Conjugated Polymers and Carbon Materials*. Vol. 246. (Eds M.Leclerc, J.-F.Morin). (Wiley-VCH, 2017). P. 59
108. J.Murage, J.W.Eddy, J.R.Zimbalist, T.B.McIntyre, Z.R.Wagner, F.E.Goodson. *Macromolecules*, **41**, 7330 (2008); https://doi.org/10.1021/ma801275y
109. T.-H.Kao, Z.Qiao, P.Y.Ho, O.Ditzer, N.Sun, B.Voit, F.Lissel. *J. Polym. Sci*., **60**, 1899 (2022); https://doi.org/10.1002/pol.20220016
110. L.Zhang, W.Zhan, Y.Dong, T.Yang, C.Zhang, M.Ouyang, W.Li. *ACS Appl. Mater. Interfaces*, **13**, 20810 (2021); https://doi.org/10.1021/acsami.1c02745
111. L.Chen, Z.Lin, L.Liu, X.Zhang, W.Shi, D.Ge, Y.Sun. *ACS Biomater. Sci. Eng*., **5**, 4861 (2019); https://doi.org/10.1021/acsbiomaterials.9b00461
112. K.Neumann, C.Schwarz, A.Köhler, M.Thelakkat. *J. Phys. Chem. C*, **118**, 27 (2014); https://doi.org/10.1021/jp407014q
113. S.Goker, S.O.Hacioglu, G.Hizalan, E.Aktas, A.Cirpan, L.Toppare. *Macromol. Chem. Phys.*, **218**, 1600544 (2017); https://doi.org/10.1002/macp.201600544
114. T.Zheng, A.M.Schneider, L.Yu. In *Synthetic Methods for Conjugated Polymers and Carbon Materials*. (Eds M.Leclerc, J.-F.Morin). (Wiley-VCH, 2017). P. 1; https://doi.org/10.1002/9783527695959.ch1
115. Z.Liang, A.Neshchadin, Z.Zhang, F.-G.Zhao, X.Liu, L.Yu. *Polym. Chem*., **14**, 4611 (2023); https://doi.org/10.1039/D3PY00815K
116. A.Krishna, A.V.Lunchev, A.C.Grimsdale. In *Synthetic Methods for Conjugated Polymers and Carbon Materials*. (Eds M.Leclerc, J.-F.Morin). (Wiley-VCH, 2017). P. 59; https://doi.org/10.1002/9783527695959.ch1
117. H.Wang, W.Ding, G.Wang, C.Pan, M.Duan, G.Yu. *J. Appl. Polym. Sci*., **133** (47), 44182 (2016); https://doi.org/10.1002/app.44182
118. T.Yamamoto, S.-B.Kim, T.Koizumi. *Polym. J*., **41**, 810 (2009); https://doi.org/10.1295/polymj.PJ2009102
119. S.Xu, E.H.Kim, A.Wei, E.Negishi. *Sci. Technol. Adv. Mater*., **15**, 044201 (2014); https://doi.org/10.1088/1468-6996/15/4/044201
120. H.-W.Chang, K.-H.Lin, C.-C.Chueh, G.-S.Liou, W.-C.Chen. *J. Polym. Sci. Part A: Polym. Chem*., **47**, 3957 (2009); https://doi.org/10.1002/pola.23465
121. M.Goshaev, O.S.Otroshchenko, A.S.Sadykov. *Russ. Chem. Rev*., **41**, 1046 (1972); https://doi.org/10.1070/RC1972v041n12ABEH002112
122. Ya.O.Mezhuev, Yu.V.Korshak, M.I.Shtilman. *Russ. Chem. Rev*., **86**, 1271 (2017); https://doi.org/10.1070/RCR4755
123. C.Takahashi, S.Moriya, N.Fugono, H.C.Lee, H.Sato. *Synth. Met*., **129**, 123 (2002); https://doi.org/10.1016/S0379-6779(02)00010-3
124. J.H.Sim, K.Yamada, S.H.Lee, S.Yokokura, H.Sato. *Synth. Met*., **157**, 940 (2007); https://doi.org/10.1016/j.synthmet.2007.09.009
125. H.-Y.Lin, G.-S.Liou. *J. Polym. Sci. Part A: Polym. Chem*., **11**, 285 (2008); https://doi.org/10.1002/pola.23155
126. Z.Cao, Y.Abe, T.Nagahama, K.Tsuchiya, K.Ogino. *Polym*., **54** (1), 269 (2013); https://doi.org/10.1016/j.polymer.2012.11.028
127. Y.Yang, Q.Zhang, S.Zhang, S.Li. *Polymer*, **54**, 5698 (2013); https://doi.org/10.1016/j.polymer.2013.08.039
128. T.Geng, Z.Zhu, X.Wang, H.Xia, Y.Wang, D.Li. *Sens. Actuators B: Chem*., **244**, 334 (2017); https://doi.org/10.1016/j.snb.2017.01.005
129. K.Ogino, A.Kanegae, R.Yamaguchi, H.Sato, J.Kurjata. Macromol. *Rapid Commun*., **20**, 103 (1999); https://doi.org/10.1002/(SICI)1521-3927(19990301)20:3<103::AID-MARC103>3.0.CO;2-Q
130. J.Lee, J.Park, H.Choi, Y.R.Yoon, M.Seo, S.Song, B.-K.Kim, S.Y.Kim. *Polym. Bull*., **78**, 965 (2021); https://doi.org/10.1007/s00289-020-03146-y
131. V.M.Niemi, P.Knuuttila, J.-E.Osterholm, J.Korvola. *Polymer*, **33**, 1559 (1992); https://doi.org/10.1016/0032-3861(92)90138-M
132. F.Bekkar, F.Bettahar , I.Moreno, R.Meghabar, M.Hamadouche, E.Hernáez, J.L.Vilas-Vilela, L.Ruiz-Rubio. *Polymers*, **12**., 2227 (2020); https://doi.org/10.3390/polym12102227
133. S.-H.Hsiao, J.-W.Lin. *Polym. Chem*., **5**, 6770 (2014); https://doi.org/10.1039/C4PY00610K
134. G.Wang, Z.Liu, X.Wang, J.Liu, Y.Chen, B.Liu. *ACS Omega*, **4** (12), 15215 (2019); https://doi.org/10.1021/acsomega.9b02101
135. N.Guven, O.S.Cemaloglu, P.Camurlu. *J. Electrochem. Soc*., **169**, 026511 (2022); https://doi.org/10.1149/1945-7111/ac4f71
136. W.Fu, H.Chen, Y.Han, W.Wang, R.Zhanga, J.Liu. *New J. Chem*., **45**, 19082 (2021); https://doi.org/10.1039/D1NJ04074J
137. G.Fomo, T.Waryo, U.Feleni, P.Baker, E.Iwuoha. In *Functional Polymers*. (Eds M.A.J.Mazumder, H.Sheardown, A.Al-Ahmed). (Berlin: Springer, 2019). P. 105; https://doi.org/10.1007/978-3-319-95987-0
138. M.Renfige, E.J.G.Lopez, L.Macor, C.Solis, J.E.Durantini, G.Morales, L.Otero, E.N.Durantini, D.A.Heredia, M.Gervaldo. *Electrochim. Acta*, **486**, 144120 (2024); https://doi.org/10.1016/j.electacta.2024.144120
139. S.Balakrishnan, R.Venugopal, A.Harikumar, B.Deb, J.Joseph. *ACS Appl. Polym. Mater*., **5**, 4170 (2023); https://doi.org/10.1021/acsapm.3c00393
140. M.Nowacki, M.Wałęsa-Chorab. *Prog. Org. Coat*., **182**, 107691 (2023); https://doi.org/10.1016/j.porgcoat.2023.107691
141. M.Wałęsa-Chorab, W.G.Skene. *Prog. Org. Coat*., **187**, 108113 (2024); https://doi.org/10.1016/j.porgcoat.2023.108113
142. K.Kanazawa, S.Uemura. *Eur. Polym. J.*, **119**, 322 (2019); https://doi.org/10.1016/j.eurpolymj.2019.08.010
143. Y.Pan, P.Gao, H.Chen, X.-P.Zhang, Y.Han, Z.Gu, J.Xu, R.Zhang, J.Liu. *J. Mol. Struct*., **1292**, 136182 (2023); https://doi.org/10.1016/j.molstruc.2023.136182
144. E.J.W.List, R.Guentner, P.S.De Freitas, U.Scherf. *Adv. Mater*., **14**, 374 (2002); https://doi.org/10.1002/1521-4095(20020304)14:5<374::AID-ADMA374>3.0.CO;2-U
145. J.L.Reddinger, J.R.Reynolds. In *Radical Polymerisation Polyelectrolyte*. (Eds I.Capek, J.Hernfández-Barajas, D.Hunkeler, J.L.Reddinger, J.R.Reynolds, C.Wandrey). (Berlin, Heidelberg: Springer, 1999). P. 57
146. P.Marrec, C.Dano, N.Gueguen-Simonet, J. Simonet. *Synth. Met*., **89**, 171 (1997); https://doi.org/10.1016/S0379-6779(97)81214-3
147. C.Cao, M.Xiao, X.Yang, J.Zhang, F.Huang, Y.Cao. *J. Mater. Chem. C*, **6**, 8020 (2018); https://doi.org/10.1039/C8TC02021C
148. L.Giraud, S.Grelier, E.Grau, G.Hadziioannou, C.Brochon, H.Cramail, E.Cloutet. *J. Mater. Chem. C*, **8**, 9792 (2020); https://doi.org/10.1039/D0TC01645D
149. M.Oh, S.Jo, T.-H.Huh, Y.-J.Kwark, T.S.Lee. *Polymer*, **237**, 124384 (2021); https://doi.org/10.1016/j.polymer.2021.124384
150. P.A.Sobarzo,A.F.González, E.Schott, L.H.Tagle, A.Tundidor-Camba, C.González-Henríquez, I.A.Jessop, C.A.Terraza. *Polymers*, **11**, 216 (2019); https://doi.org/10.3390/polym11020216
151. Y.Liu, Y.Xin, J.Li, G.Zhao, B.Ye, S.Xu, S.Cao. *React. Funct. Polym*., **67**, 253 (2007); https://doi.org/10.1016/j.reactfunctpolym.2006.12.003
152. K.B.Labasan, H.-J.Lin, F.Baskoro, J.J.H.Togonon, H.Q.Wong, C.-W.Chang, S.D.Arco, H.-J.Yen. *ACS Appl. Mater. Interfaces*, **13**, 17467 (2021); https://doi.org/10.1021/acsami.1c00065
153. C.Su, M.Sun, P.Guo, L.Xu. *J. Electrochem. Energy Conv. Stor*., **18**, 031011 (2021); https://doi.org/10.1115/1.4049574

154. Y.-T.Chern, S.-J.Zhang, S.-J.Ho, Y.-J.Shao, Y.-J.Wang, G.-S.Liou. *ACS Appl. Polym. Mater*., **6**, 5256 (2024); https://doi.org/10.1021/acsapm.4c00432
155. X.Lv, M.Shao, X.Zhu, L.Xu, M.Ouyang, C.Zhou, J.Dong, C.Zhang. *ACS Appl. Polym. Mater*., **5**, 3595 (2023); https://doi.org/10.1021/acsapm.3c00250
156. K.L.O.Chin, P.J.Ong, Q.Zhu, J.Xu, M.H.Chua. *Molecules*, **29**, 2340 (2024); https://doi.org/10.3390/molecules29102340
157. E.Cucu, Erdin Dalkılıç R.Altundas, A.E.Sadak. *Micropor. Mesopor. Mater*., **330**, 111567 (2022); https://doi.org/10.1016/j.micromeso.2021.111567
158. W.J.Jang, J.-H.Jang, D.B.Kim, J.M.Kim, H.Kang, B.-G.Kang. *Eur. Polym. J*., **216**, 113284 (2024); https://doi.org/10.1016/j.eurpolymj.2024.113284
159. B.-G.Kang, N.-G.Kang, J.-S.Lee. *Macromolecules*, **43**, 8400 (2010); https://doi.org/10.1021/ma1014353
160. T.V.Nguyen, T.Maeda, H.Nakazumi, S.Yagi. *Chem. Lett*., **45**, 291 (2016); https://doi.org/10.1246/cl.151101
161. J.Tydlität, M.Fecková, P.le Poul, O.Pytela, M.Klikar, J.Rodríguez-López, F.Robin-le Guen, S.Achelle. *Eur. J. Org. Chem*., 1921 (2019); https://doi.org/10.1002/ejoc.201900026
162. T.Zhang, I.E.Brumboiu, C.Grazioli, A.Guarnaccio, M.Coreno, M.de Simone, A.Santagata, H.Rensmo, B.Brena, V.Lanzilotto, C.Puglia. *J. Phys. Chem. C*, **122**, 17706 (2018); https://doi.org/10.1021/acs.jpcc.8b06475
163. P.Agarwalaa, D.Kabra. *J. Mater. Chem. A*, **5**, 1348 (2017); https://doi.org/10.1039/C6TA08449D
164. P.Cias, C.Slugovc, G.Gescheidt. *J. Phys. Chem. A*, **115**, 14519 (2011); https://doi.org/10.1021/jp207585j
165. G.E.Eperon, V.M.Burlakov, P.Docampo, A.Goriely, H.J.Snaith. *Adv. Funct. Mater.*, **24**, 151 (2013); https://doi.org/10.1002/adfm.201302090
166. Q.Zhang, P.-I.Wang , G.L.Ong, S.H.Tan, Z.W.Tan, Y.H.Hii, Y.L.Wong, K.S.Cheah, S.L.Yap,T.S.Ong, T.Y.Tou, C.H.Nee, D.J.Liaw, S.S.Yap. *Polymers*, **11**, 840 (2019); https://doi.org/10.3390/polym11050840
167. R.Rybakiewicz, M.Zagorska, A.Pron. *Chem. Pap*., **71**, 243 (2016); https://doi.org/10.1007/s11696-016-0097-0
168. C.Su, F.Yang, L.Ji, L.Xu, C.Zhang. *J. Mater. Chem. A*, **2**, 20083 (2014); https://doi.org/10.1039/C4TA03413A
169. H.Zhuang, Q.Zhou, Q.Zhang, H.Li, N.Li, Q.Xu, J.Lu. *J. Mater. Chem*. *C*, **3**, 416 (2015); https://doi.org/10.1039/C4TC01844C
170. A.K.Jena, A.Kulkarni, T.Miyasaka. *Chem Rev*., **119**, 3036 (2019); https://doi.org/10.1021/acs.chemrev.8b00539
171. T.Miyasaka, A.Kulkarni, G.M.Kim, S.Oz, A.K.Jena. *Adv. Energy Mater*., **10**, 1902500 (2020); https://doi.org/10.1002/aenm.201902500
172. C.-L.Chen, S.-S.Zhang, T.-L.Liu, S.-H.Wu, Z.-C.Yang, W.-T.Chen, R.Chen, W.Chen. *Rare Met*., **39**, 131 (2020); https://doi.org/10.1007/s12598-019-01341-z
173. Q.Fan, G.V.Biesold-McGee, J.Ma, Q.Xu, S.Pan, J.Peng, Z.Lin. *Angew. Chem., Int. Ed. Engl*., **59**, 1030 (2020); https://doi.org/10.1002/anie.201904862
174. J.Y.Kim, J.-W.Lee, H.S.Jung, H.Shin, N.-G.Park. *Chem. Rev*., **120**, 7867 (2020); https://doi.org/10.1021/acs.chemrev.0c00107
175. P.Tonui, S.O.Oseni, G.Sharma, Q.Yan, G.T.Mola. *Renew. Sustain. Energy Rev*., **91**, 1025 (2018); https://doi.org/10.1016/j.rser.2018.04.069
176. P.Vivo, J.K.Salunke, A.Priimagi. *Materials*, **10**, 1087 (2017); https://doi.org/10.3390/ma10091087
177. J.Urieta-Mora, I.García-Benito, A.Molina-Ontoria, N.Martín. *Chem. Soc. Rev*., **47**, 8541 (2018); https://doi.org/10.1039/c8cs00262b
178. J.H.Lee, M.H.Jang, C.H.Lee, J.-J.Lee, S.Y.Lee, J.W.Jo. *Dyes Pigm*., **200**, 110162 (2022); https://doi.org/10.1016/j.dyepig.2022.110162
179. S.Yi, W.Deng, S.Sun, L.Lan, Z.He, W.Yang, B.Zhang. *Polymers*, **10**, 52 (2018); https://doi.org/10.3390/polym10010052
180. D.Bi, G.Boschloo, A.Hagfeldt. *NANO: Brief Rep. Rev.*, **09** (05), 1440001 (2014); https://doi.org/10.1142/S1793292014400013
181. Y.Ko, Y.Kim, C.Lee, Y.Kim, Y.Jun. *ACS Appl. Mater. Interfaces*, **10**, 11633 (2018); https://doi.org/10.1021/acsami.7b18745
182. K.T.Cho, S.Paek, G.Grancini, C.Roldan-Carmona, P.Gao, Y.Lee, M.K.Nazeeruddin. *Energy Environ. Sci*., **10**, 621 (2017); https://doi.org/10.1039/C6EE03182J
183. B.L.Watson, N.Rolston, K.A.Bush, L.Taleghania, R.H.Dauskardt. *J. Mater. Chem. A*, **5**, 19267 (2017); https://doi.org/10.1039/C7TA05004F
184. B.Xu, Z.Zhu, J.Zhang, H.Liu, C.-C.Chueh, X.Li, A.K.-Y.Jen. *Adv. Eng. Mater*., **7**, 1700683 (2017); https://doi.org/10.1002/aenm.201700683
185. S.Wang, Z.Huang, X.Wang, Y.Li, M.Günther, S.Valenzuela, P.Parikh, A.Cabreros, W.Xiong, Y.S.Meng. *J. Am. Chem. Soc*., **140**, 16720 (2018); https://doi.org/10.1021/jacs.8b09809
186. A.F.Latypova, N.A.Emelianov, D.O.Balakirev, P.K.Sukhorukova, N.K.Kalinichenko, P.M.Kuznetsov, Y.N.Luponosov, S.M.Aldoshin, S.A.Ponomarenko, P.A.Troshin, L.A.Frolova. *ACS Appl. Energy Mater*., **5**, 5395 (2022); https://doi.org/10.1021/acsaem.1c03119
187. W.Zhou, Z.Wen, P.Gao. *Adv. Energy Mater*., **8**, 1702512 (2018); https://doi.org/10.1002/aenm.201702512
188. Y.Xu, T.Bu, M.Li, T.Qin, C.Yin, N.Wang, R.Li, J.Zhong, H.Li, Y.Peng, J.Wang, L.Xie, W.Huang. *ChemSusChem.*, **10**, 2578 (2017); https://doi.org/10.1002/cssc.201700584
189. S.Valero, S.Collavini, S.F.Völker, M.Saliba, W.R.Tress, S.M.Zakeeruddin, M.Grätzel, J.L.Delgado. *Macromolecules*, **52**, 2243 (2019); https://doi.org/10.1021/acs.macromol.9b00165
190. Y.Xie, X.Wang, Q.Chen, S.Liu, Y.Yun, Y.Liu, C.Chen, J.Wang, Y.Cao, F.Wang, T.Qin, W.Huang. *Macromolecules*, **52**, 4757 (2019); https://doi.org/10.1021/acs.macromol.9b00372
191. X.Sun, X.Deng, Z.Li, B.Xiong, C.Zhong, Z.Zhu, Z.Li, A.K.-Y.Jen. *Adv. Sci*., **7**, 1903331 (2020); https://doi.org/10.1002/advs.201903331
192. X.Sun, Z.Li, X.Yu, X.Wu, C.Zhong, D.Liu, D.Lei, A.K.-Y.Jen, Z.Li, Z.Zhu. *Angew. Chem., Int. Ed*., **60**, 7227 (2021); https://doi.org/10.1002/anie.202016085
193. M.M.Elnaggar, L.G.Gutsev, N.A.Emelianov, P.M.Kuznetsov, L.A.Frolova, L.A.Frolova, S.M.Aldoshin, P.A.Troshin. *ACS Appl. Energy Mater*., **5**, 5388 (2022); https://doi.org/10.1021/acsaem.1c03040
194. B.Li, K.S.Valer Yang, Q.Liao, Y.Wang, M.Su, Y.Li, Y.Shi, X.Feng, J.Huang, H.Sun, X.Guo. *Adv. Funct. Mater*., **31**, 2100332 (2021); https://doi.org/10.1002/adfm.202100332
195. R.Chen, S.Liu, X.Xu, F.Ren, J.Zhou, X.Tian, Z.Yang, X.Guanz, Z.Liu, S.Zhang, Y.Zhang, Y.Wu, L.Han, Y.Qi, W.Chen. *Energy Environ. Sci*., **15**, 2567 (2022); https://doi.org/10.1039/D2EE00433J
196. X.Wu, D.Gao, X.Sun, S.Zhang, Q.Wang, B.Li, Z.Li, M.Qin, X.Jiang, C.Zhang, Z.Li, X.Lu, N.Li, S.Xiao, X.Zhong, S.Yang, Z.Li, Z.Zhu. *Adv. Mater*., **35**, 2208431 (2023); https://doi.org/10.1002/adma.202208431
197. M.Luo, X.Zong, M.Zhao, Z.Sun, Y.Chen, M.Liang, Y.Wu, S.Xue. *Chem. Eng. J.*, **442**, 136136 (2022); https://doi.org/10.1016/j.cej.2022.136136
198. K.Mahesh, S.Karpagam, T.Putnin, H.Le, T.-T.Bui, K.Ounnunkad, F.Goubard. *J. Photochem. Photobiol. A: Chem.*, **371**, 238 (2019); https://doi.org/10.1016/j.jphotochem.2018.11.024
199. Z.-G.Zhang, Y.Yang, S.Zhang, J.Min, J.Zhang, M.Zhang, X.Guo, Y.Li. *Synth. Met*., **161**, 1383 (2011); https://doi.org/10.1016/j.synthmet.2011.05.005
200. S.J.Hyun, N.-G.Park. *Small*, **11**, 10 (2015); https://doi.org/10.1002/smll.201402767

201. B.Zhang, Y.Zhou, Q.Xue, J.Tian, Q.Yao, Y.Zang, L.Wang, W.Yang, H.-L.Yip, Y.Cao. *Solar RRL*, **3**, 1900265 (2019); https://doi.org/10.1002/solr.201900265
202. B.Niu, H.Liu, Y.Huang, E.Gu, M.Yan, Z.Shen, K.Yan, B.Yan, J.Yao, Y.Fang, H.Chen, C.-Z.Li. *Adv. Mater*., **35**, 2212258 (2023); https://doi.org/10.1002/adma.202212258
203. X.Xu, X.Ji, R.Chen, F.Ye, S.Liu, S.Zhang, W.Chen, Y.Wu, W.-H.Zhu. *Adv. Funct. Mater*., **32**, 2109968 (2022); https://doi.org/10.1002/adfm.202109968
204. A.K.Harit, E.D.Jung, J.M.Ha, J.H.Park, A.Tripathi, Y.W.Noh, M.H.Song, H.Y.Woo. *Small*, **18**, 2104933 (2022); https://doi.org/10.1002/smll.202104933
205. S.-G.Kim, K.Zhu. *Adv. Energy Mater*., **13**, 2300603 (2023); https://doi.org/10.1002/aenm.202300603
206. M.S.Mikhailov, N.S.Gudim, L.V.Mikhalchenko, M.I.Knysh, E.A.Knyazeva, O.A.Rakitin. *Russ. Chem. Bull*., **73**, 2199 (2024); https://doi.org/10.1007/s11172-024-4341-4
207. J.Lee, H.Kang, G.Kim, H.Back, J.Kim, S.Hong, B.Park, E.Lee, K.Lee. *Adv. Mater.*, **29**, 1606363 (2017); https://doi.org/10.1002/adma.201606363
208. G.Wang, Y.Huang, X.Tang, J.Li, J.Dai, B.Liu, J.Zhang., J. Xiong. *Dyes Pigm*., **222**, 111843 (2024); https://doi.org/10.1016/j.dyepig.2023.111843
209. M.Zhao, Q.Wu, P.Liu, M.Luo, J.He, S.Xue, Y.Xiong, X.Zong. *Mater. Today Energy*, **42**, 101549 (2024); https://doi.org/10.1016/j.mtener.2024.101549
210. M.Mahdi Tavakoli, R.Tavakoli. *Phys. Stat. Sol. Rep. Res. Lett.*, **15**, 2000449 (2021); https://doi.org/10.1002/pssr.202000449
211. S.Wu, Z.Li, J.Zhang, X.Wu, X.Deng, Y.Liu, J.Zhou, C.Zhi, X.Yu, W.C.H.Choy, Z.Zhu, A.K.-Y.Jen. *Adv. Mater*., **33** (51), 2105539 (2021); https://doi.org/10.1002/adma.202105539
212. F.Zhang, Y.Hou, S.Wang, H.Zhang, F.Zhou, Y.Hao, S.Ye, H.Cai, J.Song, J.Qu. *Solar RRL*, **5**, 2100190 (2021); https://doi.org/10.1002/solr.202100190
213. I.Lee, N.Rolston, P.-L.Brunner, R.H.Dauskardt. *ACS Appl. Mater. Interfaces*, **11**, 23757 (2019); https://doi.org/10.1021/acsami.9b05567
214. N.Yaghoobi Nia, M.Mendez, B.Paci, A.Generosi, A.Di Carlo, E.Palomares. *ACS Appl. Energy Mater*., **3**, 6853 (2020); https://doi.org/10.1021/acsaem.0c00956
215. P.L.Taberna, S.Mitra, P.Poizot, P.Simon, J.-M.Tarascon. *Nature Mater*., **5**, 567 (2006); https://doi.org/10.1038/nmat1672
216. M.Morcrette, P.Rozier, L.Dupont, E.Mugnier, L.Sannier, J.Galy, J.-M.Tarascon. *Nature Mater*., **2**, 755 (2003); https://doi.org/10.1038/nmat1002
217. N.Du, H.Zhang, B.D.Chen, J.B.Wu, X.Y.Ma, Z.H.Liu, Y.Q.Zhang, D.R.Yang, X.H.Huang, J.P.Tu. *Adv. Mater*., **19** (24), 4505 (2007); https://doi.org/10.1002/adma.200602513
218. X.Yue, J.Zhao, L.Kong. *Int. J. Electrochem. Sci*., 16, 210238 (2021); https://doi.org/10.20964/2021.02.02
219. F.A.Obrezkov, A.F.Shestakov, S.Vasiliyev, K.J.Stevenson, P.A.Troshin. *J. Mater. Chem. A*, **9**, 2864 (2021); https://doi.org/10.1039/D0TA09427G
220. F.A.Obrezkov, A.I.Somova, E.S.Fedina, K.J.Stevenson, P.A.Troshin. *Energy Technol*., **9**, 2000772 (2021); https://doi.org/10.1002/ente.202000772
221. R.R.Kapaev, F.A.Obrezkov, K.J.Stevenson, P.A.Troshin. *Chem. Commun*., **55**, 11758 (2019); https://doi.org/10.1039/C9CC05745E
222. F.A.Obrezkov, V.Ramezankhani, I.Zhidkov, V.F.Traven, E.Z.Kurmaev, K.J.Stevenson, P.A.Troshin. *J. Phys. Chem. Lett*., **10**, 5440 (2019); https://doi.org/10.1021/acs.jpclett.9b02039
223. F.A.Obrezkov, A.F.Shestakov, V.F.Traven, K.J.Stevenson, P.A.Troshin. *J. Mater. Chem. A*, **7**, 11430 (2019); https://doi.org/10.1039/C8TA11572A
224. L.I.Tkachenko, G.V.Nikolaeva, A.G.Ryabenko, N.N.Dremova, I.K.Yakushchenko, E.I.Yudanova, O.N.Efimov. *Russ. J. Electrochem*. **54**, 1222 (2018); https://doi.org/10.1134/S1023193518130487
225. E.V.Beletskii, E.V.Alekseeva, O.V.Levin. *Russ. Chem. Rev*., **91** (3), RCR5030 (2022); https://doi.org/10.1070/RCR5030
226. J.K.Feng, Y.L.Cao, X.P.Ai, H.X.Yang. *J. Power Sources*, **177**, 199 (2008); https://doi.org/10.1016/j.jpowsour.2007.10.086
227. C.Su, Y.Ye, L.Xua, C.Zhang. *J. Mater. Chem*., **22**, 22658 (2012); https://doi.org/10.1039/C2JM34752K
228. C.Su, Y.Ye, L.Xua, C.Zhang. *J. Mater. Chem. A*, **2**, 20083 (2014); https://doi.org/10.1039/C4TA03413A
229. W.Huang, T.Jia, G.Zhou, S.Chen, Q.Hou, Y.Wang, S.Luo, G.Shi, B.Xu. *Electrochim. Acta*, **283**, 1284 (2018); https://doi.org/10.1016/j.electacta.2018.07.062
230. C.N.Gannett, B.M.Peterson, L.Shen, J.Seok, B.P.Fors, H.D.Abruna. *ChemSusChem*., **13**, 2428 (2020); https://doi.org/10.1002/cssc.201903243
231. F.A.Obrezkov, E.S.Fedina, A.I.Somova, A.V.Akkuratov, K.J.Stevenson. *ACS Appl. Energy Mater*., **4**, 11827 (2021); https://doi.org/10.1021/acsaem.1c02597
232. Z.Yu, L.Huang, Z.Sun, Fengshi Cai, M.Liang, Z.Luo. *J. Power Sources*, **550**, 232149 (2022); https://doi.org/10.1016/j.jpowsour.2022.232149
233. M.Wang, X.Xing, I.F.Perepichka, Y.Shi, D.Zhou, P.Wu, H.Meng. *Adv. Energy Mater*., **9**, 1900433 (2019); https://doi.org/10.1002/aenm.201900433
234. R.J.Mortimer, A.L.Dyer, J.R.Reynolds. *Displays*, **27**, 18 (2006); https://doi.org/10.1016/j.displa.2005.03.003
235. C.-W.Kuo, J.-C.Chang, L.-T.Lee, J.-K.Chang, Y.-T.Huang, P.-Y.Lee, T.-Y.Wu. *J. Taiwan Inst. Chem. Eng*., **131**, 104173 (2022); https://doi.org/10.1016/j.jtice.2021.104173
236. S.-H.Hsiao, Y.-C.Liao. *Polymers*, **9**, 497 (2017); https://doi.org/10.3390/polym9100497
237. W.Yang, J.Zhao, C.Cui , Y.Kong, P.Li. *Int. J. Electrochem. Sci*., **7**, 7960 (2012); https://doi.org/10.1016/S1452-3981(23)17968-5
238. Y.Gao, W.Zhang, D.Li, X.Lin, X.Qiao, H.Niu, W.Wang. *Synth. Met*., **274**, 116732 (2021); https://doi.org/10.1016/j.synthmet.2021.116732
239. F.Ma, F.Liu, Y.Hou, H.Niu, C.Wang. *Synth. Met*., **259**, 116235 (2020); https://doi.org/10.1016/j.synthmet.2019.116235
240. L.Zhang, F.Luo, W.Li, S.Yan, Z.Chen, R.Zhao, N.Ren, Y.Wu, Y.Chen, C.Zhang. *Phys. Chem. Chem. Phys*., **21**, 24092 (2019); https://doi.org/10.1039/C9CP04308J
241. S.Yan, H.Fu, Y.Dong, W.Li, Y.Dai, C.Zhang. *Electrochim. Acta*, **354**, 136672 (2020); https://doi.org/10.1016/j.electacta.2020.136672
242. P.-I.Wang, W.-R.Shie, J.-C.Jiang, L.-J.Lib, D.-J.Liaw. *Polym. Chem*., **7**, 1505 (2016); https://doi.org/10.1039/C5PY01971K
243. H.-J.Yen, G.-S.Liou. *Chem. Mater*., **21**, 4062 (2009); https://doi.org/10.1021/cm9015222
244. B.Wang, L.Wang, H.Chen, Y.Jia, Y.Ma. *Adv. Opt. Mater*., **11**, 2201572 (2023); https://doi.org/10.1002/adom.202201572
245. X.-J.Lv, L.-B.Xu, L.Qian, Y.-Y.Yang, Z.-Y.Xu, J.Li, C.Zhang. *Chin. J. Polym. Sci.*, **39**, 537(2021); https://doi.org/10.1007/s10118-021-2525-z
246. S.Topal, O.Savlug Ipek, E.Sezer, T.Ozturk. *Chem. Eng. J*., **434**, 133868 (2022); https://doi.org/10.1016/j.cej.2021.133868
247. M.Shao, X.Lv, C.Zhou, M.Ouyang, X.Zhu, H.Xu, Z.Feng, D.S.Wright, C.Zhang. *Sol. Energy Mater. Sol. Cells*, **251**, 112134 (2023); https://doi.org/10.1016/j.solmat.2022.112134
248. Z.Zhao, K.Xia, Y.Hou, Q.Zhang, Z.Ye, J.Lu. *Chem. Soc. Rev*., **50**, 12702 (2021); https://doi.org/10.1039/D1CS00800E
249. P.Semenza. *Inf. Disp*., **27** (10), 14 (2011); https://doi.org/10.1002/j.2637-496X.2011.tb00433.x
250. R.Young. *Inf. Disp*., **35** (3), 24 (2019); https://doi.org/10.1002/msid.1035
251. M.Mizusaki, M.Shibasaki, H.Tsuchiya, Y.Tsukamoto, T.Umeda, K.Nakamura, T.Ohshita, S.Shimada. In *SID Symposium Digest of Technical Papers*. Vol. 50. (Ed. K.J.Fitzsimmons). (North Carolina: Wiley Online Library, 2019). P. 44
252. S.Jadoun, U.Riaz. In *Polymers for Light-Emitting Devices and Display*. (Eds Inamuddin, R.Boddula, M.I.Ahamed, A.M.Asiri). (Scrivener Publishing LLC, 2020). P. 77

253. W.Shi, S.Fan, F.Huang, W.Yang, R.Liua, Y.Cao. *J. Mater. Chem*., **16**, 2387 (2006); https://doi.org/10.1039/B603704F
254. Z.Yao, W.Zong, K.Wang, P.Yuan, Y.Liu, S.Xu, S.Cao. *React. Funct. Polym*., **163**, 104898 (2021); https://doi.org/10.1016/j.reactfunctpolym.2021.104898
255. F.Peng, J.Xu, Y.Zhang, R.He, W.Yang, Y.Cao. *Polym. Chem*., **10**, 1367 (2019); https://doi.org/10.1039/C8PY01677A
256. J.Xu, Z.Wang, Y.Huang, S.Hu, W.Zhou, J.Liu, A.Liang, M.Cai. *Opt. Mater*., **115**, 111072 (2021); https://doi.org/10.1016/j.optmat.2021.111072
257. W.J.Jang, J.-H.Jang, D.B.Kim, J.M.Kim, H.Kang, B.-G.Kang. *Eur. Polym. J*., **216**, 113284 (2024); https://doi.org/10.1016/j.eurpolymj.2024.113284
258. J.Y.Park, J.Jang, X.Shen, J.-H.Jang, S.L.Kwak, H.Choi, B.R.Lee, D.Hwang. *Macromol. Res*., **31**, 721 (2023); https://doi.org/10.1007/s13233-023-00151-8
259. S.Lee, H.Kim, Y.Kim. *InfoMat*., **3**, 61 (2021); https://doi.org/10.1002/inf2.12123
260. Y.Liu, S.Yan, Z.Ren. *Chem. Eng. J*., **417**, 128089 (2021); https://doi.org/10.1016/j.cej.2020.128089
261. M.Li, Y.Zhang, N.Yu, W.Chen, H.Gong, Y.Zheng, M.Ni, Y.Han, N.Sun, L.Bai, X.An, J.Yang, Y.Lin, W.Huang, Z.Zhuo, X.Liang, L.Wang, L.Sun, M.Xu, J.Lin, W.Huang. *Adv. Mater*., **36**, 2307605 (2024); https://doi.org/10.1002/adma.202307605
262. J.Jiao, C.Yang, Z.Wang, C.Yan, C.Fang. *Results Engin.*, **18**, 101158 (2023); https://doi.org/10.1016/j.rineng.2023.101158
263. B.Lynn, P.-A.Blanche, N.Peyghambarian. *J. Polym. Sci. B: Polym. Phys*., **52**, 193 (2014); https://doi.org/10.1002/polb.23412
264. K.Zhang, H.Yang, M.Li, J.Li, W.Wu, S.Xu, Y.Liu, S.Cao. *Dyes Pigm*., **180**, 108473 (2020); https://doi.org/10.1016/j.dyepig.2020.108473
265. H.N.Giang, T.Sassa, T.Fujihara, S.Tsujimura, K.Kinashi, W.Sakai, S.Wada, N.Tsutsumi. *ACS Appl. Electron. Mater*., **3**, 2170 (2021); https://doi.org/10.1021/acsaelm.1c00162
266. N.Tsutsumi, S.Sakamoto, K.Kinashi, B.J.Jackin, W.Sakai. *ACS Omega*., **7**, 12120 (2022); https://doi.org/10.1021/acsomega.2c00370
267. K.Kinashi, M.Matsumura, W.Sakai, N.Tsutsumi. *ACS Appl. Electron. Mater*., **1**, 238 (2019); https://doi.org/10.1021/acsaelm.8b00075
268. G.Chen, W.Wei, S.Li, X.Zhou, Z.Li, H.Peng, X.Xie. *Mater. Chem. Front*., **6**, 3531 (2022); https://doi.org/10.1039/D2QM00744D
269. A.V.Vannikov, A.D.Grishina. *Russ. Chem. Rev*., **72**, 471 (2003); https://doi.org/10.1070/RC2003v072n06ABEH000808
270. W.E.Moerner, S.M.Silence, F.Hache, G.C.Bjorklund. *J. Opt. Soc. Am. B*, **11**, 320 (1994); https://doi.org/10.1364/JOSAB.11.000320
271. Y.Cheng, Y.Xiong, M.Pan, L.Li, L.Dong. *Mater. Lett*., **330**, 133268 (2023); https://doi.org/10.1016/j.matlet.2022.133268
272. W.-J.Yoo, S.Yang, J.Jang, M.Oh, M.Rim, H.Ko, J.Koo, S.-I.Lim, Y.-J.Choi, K.-U.Jeong. *J. Mater. Chem. C*, **10**, 11316 (2022); https://doi.org/10.1039/D2TC02066A
273. I.Butnaru, C.-P.Constantin, M.-D.Damaceanu. *J. Photochem. Photobiol. A: Chem.*, **435**, 114271 (2023); https://doi.org/10.1016/j.jphotochem.2022.114271
274. W.Dong, T.Fei, U.Scherf. *RSC Adv*., **8**, 5760 (2018); https://doi.org/10.1039/C7RA13536J
275. Z.-Q.Shi, N.-N.Ji, H.-L.Hu. *Dalton Trans*., **49**, 12929 (2020); https://doi.org/10.1039/D0DT02213F
276. M.-H.Lee, C.-C.Lin, W.Kutner, J.L.Thomas, C.-Y.Lin, Z.Iskierko, Y.-S.Ku, C.-Y.Lin, P.Borowicz, P.S.Sharma, Y.-W.Lan, C.-H.Yang, H.-Y.Lin. *Biosens. Bioelectron.: X*, **13**, 100258 (2023); https://doi.org/10.1016/j.biosx.2022.100258
277. V.Bharadwaj, N.Singh, S.K.Sahoo. *Sens. Biosens. Opt. Act. Nanomater. Micro Nano Technol*., 401 (2022); https://doi.org/10.1016/B978-0-323-90244-1.00001-X
278. X.Wang, Y.Wang, G.Chai, G.Yang, C.Wang, W.Yan. *J. CO_2 Util*., **51**, 101654 (2021); https://doi.org/10.1016/j.jcou.2021.101654
279. T.-Y.Huang, C.-H.Chen, C.-C.Lin, Y.-J.Lee, C.-L.Liu, G.-S.Liou. *J. Mater. Chem. C*, **7**, 11014 (2019); https://doi.org/10.1039/C9TC03607E
280. T.-H.Lee, J.-H.Tsai, H.-Y.Chen, P.-T.Huang. *Polym*., **13** (10), 1629; https://doi.org/10.3390/polym13101629
281. J.-H.Tsai, M.-C.Tsai, T.-H.Lee, P.-T.Huang. *J. Chin. Chem. Soc*., **67**, 1174 (2020); https://doi.org/10.1002/jccs.201900367